

2011

Characterization of the HIV-1 Restriction Factor Herc5

Jessica G.K. Tong

Follow this and additional works at: <https://ir.lib.uwo.ca/digitizedtheses>

Recommended Citation

Tong, Jessica G.K., "Characterization of the HIV-1 Restriction Factor Herc5" (2011). *Digitized Theses*. 3326.

<https://ir.lib.uwo.ca/digitizedtheses/3326>

This Thesis is brought to you for free and open access by the Digitized Special Collections at Scholarship@Western. It has been accepted for inclusion in Digitized Theses by an authorized administrator of Scholarship@Western. For more information, please contact wlsadmin@uwo.ca.

Characterization of the HIV-1 Restriction Factor Herc5

(Spine Title: Characterization of the HIV-1 Restriction
Factor Herc5)

(Thesis format – Monograph)

By Jessica G. K. Tong

Graduate program in Microbiology and Immunology

A thesis submitted in partial fulfillment
Of the requirements for the degree of
Master of Science

School of Graduate and Postdoctoral Studies
The University of Western Ontario
London, Ontario, Canada

© Jessica G. K. Tong 2011

THE UNIVERSITY OF WESTERN ONTARIO
SCHOOL OF GRADUATE AND POSTDOCTORAL STUDIES

CERTIFICATE OF EXAMINATION

Supervisor

Dr. Stephen Barr

Graduate Chair

Dr. Martin McGavin

Examiners

Dr. John McCormick

Dr. Joe Mymryk

Dr. Jane Rylett

The thesis by

Jessica G. K. Tong

entitled:

Characterization of the HIV-1 Restriction Factor Herc5

is accepted in partial fulfillment of the
requirements for the degree of
Master of Science

Date _____

Chair of the Thesis Examination Board

Abstract

Herc5 is a potent HIV-1 restriction factor able to restrict HIV-1 by two mechanisms: 1) conjugation of ISG15 to gag polyprotein via E3 ligase activity, and 2) restricting the production of HIV-1 proteins by an unknown mechanism that is independent of its E3 ligase function. Herc5 mutations of the RCC1-like domain (RLD) and Spacer domains were generated to dissect this mechanism. Based on HIV-1 release assays, the RLD is important for preventing the production of viral proteins. Herc5 transfected cells show defects in cell cycle progression at the G2/M phase as well as abnormal nuclear morphology. C994A and Δ Spacer constructs did not impact these phenotypes. However, Δ RLD Herc5 constructs had normal cell cycle and nuclear morphology. Based on the results found, the RLD was found to be an important mediator of Herc5 cellular and antiviral activity.

Table of Contents

Certificate of Examination	p. ii
Abstract	p. iii
List of Figures	p. vii
Common Abbreviations	p. viii
<u>Chapter 1: Introduction</u>	p. 1
1.1 Overview of ubiquitination	p. 1
1.2 HECT E3 ligases	p. 2
1.3 Ubiquitin-like proteins / modifiers	p. 6
1.31 SUMO (small ubiquitin-like modifier)	p. 7
1.32 NEDD8 (neural precursor cell expressed, developmentally down-regulated 8)	p. 9
1.33 ISG15 (interferon stimulated gene 15)	p. 11
1.4 HIV Replication	p. 11
1.41 Virus structure	p. 11
1.42 HIV life cycle	p. 12
• Viral entry and uncoating	p. 12
• Reverse transcription	p. 13
• Nuclear entry and integration	p. 14
• Transcription	p. 16
• Nuclear export of viral RNA and translation	p. 17
• Assembly	p. 19
• Budding and maturation	p. 22
1.5 Interferon response	p. 23
1.51 Restriction factors	p. 26
1.52 Interferon stimulated gene (ISG15)	p. 26
1.6 HECT domain and RCC1-like domain containing protein (Herc) Family	p. 32

1.61 Herc5	p. 33
1.7 Preliminary data	p. 38
1.8 Hypothesis and aims	p. 42
<u>Chapter 2: Materials and Methods</u>	p. 42
2.1 Plasmid constructs	p. 42
2.2 Cell culture, plasmids, and transfection	p. 48
2.21 Transfections	p. 48
• Lipofectamine transfection	p. 48
• FuGene transfection	p. 48
• Superfect transfection	p. 48
2.3 mRNA expression of protein constructs	p. 49
2.4 HIV-1 release assay	p. 49
2.5 Growth analysis	p. 50
2.6 Confocal microscopy	p. 52
2.7 Propidium iodide staining for cell cycle analysis	p. 52
2.8 Statistics	p. 53
<u>Chapter 3: Results</u>	p. 53
3.1 Generation of Herc5 mutants and RNA expression	p. 53
3.2 Effect of Herc5 on cell viability and growth	p. 57
3.3 Propidium iodide staining for cell cycle analysis	p. 58
3.4 Nuclear morphology	p. 63
3.5 Rev localization	p. 66
<u>Chapter 4: Discussion</u>	p. 68
4.1 Summary and interpretation of data	p. 68
4.2 Future directions	p. 77

4.21 Quantification of cytoplasmic rev in the presence of Herc5 vs. pGL3 and Δ RLD transfected HeLa cells	p. 77
4.22 qRTPCR of HIV mRNA in cytoplasm and nuclear fractions to evaluate shuttling bility in the presence of Herc5 and mutant constructs	p. 77
4.23 Quantification of cytoplasmic Ran-GTP in the presence of Herc5 vs. pGL3 negative control and mutant constructs	p. 78
4.24 Generation of RLD active site mutants to evaluate the impact on Herc5 GEF activity (if any), mRNA shuttling capacity, nuclear morphology, cell cycle progression, growth curve, and rev localization	p. 79
4.25 Generation of an RLD only construct lacking spacer and HECT domains of Herc5	p. 79
4.26 Generation of point mutants at lysine residues in the spacer domain to determine if autoISGylation in this domain leads to Herc5 turnover	p. 80
4.27 Evolutionary comparison of Herc5 across various primate species	p. 81
<u>Supplementary Figures</u>	p. 83
<u>References</u>	p. 90
<u>VITA</u>	p. 107

List of Figures

Fig. i- HIV-1 structure and genome organization

Fig. ii- Rev shuttling

Fig. iii- Interferon signalling

Fig. iv- The crystal structure of ISG15

Fig. v- Herc family of proteins

Fig. vi- Herc5 RLD vs. RCC1

Fig. vii- HERC5 ISGylation leads to gag polyprotein restriction in U2OS cells

Fig. viii- Herc5 restriction of HIV-1

Fig. ix- qRT-PCR of gag mRNA in HIV-1 infected cells

Fig x- RLD mutant design

Table i- Primers used for pCS2+ Herc5 RLD mutants and Spacer domain deletion

Table ii- PCR conditions for pCS2+ Herc mutants.

Table iii- PCR conditions for RTPCR of Herc5 CS2+ mutants

Fig. 1- Western blot for protein expression of pFLAG Herc5 RLD mutants in comparison to pCS2⁺ WT Herc5

Fig. 2- RTPCR of CS2+ Herc5 constructs from U2OS transfected cells

Fig. 3- Growth comparison of Herc5 constructs in HeLa cells

Fig. 4- Propidium Iodide staining for cell cycle analysis of HeLa cells transfected with Herc5 constructs

Fig. 5- Lobed nuclear morphology of Herc5 transfected cells

Fig. 6- Rev Localization in HeLa cells transfected with Herc5 mutant constructs

Supplementary Figure 1- HECT vs. RING E3 ligases

Supplementary Figure 2- pCS2+ plasmid map

Supplementary Table 1- Primers used for generation of pFLAG Herc5 RLD mutants

Supplementary Table 2- PCR conditions used for pFLAG Herc5 RLD mutants

Supplementary Table 3- Statistical analysis/ two-way ANOVA output for growth curve

Common Abbreviations

ISG15 – Interferon Stimulated Gene 15

Herc5 – HECT domain and RCC1-like domain containing protein 5

HIV-1 – Human Immunodeficiency Virus-1

RCC1 - Regulator of chromosome condensation 1

HECT - Homologous to the E6-AP (ube3A) Carboxyl Terminus

RLD- RCC1-like Domain

PR – Protease

IN – Integrase

RT – Reverse Transcriptase

PI- Propidium iodide

Env – Envelope proteins

RRE – Rev response element

PM – Plasma membrane

IFN- Interferon

WT Herc5- Wild type Herc5

C994A Herc5 – Herc5 with a point mutation at 994 (cysteine converted into alanine)

Δ spacer – Herc5 with the spacer domain deleted

Δ RLD – Herc5 with the RLD deleted

Δ 1-2 RLD Herc5- Herc5 with the first two blades of the RLD deleted

Δ 1-5 RLD Herc5- Herc5 with the first 5 blades of the RLD deleted

pGL3 - Promoterless vector used as a negative control.

GEF - Guanine exchange factor

GTPase - Hydrolase enzymes that can bind and hydrolyze guanosine triphosphate (GTP)

Chapter 1: Introduction

1.1 Overview of Ubiquitination

Ubiquitination of proteins has a large role in maintaining homeostasis in the host by altering a wide variety of cellular processes such as, apoptosis, cell cycle, DNA transcription, and antiviral immune responses. The conjugation of ubiquitin to target proteins requires three enzymatic reactions from three classes of enzymes, the E1, E2, and E3, in sequential steps [1]. The initiation of this process involves the activation of ubiquitin by E1 through an ATP dependent mechanism, forming a ubiquitin-adenylate intermediate and results in binding to a cysteine residue of the E1 via a thioester bond. This activated ubiquitin is then passed to a cysteine residue on the E2 enzyme via a trans-thiolation reaction. The E2 then passes ubiquitin to an E3 ligase enzyme which conjugates the c-terminus of ubiquitin to a lysine residue on a target protein. The process of ubiquitination can lead to formations of poly-ubiquitin chains on target substrates. The length and binding site of the poly-ubiquitin chain on the substrate can have a variety of affects including alternative protein trafficking, degradation, or signalling events to occur. The variety of ubiquitin linkages derives from the diversity of E1, E2, and E3 enzymes that are able to conjugate ubiquitin to targets, E3s being the most diverse class amongst ubiquitinating enzymes with over a hundred known E3 ligases [2,3].

There are two main classes of E3 ligases: RING (Really Interesting New Gene) domain E3 ligases and HECT (Homologous to the E6-AP Carboxyl terminus) domain. These two classes differ in the way they interact with ubiquitin and their target substrate [3]. RING E3 ligases act as scaffold proteins, binding both E2 and substrate protein,

which brings them in close proximity to one another and facilitates the direct transfer of ubiquitin from the E2 to the target substrate. HECT (Homologous to the E6-AP (ube3A) Carboxyl Terminus) domain E3 ligases however, form an E3-ubiquitin thiol-ester conjugate intermediate. In this instance, ubiquitin is transferred from the E2 enzyme to the HECT E3 ligase which then catalytically conjugates ubiquitin to the amine group of a lysine residue on a bound substrate, the specifics of which are unknown [3] (Supplementary Figure 1). For substrate proteins to be capable of accepting ubiquitin each must contain either a ubiquitin associated domain, ubiquitin interacting motif, ubiquitin E2 variant or CUE-1 homologous sequence. Each of these ubiquitin binding domains is commonly affiliated with specific protein and cellular activities such as ubiquitin linkage patterns, DNA repair, degradation, and signalling which may in part be responsible for the diversity of ubiquitin functions [4-6].

1.2 HECT E3 ligases

HECT domain containing proteins were first discovered in E6 associated protein (E6-AP), a cellular factor which associates with the Human Papilloma Viruses 16 and 18 (HPV16 and HPV18). This HECT domain containing protein targets p53 for ubiquitination and proteasomal degradation which enhances viral replication for HPV16 and HPV18 [7,8]. Sequence analysis of the C-terminus of E6-AP shows 28 proteins containing similar C-terminal sequences which formed a new class of proteins subsequently designated HECT domain containing proteins [9]. C-terminal HECT domains perform the catalytic function of conjugating ubiquitin on to its target substrates, while the N-terminus of most HECT containing proteins are reserved for recognizing and maintaining substrate specificity [10-12]. These N-terminal regions of HECT containing

proteins are subcategorized into three different groups: 1) RLD (RCC1-like domain) containing HECT proteins, 2) WW domain containing HECT proteins called NEDD4/NEDD4-like E3s, and 3) Singular HECT proteins which neither contain an RLD or a WW domain [13-15].

The precise mechanism by which the HECT domain conjugates ubiquitin to a substrate remains unclear. However, all HECT E3 ligases have at least 4 biochemical activities: i) they bind to specific E2s ii) they form ubiquitin-thioester intermediates on their active-site cysteine when ubiquitin is transferred from the E2 iii) it conjugates ubiquitin on lysine residues of target proteins by catalyzing the formation of an isopeptide bond iv) it conjugates additional ubiquitin molecules on the lysine residues of the already conjugated ubiquitin forming a chain [16]. Crystal structure analysis of the HECT domain of E6-AP shows that the HECT is a bi-lobed structure made up of the N-lobe and the C-lobe which are connected by a flexible hinge made up of 3 amino acids. This structure is maintained through most HECT domain containing proteins and is important for the catalytic activity of the domain as well as its interaction with a specific E2. The N-lobe of the E6-AP HECT domain forms a V shaped groove which is responsible for interaction with its E2, UbcH7, while the C-lobe contains the active-site cysteine residue responsible for accepting the ubiquitin transfer [16]. Once the UbcH7 is bound to the groove of the N-lobe, the active-site cysteine residues on both UbcH7 and E6-AP are only 41Å apart and have an open line of sight between them for the easy transfer of ubiquitin. Interestingly it has been proposed that the N-lobe binding of the E2 is stable and is maintained throughout the entire E1-E2-E3 enzymatic cascade facilitating the efficient transfer of ubiquitin.

This bi-lobed HECT domain structure is clearly an important feature for the proper functioning of HECT proteins such as WWP1. Two models have been proposed to describe how the HECT domain structure relates to the mechanism by which WWP1 HECT E3 acts to ubiquitinate target substrates. 1) the C-lobe rotates along the hinge region and acquires ubiquitin molecules from the bound E2 on the N-lobe via a thioester bond and tethers to the active-site cysteine residue which subsequently modifies the target protein through an isopeptide bond. This continuously occurs until the growing ubiquitin chain interferes with the flexibility of the hinge region and consequently interrupts further ubiquitination. 2) Ubiquitin chain elongation occurs before the conjugation of the poly-ubiquitin chain on the target protein. Here the transfer of ubiquitin from the E2 to the E3 occurs in the same fashion as the first model but differs in that it proposes that the ubiquitin chain forms on the active-cysteine residue on the C-lobe of the HECT domain. The C-lobe continuously rotates along the hinge region to bring the C-lobe lysine residues of attached ubiquitin within close proximity of the thioester bond between the E2-ubiquitin conjugate on the N-lobe. This consequently forms the ubiquitin chain and stops when the ubiquitin chain interferes with the flexibility of the hinge region. This poly-ubiquitin chain is collectively transferred to the target protein in one step [17].

It has been noted repeatedly in literature that different HECT domains favour certain conformations of ubiquitin chains. For example, E6-AP favours K48 linkages of ubiquitin (linkages of ubiquitin at the 48th residue-lysine) which subsequently leads to proteasomal degradation of these protein targets [18,19]. In contrast, the HECT proteins NEDD4 and Itch have been shown to favour K63 linkages of ubiquitin (chains of

ubiquitin linked at the lysine residue at the 63rd amino acid) for proteasome-independent processes such as DNA repair, endocytosis, and NF- κ B activation [20,21]. Mutational analysis suggests that the C-lobe of HECT domains carries the specificity for these various ubiquitin linkages. Chimeras in which the C-lobe and linker of the HECT domain of the protein Rsp5 (typically promotes K63 linked ubiquitin chains) are replaced with the C-lobe and linker of E6-AP (favouring K48 linked ubiquitin) show almost exclusive production of K48 linked ubiquitin chains on target proteins [22]. When only the C-terminal portion of the C-lobe of Rsp5 was replaced with the C-terminal portion of the C-lobe of E6-AP, the same K48 linked ubiquitin chains were formed again almost exclusively. This data which strongly suggests this C-terminal region (60 amino acids) of the C-lobes of Rsp5 is responsible for the patterns of ubiquitylation [22] however it is unclear whether this parallels all HECT domains.

The regulation of the function of E3 ligases especially HECT E3s is physiologically crucial in maintaining human health. For example, dysregulation of the E6-AP HECT domain containing protein in which there is inappropriate activation of the E3 ligase has been linked to the development of cervical cancer. The highest risk factor for the development of cervical cancer is HPV. One of the most effective modes of restricting HPV replication is through the tumour suppressor protein p53 [10]. For efficient replication of HPV the E6 protein, encoded in the viral genome, hijacks the cellular protein E6-AP which together promote the recognition, binding, and ubiquitination of p53 leading to its proteasomal degradation and enhancing viral replication [23].

The onset of Liddle's Syndrome is also due to dysregulated ubiquitination. This disease is characterized by high blood pressure and low levels of aldosterone and renin due to an excessive reabsorption of sodium from the nephron in the kidneys. The dysregulation in reabsorption is due to a high number of epithelial sodium channels on the apical side (facing the urinary tract) causing an increase in flux of sodium back into the body. These channels are made up of three homologous transmembrane subunits, α , β , and γ . The C-terminus of each of these subunits has a PY motif which allows for the binding of the WW domains of NEDD4-1 and NEDD4-2 HECT domain containing proteins and ubiquitination of the N-termini of the subunits leading to the sequestration of the channel and degradation. In Liddle's syndrome patients, the gene encoding either the β or γ subunit is mutated causing a deformed or deleted PY motif which subsequently eliminates NEDD4-1 and NEDD4-2 binding and leads to an accumulation of epithelial sodium channels at the membrane [10,24,25]. This excessive sodium retention causes constipation, fatigue, heart palpitations, and chronic hypertension.

1.3 Ubiquitin-like proteins/ modifiers

Similarly to ubiquitin, other posttranslational modifications exist which alter proteins using the same E1-E2-E3 enzyme cascade reaction. This constitutes a growing family of proteins called ubiquitin-like modifiers (Ubls). ISG15 was the first and least characterized protein of this family of proteins. These proteins do not share much sequence homology with ubiquitin however some show a great amount of structural similarity. Ubls also are functionally distinct from ubiquitin. Although they may be involved in protein degradation, they have a diverse range of regulatory functions including, protein stability, altering protein affinity, or changing localization.

1.31 SUMO (Small Ubiquitin-like Modifier)

The process of SUMOylation (conjugation of sumo on proteins) has a variety of functions in the cell including cell cycle regulation, transcription, localization, localization, degradation, and chromosomal organization [26]. Before conjugation, a pro-form of SUMO is cleaved at the C-terminus by SUMO specific proteases (SENPs) to create activated SUMO. From this stage, the heterodimer Uba2/Aos1 binds SUMO in an ATP dependent manner, acting as its E1 enzyme. The E1 dimer then passes SUMO to its E2 enzyme, Ubc9 - the only known E2 for SUMO, and is attached to an active-site cysteine residue (similarly to ubiquitin). Ubc9 then interacts with one of a number of different E3 ligases found for SUMO.

Two-thirds of SUMOylation target proteins contain at least one ψ KxE/D motif where ψ represents a large hydrophobic residue such as valanine, leucine, or methionine, and x is any residue. It is possible that the pool of SUMOylatable proteins is much larger than previously thought seeing as one-third to half of human proteins contain this motif [27,28]. Currently most SUMOylatable proteins are found in the nucleus. Some of these proteins are involved in repressing DNA transcription by binding to transcriptional inhibitors/co-repressors of transcription and enhancing their function or by binding to transcription factors and co-activators and inhibiting their activity [29,30, 40].

Some nuclear SUMOylated proteins are involved in RNA editing by co-localizing with the RNA editing protein, ADAR1. ADAR1 functions to destabilize dsRNA through the conversion of adenosine into inosine. Since inosine functions as a guanosine during translation, the conversion of adenosine into inosine leads to amino acid changes and results in alterations of protein function, and alternative RNA splicing [31,32].

SUMOylation of proteins has also been shown to counteract their ubiquitination and subsequent degradation. The E3 ubiquitin ligase and tumor suppressor protein vonHippel-Lindau (VHL) has been shown to be regulated by both SUMOylation and ubiquitination. One of VHLs most researched targets is HIF1 α , a transcription factor leading to the upregulation of cyclinD1, the progression of cell cycle, and related to tumorigenesis [38]. Ubiquitination of HIF1 α by VHL has been shown to destabilize the protein and lead to its degradation and protection against tumorigenesis [38, 39]. However, mutations in VHL or hypermethylation in its gene can lead to the development of renal cell carcinomas and sporadic hemangioblastomas of the CNS due to increased levels of HIF1 α [39]. The lysine residues at position 171 and 196 of VHL are targeted by both ubiquitin and SUMO and are the main regulators of the protein; where ubiquitination leads to its degradation and SUMOylation causing increased stability [38]. Moreover, SUMOylation of VHL is able to out-compete ubiquitin for binding at these lysine residues and stabilize VHL expression. This may in part be due to the alternative trafficking patterns of ubiquitinated versus SUMOylated VHL. It is possible that the ubiquitination of VHL leads to proteasomal degradation in the cytoplasm as opposed to SUMOylated VHL which is stabilized and maintains transcriptional regulation within the nucleus [38].

Upon recognition of ssRNA viruses (like Human Immunodeficiency Virus [HIV]), RIG-I activates itself by unfolding from an autoinhibitory conformation, a process initiated by ubiquitination of the lysine residue at position 172. After which, RIG-I induces a cascade of reactions that lead to the transcription and production of interferon (for more information on interferon, see section 1.5). It has been suggested that

SUMOylation of RIG-I has a positive regulatory affect on the activity of the protein. Particularly, SUMOylation of RIG-I increases its ubiquitination and enhances activation and interaction with the downstream adaptor protein, cardif which also enhances expression interferon [45].

Many viruses however have their own means of circumventing these cellular defences or even utilizing SUMOylation for their own benefit. For example, the non-structural protein1 (NS1) of Influenza A is essential for efficient replication of virus in human cells. Particularly, NS1 antagonizes the interferon response [41]. It does so by binding to viral ssRNA and sequestering it so that ssRNA binding proteins like RIG-I are less readably activated by viral RNA and therefore impedes interferon mRNA production [42]. NS1 is also able to impede the translation of interferon mRNA through the formation of an inhibitory complex with specific nuclear mRNA export proteins as well as proteins which form the nuclear pore thus trapping mRNA in the nucleus and preventing access to cytoplasmic ribosomes. Therefore the production of interferon is disrupted at two stages by the NS1 protein, at the transcription level as well as translation [43]. It has recently been shown that the C-terminus of NS1 is SUMOylated at lysine residues K219 and K221 and contributes to protein stability. It has also been shown that SUMOylation of NS1 also marginally increases the replication rate of H5N1 and viral titres [44].

1.32 NEDD8 (Neural precursor cell expressed, developmentally down-regulated

8)

Of all ubiquitin like proteins (Ubls), NEDD8 shows the highest degree of sequence similarity to ubiquitin (~60%). Like the E1 for SUMO, the NEDD8 E1 is a heterodimer composed of the proteins, APPBP1 and Uba3. Like ubiquitin and SUMO, NEDD8 is transferred via thioester bonds to the E2, Ubc12, and the E3 ligase (of which there are no specific NEDD8 only ligases) [46]. The most well characterized NEDD8 target is the cullin family of proteins. Cullins are scaffold proteins for the SCF (Skp1/cullin/Fbox) complex, a multi-subunit ubiquitin E3 family. The SCF family of E3 ubiquitin ligases are predominantly involved in the regulation of cell cycle progression, proteasomal degradation, and transcriptional regulation. The Rbx E3 ligase is a dual conjugating ligase as it also acts to conjugate NEDD8 to cullins. NEDD8 modification of cullin by Rbx subsequently enhances SCF mediated ubiquitination as well as increased proteasomal degradation. NEDD8 modification of cullin aids in the recruitment of the E2 enzyme, ubc4, to the SCF complex and accelerates their association by increasing Ubc4 affinity for SCF [47,48,49].

Since many SCF E3 ligases are essential for cell cycle progression it is no wonder that NEDDylation is also a required for cell cycle. In mice lacking Uba3, one of the proteins of the NEDD8 E1 enzyme, mitotic and endoreduplicative cell cycle events are arrested [51]. Endoreduplication involves the replication of the nuclear genome in the absence of cell cycle progression and leads to a build up of nuclear gene content. The significance of this phenomenon is currently speculative, however some suggest that in embryogenesis endoreduplication is responsible and necessary for a mass production of proteins that are required for the high metabolic demands of the developing fetus [50]. It has also been shown to be involved in DNA damage resistance and cell differentiation.

NEDDylation of cullin 1 and cullin3 of different SCF E3 ligases are required for the transition of mitotic cell cycle to endoreduplicative cell cycle and the continuance of endoreduplicative cell growth [51]. Fetal mice lacking NEDDylation capabilities died *in utero* at the preimplantation stage of embryogenesis due to a number of complications relating to DNA damage and even carcinogenesis [51].

Interestingly certain viruses have evolved to incorporate NEDD8 sequences into their genome. Bovine Viral Diarrhea Virus (BVDV) is a positive sense (+) ssRNA virus made up of one open reading frame which codes for a large polyprotein that is cleaved to form 14 different structural and non-structural viral proteins. The insertion of the NEDD8 sequence into the p821 strain of BVDV occurs between the third and fourth codons of the NS3 gene and subsequently leads to a different N-terminal amino acid sequence. It has been shown that this insertion of NEDD8 into the NS3 sequence acts as a processing signal to yield NS3, an RNA helicase necessary for the synthesis of the negative sense RNA strand and infectious virus particles[52,53].

1.33 ISG15 (Interferon Stimulated Gene 15)

(Refer to section 1.52)

1.4 HIV replication

1.41 Virus structure

HIV is an enveloped virus with two (+) ssRNA genomes that belong to the virus family *Retroviridae* or retroviruses. This class of virus is unique in that their ssRNA genomes are converted into dsDNA and are then integrated into the host genome where it becomes

a provirus and replicates itself in parallel with the host cell using host cell machinery [140]. HIV encodes for 9 open reading frames (ORFs). The three largest are the polyproteins Gag, Pol, and Env which are later proteolytically processed into individual proteins that are common to every member of the retrovirus family. The gag polyprotein is cleaved into 4 different proteins, the matrix, the capsid, the nucleocapsid, and P6 which eventually make up the structural components of the virus [68]. The Pol polyprotein is cleaved into the protease, reverse transcriptase, and integrase which provide enzymatic functions which are necessary for the HIV lifecycle and are packaged within the mature virus [69]. The Env polyprotein encodes for cell surface receptor gp120 as well as transmembrane protein gp41. These two proteins make up the outer envelope proteins of HIV [67]. HIV also encodes for 6 accessory proteins, 3 of which (Viral Protein R [vpr], Virion Infectivity Factor [vif], and Negative Regulatory Factor [nef]) are packaged with the virus [66]. Trans-activator of Transcription (Tat) and Regulator of Virion Expression (rev) are necessary for gene regulatory functions and Viral Protein U (vpu) assists in virus assembly; these proteins make up the remaining accessory proteins. In total, HIV is made up of 15 proteins and two copies of (+) ssRNA genome (Fig. i).

1.42 HIV life cycle

Viral entry and uncoating

HIV infection occurs when the envelope protein gp120 binds to the CD4 receptor found on CD4+ T cells. Mucosal sites, such as the genital mucosa, have a large CD4+ T cell population and act as a major site for viral infection. After gp120 binds to the CD4 receptor, a conformational change occurs to allow for additional binding to the cellular co-receptor CXCR4 [65]. HIV strains which target CD4 T cells predominately are

termed T cell line tropic. Some HIV strains have shown different cell tropism and infect macrophages predominantly. These macrophage tropic viruses also bind to CD4 but use the co-receptor CCR5 as a co-receptor for entry [73]. Once adherence to the cell is established, gp41 on the HIV envelope is exposed and also reaffirms adherence on the cellular membrane. Gp41 also aids in bringing HIV and the cell in close contact to promote the fusion of the viral and cellular envelopes [70]. This facilitates the release of the viral core, or capsid, into the cytoplasm along with a number of packaged viral proteins which are necessary for subsequent steps of viral replication (nucleocapsid, reverse transcriptase, integrase, and vpr). Within one hour of envelope fusion, the capsid is degraded or “uncoated” and the ssRNA genome is released into the cytoplasm and is then reverse transcribed by the viral protein, reverse transcriptase [71,72]. Although the mechanism of capsid uncoating is not well characterized, it has been thought that the degradation of the capsid is mediated by phosphorylation events in the cytoplasm [74,75]. It has been hypothesized that the catalytic domain of cellular cAMP, the C-PKA subunit, can target capsid proteins and phosphorylate them to destabilize the structure and release of HIV genomic RNA [74].

Reverse transcription

After the release of the viral genome and viral enzymes into the cytoplasm, the reverse transcription complex is formed. This complex is made up of the viral reverse transcriptase enzyme (RT), genomic RNA or viral RNA (vRNA) (flanked on each end by short direct repeats known as, R), and a cellular transfer RNA (tRNA)- tRNA₃^{Lys} [76]. This complex is required for the conversion of vRNA into DNA so that it may be incorporated into the host genome. tRNA₃^{Lys} acts as a primer and binds to vRNA [76].

This initiates the binding, initiation, and elongation by reverse transcriptase reading the template in a 3' to 5' direction and generating the DNA in a 5' to 3' direction. This leads to generation of a negative sense (-) DNA copy hybridized to vRNA [76]. In addition to its polymerase activity, RT also contains RNase H which selectively degrades RNA when it is part of an RNA-DNA hybrid. This degrades the parental RNA strand that is complexed with the (-) DNA and exposes the ssDNA with the exception of a small fragment of vRNA which is still bound to the (-) DNA. This small fraction of vRNA acts as a primer for the synthesis of the (+) DNA strand. Synthesis of the second strand is in the 5' to 3' and subsequently creates cDNA from the vRNA genome [76].

Nuclear Entry and Integration

Effective replication of HIV requires the active transport of generated cDNA from the cytoplasm into the nucleus and integration into the host genome without the breakdown of the nuclear envelope. Transport of HIV across the nuclear membrane requires three proteins, matrix, integrase (IN), and vpr, which associate with viral cDNA and form the pre-integration complex. Both IN and MA proteins contain nuclear localization signals which are important for the direction of the pre-integration complex into the nucleus. It is thought that the key regulator of the pre-integration complex is vpr which binds to the nuclear transport molecule importin α . This interaction has been shown to increase the affinity of importin α for the nuclear localization signals of both the matrix and IN. This leads to the heterodimerization of importin α with importin β and allows for the docking and transport of the entire pre-integration complex through the nuclear pore and into the nucleus [80].

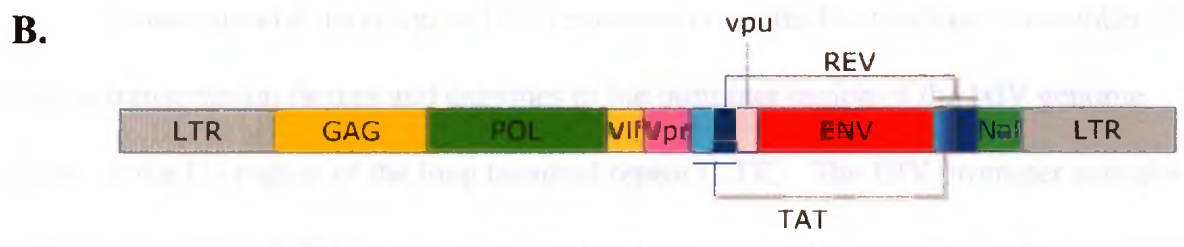
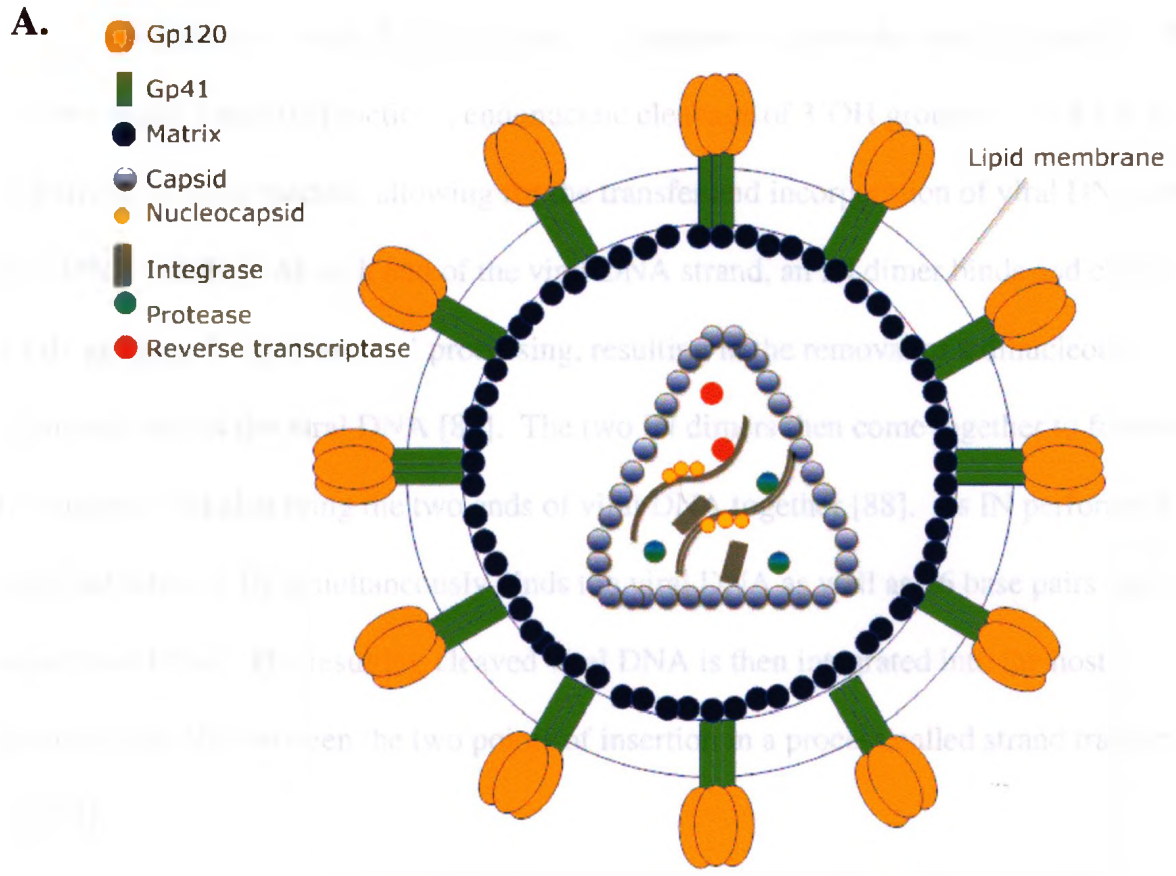


Fig. i A) The structure of HIV-1 B) Genome organization of HIV-1

Integration of viral cDNA into the host genome requires the viral enzyme IN. IN has two major catalytic functions, endonucleic cleavage of 3'OH groups of viral DNA and strand transfer reaction allowing for the transfer and incorporation of viral DNA into host DNA [81-86]. At each end of the viral DNA strand, an IN dimer binds and cleaves 3'OH groups, also known as 3' processing, resulting in the removal of a dinucleotide from each end of the viral DNA [87]. The two IN dimers then come together to form an IN tetramer and also bring the two ends of viral DNA together [88]. As IN performs its catalytic activity, IN simultaneously binds the viral DNA as well as 26 base pairs (bp) of target host DNA. The resulting cleaved viral DNA is then integrated into the host genome with 5bp between the two points of insertion in a process called strand transfer [87-92].

Transcription

Transcriptional initiation of HIV replication requires the binding of a number of cellular transcription factors and enzymes to the promoter region of the HIV genome located at the U3 region of the long terminal repeat (LTR). The HIV promoter contains two NF- κ B and three Sp1 binding sites for their respective transcription factors as well as an initiator site called, start-site region [103,104]. These sites are located upstream of the RNA polymerase II (RNAPII) TATA box region also located on the HIV promoter. The TATA box is recognized by the TATA binding protein which also binds 8-12 additional TATA associated factors [105,106]. Once all transcription factors and associated TATA associated factors are bound, RNAPII binds to TATA binding protein and is able to initiate transcription. However, only low levels of short vRNA transcripts are produced [107-109].

Highly efficient transcription of the HIV provirus requires the association of the viral protein tat to the promoter. This is only possible through the expression of TAR RNA. All HIV RNA transcripts express a TAR element (Trans-activation Response Element), a stem loop secondary structure found at the 5' end of vRNA, and serves as a binding site for tat [93,94]. The low levels of short RNA transcripts generated initially act as an attractant for tat binding. Tat-TAR interactions are stabilized by the recruitment of cyclin T1, leading to higher affinity binding of tat-TAR [95]. The cellular protein Cdk9 also binds to this complex and together with cyclin T1 constitutes the positive transcription elongation factor b (p-TEFb) [96]. P-TEFb hyperphosphorylates the carboxyl terminal domain of RNA polymeraseII and enhances its function which generates elongated RNA transcripts [96-99]. Acetylation of tat also helps to generate elongated transcripts by binding the PCAF protein which causes the dissociation of tat-p-TEFb and PCAF from TAR and RNAPII [100-102].

Nuclear Export of Viral RNA and Translation

Full length RNA transcripts function both as genomic RNA as well as mRNA for the expression of gag and pol genes. However, expression of genes downstream from gag and pol require extensive splicing of the primary transcript. With the exception of a few viral mRNA (nef, tat, and Rev) most viral transcripts require the viral protein Rev to be shuttled out of the nucleus [141,142]. After its translation in the cytoplasm, Rev relocates to the nucleus through a nuclear localization signal, an arginine rich motif on Rev which binds the cellular nuclear import factor Importin β [143]. In the nucleus, multimers of Rev bind to a stem loop structure located in the Env gene called the Rev

response element (RRE) through the same arginine rich motif and masks the nuclear localization signal [144,145].

The export of Rev-RRE complexes require a nuclear export signal which is a leucine rich sequence found on the C-terminus of Rev [146]. This allows Rev-RRE to hijack a cellular pathway for RNA export [146]. The cellular protein, Crm1, binds Rev-RRE and localizes to the nuclear pore complex and interacts with a number of nuclear proteins including Ran, a GTPase that is involved in RNA export to the cytoplasm [147-149, 138]. RNA export by Ran requires an energy gradient created by an asymmetric distribution of Ran-GTP and Ran-GDP across the nuclear membrane (high levels of nuclear Ran-GTP in the nucleus, low levels in the cytoplasm) [138]. High levels of Ran-GTP in the nucleus favour binding of Ran-GTP with nuclear export signal containing proteins such as Crm1-Rev-RRE which is very stable [148,150]. Once bound to Ran-GTP, the Crm1-Rev-RRE complex is able to be transported out of the nucleus into the cytoplasm mediated by the GTP disparity energy gradient [150]. Once in the cytoplasm RanBP1 binds Ran-GTP to catalyze the disassociation of the bound components (Crm1-Rev-RRE). This allows Rev to re-enter the nucleus via the mechanism described above and continuously shuttle vRNA back into the cytoplasm [150] (Fig. ii). Once in the cytoplasm, RNA transcripts are translated through two different mechanisms: Either by the classical 5' cap dependent translation initiation (less common), or through internal ribosomal entry sites (IRES) (more common) [151]. The classical 5' cap mechanism is maintained by all cellular proteins as well as HIV proteins which code for gag and pol [152-154]. In this mechanism, the 5' cap on the RNA transcript is recognized by the cellular factor eIF4E and leads to the unwinding of the secondary RNA structures by the

eIF4A helicase. eIF4E also acts as a scaffold for the binding of eIF4G which coordinates the binding of 40S ribosome and the initiation of translation [155, 156]. IRES mediated translation initiation allows for direct recruitment of an initiation complex (either direct recruitment of the 40S ribosomal subunit, an IRES transacting factor, or by other initiation factors) near or at the AUG start codon [157]. Although there are no consensus sequences which are characteristic of IRESs, these sites are often structurally similar in that they contain a long and structured LTR and several AUG triplets [158].

Assembly

Incorporation of viral proteins into a maturing virion requires their transport to the cell membrane. Gag polyprotein shuttling to the cell membrane and virus formation requires 3 domains: 1) the membrane domain which is post-translationally myristoylated at the N-terminus of the matrix for interaction with the cell membrane. 2) The Interaction domain, which is found at the N-terminus of the nucleocapsid, promotes gag-gag interactions at the membrane and leads to oligomerization at the plasma membrane (PM). 3) The PTAP motif or the late domain found on the N-terminus of p6 is necessary for the last stages of viral budding [159-162].

The membrane domain, along with highly basic residues, comprise a membrane targeting motif which interacts with acidic phospholipids on the PM [110]. The myristic acid addition to the matrix also allows gag to target lipid rafts on the PM. Phosphatidylinositides (PI) are a class of phosphorylated fatty acids which are implicated in cellular trafficking to various organelles. The PIs PI(4)P, PI(4,5)P₂, and PI(3,4,5)P₃

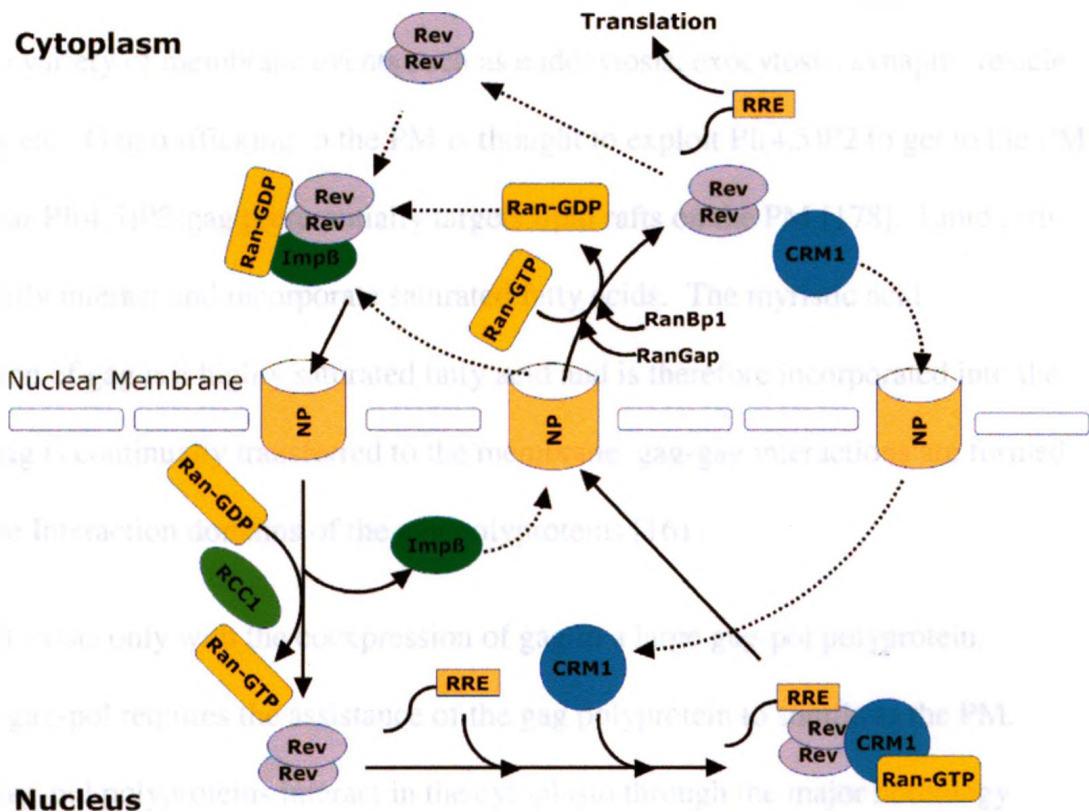


Fig. ii Rev shuttling. Once translated in the nucleus, Rev binds importin β and Ran-GDP to re-enter the nucleus. Once RCC1 performs GEF activity on Ran-GDP converting it to Ran-GTP, rev and importin β dissociate. Rev is then able to bind RRE of HIV mRNA, CRM1 nuclear exporter, and Ran-GTP. With increased Ran-GTP in the nucleus, rev uses the GTP energy gradient generated across the nuclear membrane to export HIV mRNA into the cytoplasm. Hydrolyzation of Ran-GTP in the cytoplasm by RanGAP and RanBp1 leads to the dissociation of the Rev complex and HIV mRNA is able to be translated.

are able to target to the PM and thus proteins that interact with these PIs are also trafficked to the PM. In particular PI(4,5)P2 is a major PI for PM trafficking and regulates a variety of membrane events such as endocytosis, exocytosis, synaptic vesicle trafficking etc. Gag trafficking to the PM is thought to exploit PI(4,5)P2 to get to the PM. In particular PI(4,5)P2-gag preferentially targets lipid rafts on the PM [178]. Lipid rafts preferentially interact and incorporate saturated fatty acids. The myristic acid modification of gag is a highly saturated fatty acid and is therefore incorporated into the raft. As gag is continually transferred to the membrane, gag-gag interactions are formed through the Interaction domains of the gag polyproteins [161].

Pol exists only with the coexpression of gag in a large gag-pol polyprotein. However, gag-pol requires the assistance of the gag polyprotein to shuttle to the PM. Gag and gag-pol polyproteins interact in the cytoplasm through the major homology region in the capsid region. Gag-pol therefore hitchhikes to the PM with the assistance by binding directly to myristoylated gag and targeting to the cell membrane [179]. Interestingly, gag-pol is not the only viral protein which uses gag to assist in membrane trafficking. Vpr directly binds the p6 region of gag to promote its incorporation into the maturing virion [180,181]. In addition, HIV genomic RNA contains 4 stem loop structures (SL1-4) known as a psi-site (ψ) which is recognized by the nucleocapsid of gag polyprotein and allows for packaging of genomic RNA into the virion. SL2 and SL3 are the main binding determinants of ψ and interact with the nucleocapsid through zinc finger binding [182-184]. SL1 is necessary for genomic RNA dimerization whereas SL4 is necessary for stabilization of the tertiary structure of ψ [185,186].

To form the mature structural components, gag and gag-pol precursor polyproteins must be cleaved by the viral protease (PR) located in the pol region of gag-pol. Activation of the protease occurs when dimerization of the PR domains of gag-pol leading to intramolecular cleavages (ie. The PR domains of each gag-pol cleave different processing sites within the gag-pol precursors that make up the dimer) [111, 112]. Through autocatalytic processing, the PR cuts itself out of the polyprotein by cleaving peptide bonds at either ends of its sequence [187,188]. After being released, the PR continues to cut peptide bonds within the gag-pol polyprotein to release the RT, IN, and the structural components of the virus (matrix, capsid, nucleocapsid, p6) [189].

The transmembrane envelope glycoprotein gp160 is the precursor protein of the proteolytically cleaved glycoproteins gp120 and gp41. Gp160 oligomerizes in the endoplasmic reticulum as a trimer (predominantly) and is then transported to the cell membrane via the secretory pathway. During its trafficking through the golgi, it is cleaved by the host protease, furin to produce gp120 and gp41 which form a fusion complex together through non-covalent interactions [116-118]. The mechanism by which gp41/gp120 is incorporated into the maturing virus is not fully understood, however it has been suggested that the cytoplasmic tail of gp41 recognizes the matrix domain of gag and allows for its incorporation into virions [114,115].

Budding and Maturation

The late domain on p6 of gag contains a PTAP motif that is recognized by the cellular factor TSG101 which also binds to another PTAP domain of AIP1 and a number of additional proteins to make up the ESCRT-I complex [190,191]. The AIP1 of the

ESCRT-I complex interacts with CHMP4 proteins which oligomerize at the PM and make up the ESCRT-III complex [191,192]. ESCRT-III proteins interact with an ATPase, VPS4. The N-terminus of VPS4 is responsible for the binding of ESCRT-III complex whereas the C-terminus contains a β -domain which interacts with the protein LIP5 [194]. VPS4 functions as a hexameric ring in which the N-termini are central to the ring and the β -domains are on the perimeter. When two VPS4 hexameric rings are stacked, they attain full enzymatic function and disassemble the ESCRT-III complex which provides energy for membrane fission [193]. However, the precise mechanistic details remain to be elucidated.

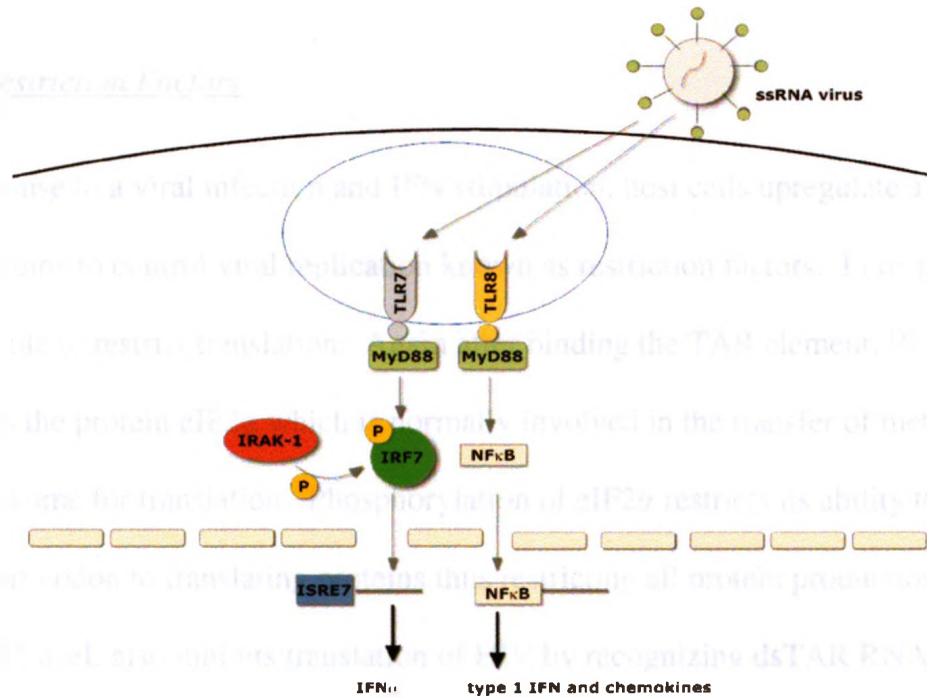
Maturation of the viral particle occurs when gag and gag-pol are cleaved to form their mature structural and enzymatic forms. Cleavage of these polyproteins is performed by the viral protease but it is unclear whether this occurs during the budding process or whether it happens after budding in the immature virion [189].

1.5 Interferon Response

Interferon (IFN) is an indispensable mechanism of defence against viral infection in vertebrates. Mice that lack a subunit of the IFN receptor (IFNR) quickly succumb to viral infections despite having a normal adaptive immune system [119]. Two pathways exist that lead to the upregulation of IFN in response to viral infection: the classical pathway and toll-like receptor (TLR) pathway. The classical pathway is used by fibroblasts, hepatocytes, and conventional dendritic cells which detect viral infection through the use of cytoplasmic receptors that recognize viral components and upregulate the transcription factors IRF3 and NF- κ B to activate IFN- β gene expression [124]. For

example, the dsRNA sensors MDA5 and RIG-I are expressed ubiquitously across most tissues and are upregulated in response to IFN. Subsequently, upon sensing dsRNA, RIG-I and MDA5 amplify the production of IFN [120, 123]. The TLR mediated pathway is mediated by plasmacytoid dendritic cells which are strong producers of IFN α . These are strong sensors of DNA viruses and RNA viruses through the use of TLRs found in endosomes. HIV infection is recognized by cells through the sensation of intracellular ssRNA by TLR 7 and 8 [121, 125]. Activation of these TLRs causes the formation of a complex between their adaptor molecule, MyD88 and TRAF6 and IRF7. IRF7 is phosphorylated by IRAK-1 which leads to its activation and expression of IFN α [122] (Fig. iii a). IFNs are cytokines which modulate cell growth, activate other antiviral cytokines, and promote an antiviral response. IFN α/β are sensed by the IFNR which is comprised of two major subunits, Interferon alpha receptor subunit 1 (IFNAR1) and IFNAR2 [126,127]. Binding of type I IFNs causes the two subunits to associate which leads to the phosphorylation, dissociation, and activation of Tyk2 and JAK1 at the cytoplasmic domain of IFNR. This allows for binding of STAT1 and STAT2 on IFNAR1 on which they are phosphorylated and subsequently translocate into the nucleus where they associate with the DNA binding protein p48 [128, 129]. This heterotrimer is known as ISGF3 which bind ISRE (IFN stimulated response element) of the IFN α/β genes. This leads to the upregulation of over 300 IFN stimulated genes such as antiviral restriction factors (Fig. iii b).

A.



B.

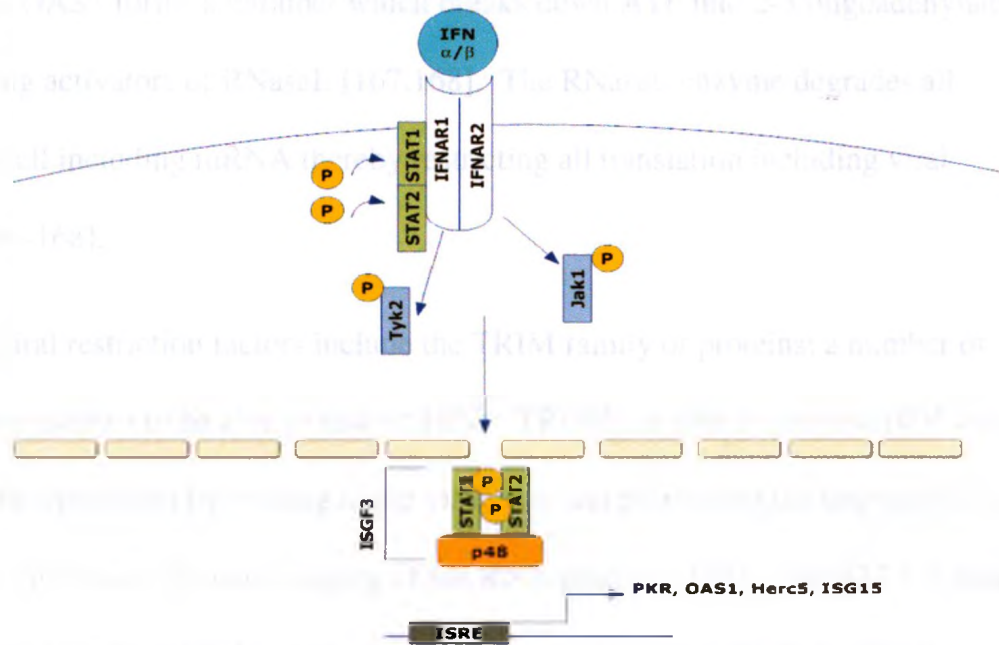


Fig. iii Interferon signalling. A) recognition of ssRNA by TLR7 or 8 causes a signalling cascade that activates transcription factors IRF7 and NF- κ B and lead to the upregulation of type 1 IFN cytokines. B) Interferon α/β are recognized by type 1 interferon receptor composed of INFAR1/INFAR2. This causes the phosphorylation and dissociation of Tyk2 and Jak1 and association of STAT1 and STAT2. These are phosphorylated and translocate to the nucleus where they bind to the DNA binding protein p48. This leads to the upregulation of a number of antiviral restriction factors including Herc5 and ISG15.

1.51 Restriction Factors

In response to a viral infection and IFN stimulation, host cells upregulate a number of proteins to control viral replication known as restriction factors. In response to HIV, PKR is able to restrict translation. Again after binding the TAR element, PKR phosphorylates the protein eIF2 α which is normally involved in the transfer of met-tRNA to the 40S ribosome for translation. Phosphorylation of eIF2 α restricts its ability to transfer the start codon to translating proteins thus restricting all protein production [163-165]. OAS1/RNaseL also inhibits translation of HIV by recognizing dsTAR RNA [167]. Once activated OAS1 forms a tetramer which breaks down ATP into 2-5 oligoadenylates which are strong activators of RNaseL [167,168]. The RNaseL enzyme degrades all ssRNA in the cell including mRNA thereby restricting all translation including viral translation [166-168].

Other viral restriction factors include the TRIM family of proteins; a number of which have been shown to be able to restrict HIV. TRIM5 α is able to prevent HIV viral uncoating in the cytoplasm by binding to the viral core and preventing the degradation of the capsid thus inhibiting the unpackaging of the RNA genome [169]. TRIM22 has been shown to restrict HIV by inhibiting the release of gag polyprotein (which is able to release from cells without any other viral proteins) and preventing the accumulation of gag at the cell membrane though the precise mechanistic details behind TRIM22 restriction of HIV need to be elucidated [170,171].

1.52 Interferon Stimulated Gene 15 (ISG15)

Interferon stimulated gene 15 (ISG15) was the first ubiquitin like modifier discovered and is strongly upregulated in response to type I interferon production and viral infection in vertebrate species [172]. Similarly to ubiquitin, ISG15 is a posttranslational modifier of proteins that requires an E3 ligase, an E1 enzyme, Ube1L and an E2 enzyme, Ubch8. The E1 enzyme, Ube1L recognizes ISG15 and passes it to the E2 enzyme through a transthiolation reaction. When ISG15 is bound to the E2, Ubch8, they bind to the E3 ligase which also binds the protein substrate and facilitates ISG15 conjugation to the substrate [175-177]. ISG15 contains two ubiquitin-like domains at the N-terminus and C-terminus which are connected by a central hinge region made up of 5 beta sheets and 1 alpha helix (Fig. iv). The C-terminus is predicted to be the main point of interaction with its E1 enzyme Ube1L, specifically through the residues K90 (lysine), W123 (tryptophan), and F149 (phenylalanine) [54]. The C-terminus also is required for the transfer of ISG15 from Ube1L to the E2 enzyme, Ubch8, which is mediated by transthiolation reactions. The N-terminus however is predicted to be responsible for the E3 mediated transfer from the E2 enzyme, Ubch8, to the target substrates [55]. There are currently two well known E3s for ISG15 conjugation, the main ISG15 conjugator being the HECT domain and RCC-1 like domain containing protein 5 (Herc5) and Estrogen-responsive finger protein (EFP) [195,196]. As a response to IFN stimulation and defence against viral protein expression, Herc5 has been shown to associate with the 60S subunit of polyribosomes (groups of ribosomes bound to mRNA) and broadly ISGylates newly synthesized proteins in an attempt to inhibit virus assembly. Although ISGylation of a broad range of newly synthesized proteins is relatively inefficient, it is believed that this is beneficial to the host cell to minimize excessive



Fig. iv The crystal structure of ISG15. Two ubiquitin –like domains are joined at a central hinge region. C-terminus is necessary for binding the E1 enzyme, Ube1L and the transfer to E2 enzyme, UbcH8. The N-terminus is required for E2 transfer to the E3 ligase and target substrate [54].

damage to host proteins. In addition, structural proteins of viruses often require very precise geometric configurations to form infectious particles; ISGylation of even a small portion of these viral proteins may lead to the restriction of virus production [62].

ISG15 is able to act as a restriction factor against HIV budding by interfering with the interaction of TSG101 with the p6 domain of gag although neither protein is directly modified with ISG15 [173]. ISG15 is also able to interfere with Vps4 recruitment to the ESCRT-III complex. Although this mechanism is not fully elucidated, it is believed that ISG15 binds to components of ESCRT-III and prevents Vps4 recognition of the complex. The result of such restriction leads to the formation of “lollipop” structures on the surface of infected cells where virus is unable to be pinched off and released from the cell [174].

It is unclear what the physiological significance of ISG15 conjugation is. However, experiments determining ISGylatable proteins have been performed to help elucidate its relevance. The proteins JAK1 and STAT1 were among the first proteins to be discovered which can be ISGylated. Both JAK1 and STAT1 are key components of the interferon activating pathway. It is possible that ISGylation of these proteins in the interferon signal transduction pathway is a method of regulating the expression of interferon either positively or negatively [56,57]. Since ISG15 is upregulated within the first 24 hours in response to cellular stressors and pathogens, it is believed that ISG15 is involved predominately in innate immune responses. However, it has also been shown to be involved in a diverse range of cellular processes such as protein trafficking and cytoskeleton organization [58].

Studies show that ISG15 can also target and conjugate to the Influenza A NS1 protein after type I interferon treatment. The NS1 protein of Influenza A is able to interfere with host mRNA processing and is also able to shut off a number of cellular defences against virus infection such as OAS1 ISGylation of the NS1 protein has shown a robust ability to inhibit virus replication. Krug and colleagues found that K41 is the predominant residue for ISG15 conjugation of NS1. This region of NS1 is responsible for binding dsRNA in order to block the activation of a number of different antiviral proteins which are activated by the recognition of dsRNA, a pathogen associated molecular pattern. It is thought that ISG15 conjugation in this region of NS1 would block NS1 from binding to dsRNA and allow for greater antiviral activity within the cell [63].

Hepatitis C Virus (HCV) replication is also strongly diminished with interferon induction and ISG15 overexpression. The NS5A protein of HCV is ISGylated at K379 of the C-terminal region which subsequently leads to protein instability. The mechanism of restriction is again unclear. Experiments with NS5A conjugated with ISG15 show that the NS5A protein is not being degraded by the 26S proteasome. However, it was shown that NS5A was both ubiquitinated and ISGylated and that these two in parallel were involved in altering the proteins' stability [64].

Interestingly, ISG15 also exists as a soluble protein which can be excreted into extracellular space as an immunomodulatory cytokine upon stimulation of type I interferons. Secretion of ISG15 as a cytokine was shown to enhance NK cell and lymphocyte proliferation and killing. ISG15 is secreted by non-hematopoietic cells and predominantly secreted by peripheral blood mononuclear cells (PBMCs). ISG15 may be

acting as a signal of cell stress or cell damage. It is possible that ISG15 found in extracellular fluid may be the product of cell death and is behaving as a danger associated molecular pattern rather than a secretory product [61].

The over expression of the ISG15 E1 protein, Ube1L, has been shown to help control the development of lung cancer by inhibiting the growth of bronchial epithelial cells and lung cancer cells. This may be due to Ube1L promoting ISGylation of cyclin D1 and causing its destabilization and abrogates cell cycle [59].

However ISG15 has also been reported to be an oncogenic factor. Many different tumors and tumor cell lines have displayed ISG15 dysregulation and elevated levels of ISG15. This may be due to constitutively activated NF- κ B found in many tumor cells which in turn continuously produces interferon and subsequently ISG15. In tumor cells where ISG15 is constantly elevated, polyubiquitination and degradation is strongly diminished however the mechanism by which ISG15 impairs ubiquitin conjugation remains to be elucidated. It is possible that ISG15 competes for the same lysine residues as ubiquitin on many different target substrates or that certain E1, E2s, and/or E3s that are common between ISG15 and ubiquitin are being sequestered or degraded by ISG15 [60].

Oddly, many of ISG15's antiviral activities have been not been examined in the presence of its main conjugator, Herc5. Thus studying the effect of Herc5 in the context of a variety of viral infections is very important for determining whether Herc5 is also able to act as a potent viral restriction factor.

1.6 HECT domain and RCC1-like domain containing protein (Herc) Family

The Herc family of proteins are made up of 6 members that possess a ubiquitin HECT domain (described in section 1.2) as well as an RLD [197,198] (Fig. v). The RLD structurally resembles the protein RCC1. Both the RCC1 and the RLD of Herc proteins have a 7 bladed β -propeller configuration where each blade is made up of 4 β -sheets (Fig. vi) [199,200]. The RCC1 protein interacts with Ran in the nucleus to catalyze the conversion of Ran-GDP to Ran-GTP as a guanine nucleotide exchange factor (GEF). The GTPase function of RCC1 is necessary for the generation of a GTP energy gradient in the nucleus for the export of mRNA to the cytoplasm (the same pathway that is hijacked by rev) [201-203]. The activity of RCC1 has also been implicated in nuclear envelope assembly, mitotic spindle formation, and cell cycle regulation [204]. RCC1 activation depends on its binding to nuclear chromatin particularly at histones 2A and 2B. Thus, RCC1 is able to interact with Ran on one face of the β -propeller while it tethers to nuclear chromatin on the other [200]. Of the RLD containing Herc proteins, Herc1 has displayed GEF activity in its RLD1 whereas the RLD domain of Herc3 displays none. It remains to be determined whether the other members of the Herc family maintain an RCC1-like GEF function [205].

The Herc family is separated into two subgroups based on their size and domain architecture. Herc 1 and Herc2 belong to the large Herc family where each is roughly 530kDa. Interestingly, these two Herc proteins also contain multiple RLDs, Herc1 with two RLDs and Herc2 with three [206]. Although not much is known about these proteins, it is thought that Herc1 may have oncogenic properties as it is over expressed in a number of tumor cell lines. It is also possible that Herc1 is involved in membrane trafficking to

the golgi [205]. Hercs 3-6 belong to the small Herc family whose sizes are approximately 120kDa [206]. Phylogenetic studies on the Herc family suggest that Herc4 may be the most ancient of the proteins from which all other Hercs derived as it is found in the nematode genome [198]. From such studies, Herc5 seems to be the newest addition to the Herc family [198].

1.61 Herc5

Herc5 is a type 1 interferon induced protein comprised of three major domains, the RLD, a spacer region, and an E3 ligase HECT domain. Currently, the HECT domain is the most well characterized region of Herc5 as it has been identified as the catalytic domain for ISG15 conjugation. Herc5 functions in conjunction with the E1 enzyme Ube1L and the E2 enzyme UbcH8 to conjugate ISG15 to target substrates [207]. These proteins are upregulated by type 1 interferons (Herc5 is upregulated 5 fold) which suggests the pathway may play an important role in innate immunity [208]. This activity has been described largely in terms of antimicrobial activity even though the physiological relevance of ISG15 conjugation has yet to be determined in this context. A cysteine residue at position 994 in the HECT domain is crucial to Herc5's ability to conjugate ISG15 to targets [208]. It has been shown that ISG15 conjugation at the RNA binding domain Influenza A Virus NS1 by Herc5 is able to attenuate virus propagation and virulence by inhibiting the interaction with Importin α and blocking nuclear import of the NS1 protein [209,210, 216]. Although Herc5 has not been directly identified in a number of antiviral activities, ISGylation has been shown to restrict Sindbis virus, Herpes simplex 1, HIV-1, and Ebola. In addition, Herc5 ISGylation has been shown to enhance the production of type 1 interferons by ISGylating interferon regulatory factor 3 (IRF3)

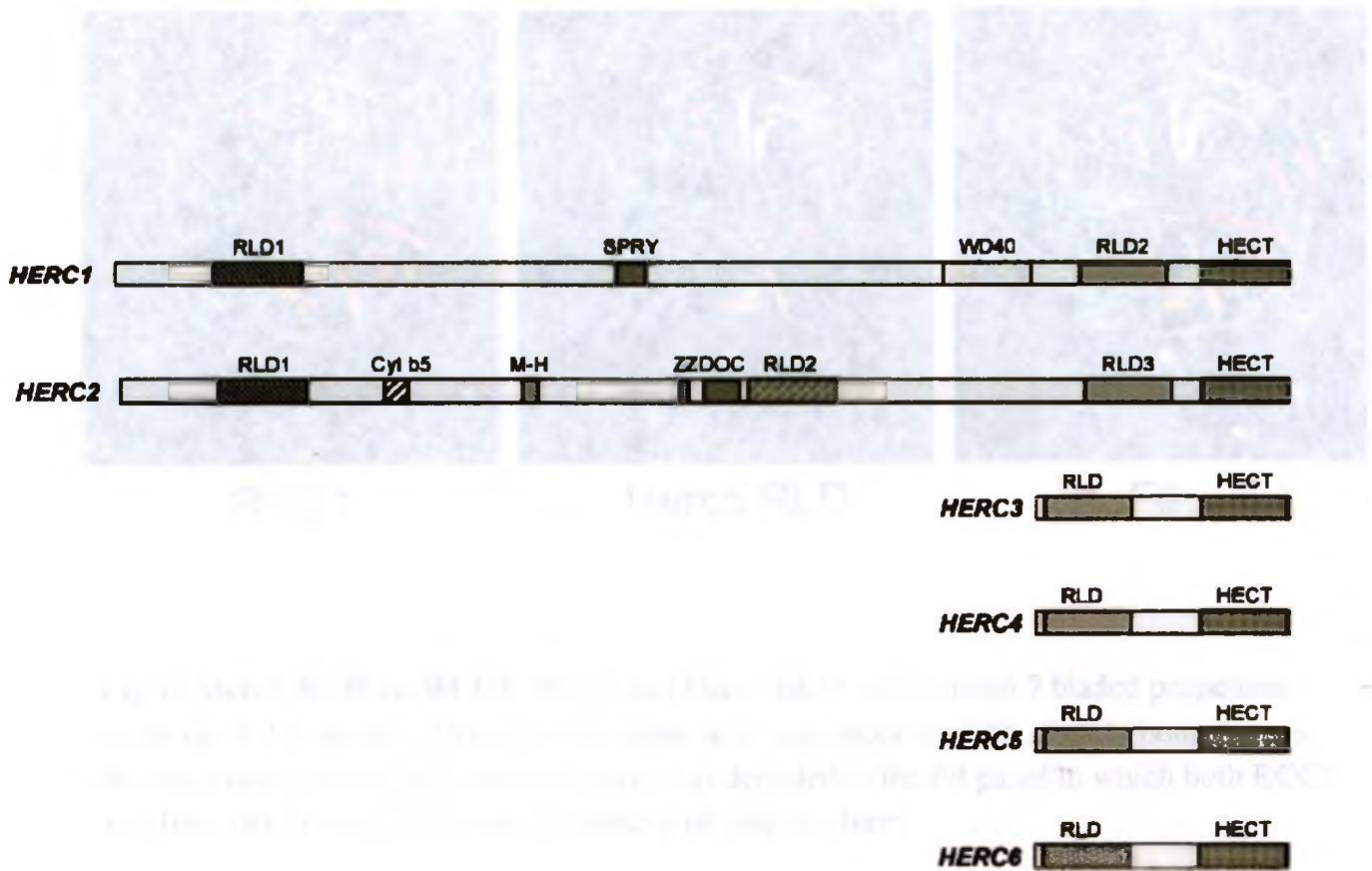


Fig. v Herc family of proteins is divided into two groups, the large and small Hercs. Both Herc1 and Herc2 belong to the large family of Herc proteins roughly 530kDa and contain multiple RLD domains. Herc3-6 all belong to the small Herc family and are roughly 120kDa [222].



Fig vi. Herc5 RLD vs. RCC1- RCC1 and Herc5 RLD both contain 7 bladed propellers made up of 4 β -sheets. Although the amino acid sequences are only slightly homologous, the structural homology is almost identical as depicted in the Fit panel in which both RCC1 and Herc5RLD are overlapped. (Courtesy of Stephen Barr)

and sustaining its function [177]. This suggests Herc5 may have broader antiviral activities than it is accredited for and thus act as a potent and versatile viral restriction factor.

The spacer domain of Herc5 shows no homology to any known protein. However, through predictive modelling, it is likely to be abundant in alpha helices similarly to coiled coil domains. Coiled coil domains are important to many intermolecular interactions including the formation of protein oligomers [212]. For example, gp41 of HIV requires coiled coil interactions to adhere to the cell membrane [213]. The ISGylating E3 ligase EFP contains a coiled coil domain which has been shown to be important for autoISGylation and the interaction with its substrates [214]. It is possible that the spacer region of Herc5 acts in a similar manner as EFP and acts as a binding domain for Herc5 substrates or as a location for autoISGylation however further characterisation of the protein is required to determine the functional role of this domain.

The RLD of Herc5 shares roughly 35% sequence homology with RCC1 however predictive modelling of the Herc5 RLD shows almost complete structural identity with RCC1 (Fig. vi). This raises the question whether the RLD of Herc5 has similar functional behaviour as RCC1 as a GEF. Like RCC1, Herc5 has been implicated in the regulation of cell cycle. Herc5 was shown to interact with the cyclin E-Cdk2 kinase which is indispensable for the transition of G1 to S phase. Herc5 is also highly expressed when the tumor suppressor proteins Rb and p53 are inhibited [215]. It is possible that Cyclin E-Cdk2 is recognized by the RLD and ISGylated by the HECT domain which stabilizes or degrades the complex to regulate cell cycle progression.

As mentioned under the HECT E3 ligase section (appendix), the N-termini of E3 ligases predominately function as the binding domains for target substrates [10-12]. Therefore, it is possible the RLD may also act as the binding domain for Herc5 substrates. Mutational studies in which the RLD of Herc5 has been removed, ISGylation was shown to be drastically reduced but not completely abolished [208]. In addition, Herc5 binding to NS1A protein is eliminated when the RLD is removed [216].

ISG15 has been implicated in many antiviral activities, including the restriction of HIV-1 at the late stages of virus release. However, many of its antiviral properties have not been investigated in the context of its main E3 conjugating ligase, Herc5. Thus far, Herc5 has only been directly implicated in antiviral activity through the restriction of both Influenza A and B and is also upregulated during the course of Hepatitis C infection [209,210,216,219]. However, it is also upregulated 4 fold in the presence of type 1 interferons and positively regulates their expression by modifying interferon regulatory factor 3 (IRF3) with ISG15 [211]. Herc5 also broadly ISGylates newly synthesized proteins upon type 1 interferon signalling [62]. The potency of ISG15 as a viral restriction factor and the implications of Herc5 in a variety of antiviral activities strongly suggest that Herc5 may in fact have greater potential for restricting viral replication than what is currently understood. Further investigation into the antiviral properties of Herc5 as a restriction factor must be conducted to better understand the physiological relevance of Herc5 during viral infection in hopes of extrapolating its activity for novel antiviral therapies.

1.7 Preliminary data

Our lab has shown that Herc5 mediated ISGylation of the HIV-1 gag structural protein is sufficient to restrict the release of virus-like particles (gag polyprotein release) from U2OS cells. The C994A Herc5 mutant that lacks E3 ligase activity is unable to restrict gag release. Herc5 transfected cells co-transfected with Ubp43, a deISGylating enzyme, are also unable to restrict gag release. This suggests that ISGylating activity of Herc5's HECT E3 ligase domain is responsible for inhibiting gag budding from cells (Fig. vii).

When cells are infected with replication competent HIV in the presence of Herc5, there is restriction of HIV-1 release from the cell as well as restriction of gag protein production in the cell. When C994A Herc5 is transfected into HIV infected cells, there is still restriction of gag production in the cell and virus release (Fig. viii). This indicates that the E3 ligase activity of Herc5 is not absolutely necessary for virus restriction and that there are two mechanisms by which Herc5 can restrict viral replication – although it is unclear what the second mechanism is. Therefore, characterizations of the RLD and spacer regions are required to understand the second mechanism of HIV restriction.

Quantification of intracellular gag mRNA in cells infected with HIV-1 indicates that in the presence of Herc5 there is a build up of gag mRNA that is not being translated into protein in comparison to the negative control (3.5x more gag mRNA) (Fig. ix). It is possible that mRNA is not being translated because there is a defect in mRNA shuttling to the cytoplasm.

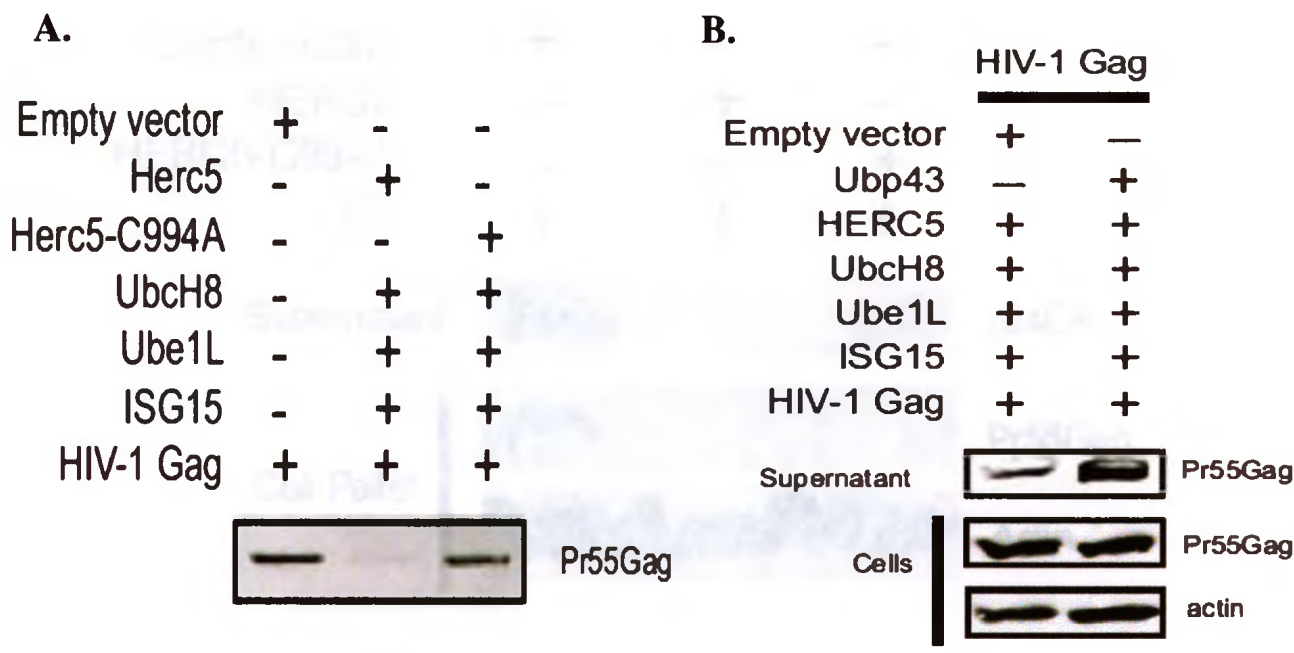


Fig. vii HERC5 ISGylation leads to gag polyprotein restriction in U2OS cells. A) gag transfected into U2OS cells in the presence of Herc5, C994A, or negative control. Gag virus like particle release was measured by western blot detection of gag polyprotein using gag antibody. B) Western blot of gag release in Herc5 transfected cells and ISG15 conjugation system in the presence or absence of de-ubiquitinating protein Ubp43. (Courtesy of Matt Woods; Woods, M., et al., 2011. Unpublished)

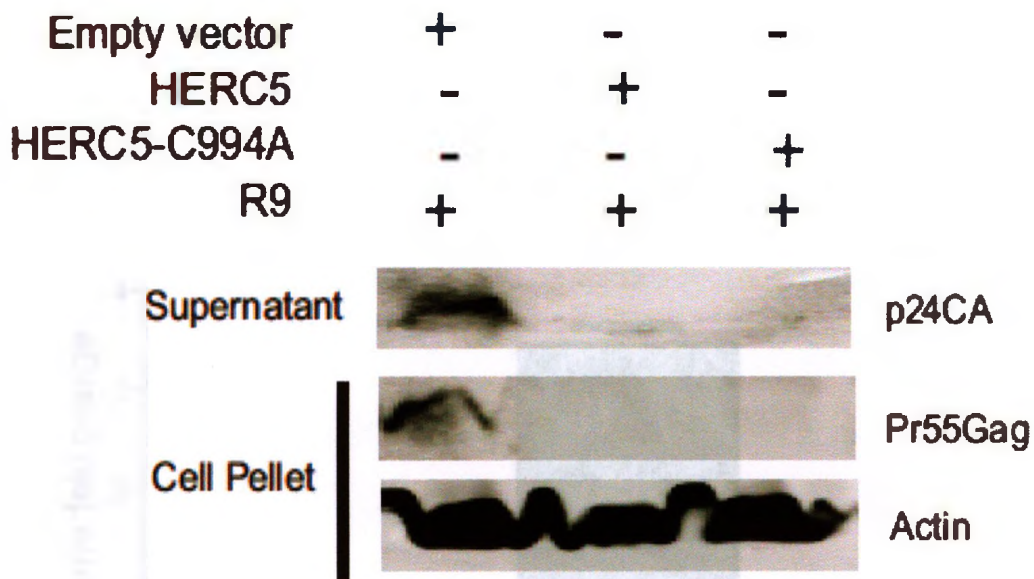


Fig. viii Herc5 restriction of HIV-1. pGL3, WT Herc5, or C994A, was co-transfected with replication competent HIV-1 (R9) in U2OS cells. Herc5 and C994A are able to restrict the release of virus into cell supernatant. Herc5 and C994A are also shown to restrict gag polyprotein production in the cell pellet in the presence of R9. (Courtesy of Matt Woods; Woods, M., et al., 2011. Unpublished)

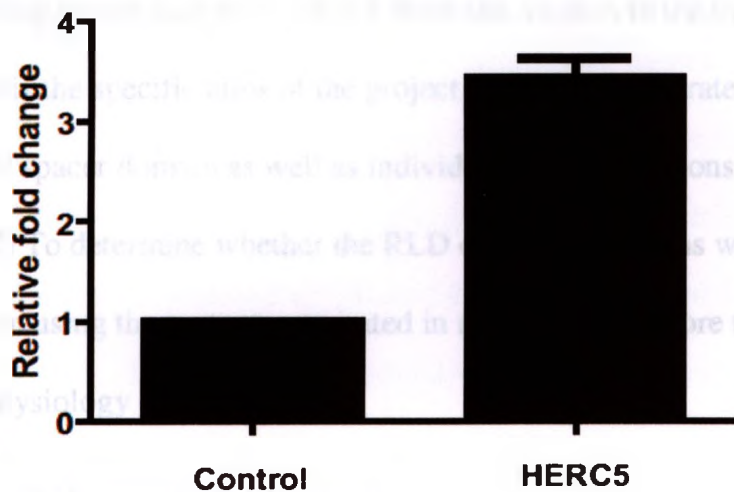


Fig. ix qRTPCR of gag mRNA in HIV-1 infected cells. qRTPCR of gag mRNA in HIV-1 infected U2OS cells co-transfected with Herc5 or pGL3. 3.5x fold increase in gag mRNA in the presence of Herc5. (n=3) (Courtesy of Matt Woods; Woods, M., et al., 2011. Unpublished)

1.8 Hypothesis and Aims

I hypothesized that the spacer and/or RLD domains of Herc5 were necessary for Herc5 mediated HIV-1 restriction since elimination of HECT domain activity did not abolish Herc5 restriction of HIV-1. I also hypothesized that the Spacer or RLD is interrupting proper export of mRNA from the nucleus to the cytoplasm. To approach my hypothesis the specific aims of the project were: **1)** to generate domain deletions of the RLD and spacer domain as well as individual bladed deletions of the RLD region of Herc5, **2)** To determine whether the RLD or spacer domains were required for HIV-1 restriction using the mutants generated in aim 1, **3)** to explore the effects of these deletion on the physiology of the host cell.

Chapter 2: Materials and Methods

2.1 Plasmid Constructs

RLD mutants via digestion, ligation, transformation- the wild type Herc5 construct in CS2+ plasmid backbone was generously supplied by K. Chin at Genome Institute of Singapore. This construct was used to subclone all mutants of Herc5 into the pFLAG plasmid backbone. Various mutations of the Herc5 RLD were generated using primers recognizing the sequences encoding each blade of the RLD creating increasingly larger truncations of the domain. All forward primers included the BglII restriction site and all reverse primers included XbaI restriction sites. Primers and template were used in PCR reactions to amplify the truncated forms of Herc5 lacking blades of the RLD (Fig. x). Primer sequences used for the generation of pFLAG RLD mutants can be found in Supplementary Table 1. PCR conditions used to amplify the RLD truncations to be

incorporated in pFLAG are found in Supplementary Table 2. PCR products were then purified using spin column PCR purification (Invitrogen and BioBasic) and used in single enzyme digests with both BglII and XbaI using buffers³ and buffer 2 respectively (New England Biolabs). Digests were done for 2 hours at 37°C and purified after each digest. After digestion of pFLAG vector with BglII and XbaI, digested DNA and vector were ligated using T4 ligase (New England Biolabs) for 20 minutes at room temperature. The product was then transformed into DH5 α competent cells and grown on LB agar plates containing ampicillin overnight (16 hours) at 37°C. Bacterial colonies grown were screened for insert by extracting plasmid DNA with Purelink Quick Plasmid Miniprep Kit (Invitrogen). Products were digested with a single enzyme (XbaI or BglII), and run on an ethidium bromide 1% agarose gel with a 1Kb ladder. Lanes with an appropriately sized DNA product (insert + product= ~7.5Kb – 8 Kb) were sent for DNA sequencing for additional sequence verification at Robarts Research Institute.

RLD mutants and spacer mutant created with modified site directed mutagenesis and transformation- RLD deletion constructs and the spacer deletion mutant were made using modified site directed mutagenesis and designed to be expressed in the CS2+ plasmid vector. WT Herc5 in pCS2+ vector was generously provided by K. Chin at the Genome Institute of Singapore, from which all RLD and spacer deletions were subcloned. Primers were designed to recognize sequences directly before and after the region to be deleted (Table i). pCS2+ plasmid map is included in Supplementary Figure 2. The QuikChange® Lightning Site-Directed Mutagenesis Kit and its corresponding protocol were used for the PCR amplification of the RLD and spacer mutants of Herc5 (Table ii). After amplification, PCR products were digested with DpnI enzyme (40 units per reaction)

at 37°C for 5 minutes to digest methylated, supercoiled parental dsDNA and isolate desired Herc5 mutants. Digested products were then transformed into XL-10 Gold ultracompetent cells. 45ul of ultracompetent cells were added to 14ml round-bottom tubes and supplemented with 2ul of β -mercaptoethanol mix (provided with cells). This was incubated on ice for 2 minutes after which 3ul of DpnI (60 units) digested PCR amplified Herc5 mutated DNA was added to the cells. This mixture was incubated on ice for 30 minutes and then heat pulsed at 42°C for 30 seconds. The reaction was then placed back on ice for 2 minutes. 0.5ml of preheated (42°C) SOC media (0.5% Yeast Extract, 2% Tryptone, 10mM NaCl, 2.5mM KCl, 10mM MgCl₂, 10mM MgSO₄, 20mM Glucose) was then added to each tube and incubated at 37°C for 1 hour while shaking at 225rpm. 300ul of each reaction was plated on ampicillin agar plates and left at 37°C overnight (>16 hours). Colonies obtained from incubated plates were then screened for desired inserts (mutated Herc5 constructs). Colonies were picked and grown in 1.5ml of LB broth supplemented with 100uM of ampicillin overnight (>16 hours). Resulting bacterial suspensions were pelleted and miniprepmed using BioBasic™ EZ-10 spin-column plasmid DNA minipreps kit to extract transformed plasmid. The resulting product was then quantified using Implen nanophotometer to determine DNA concentration. 300ng of product was loaded on a 1% Ethidium Bromide (EtBr) agarose gel and run at 120 volts for 45 minutes alongside a 1Kb DNA ladder. Products corresponding to the approximate size of product and insert were sent to Robarts Research Institute where they were sequenced verified. Confirmed mutants were then maxiprepmed with Qiagen® plasmid maxi kit and ready for transfection.

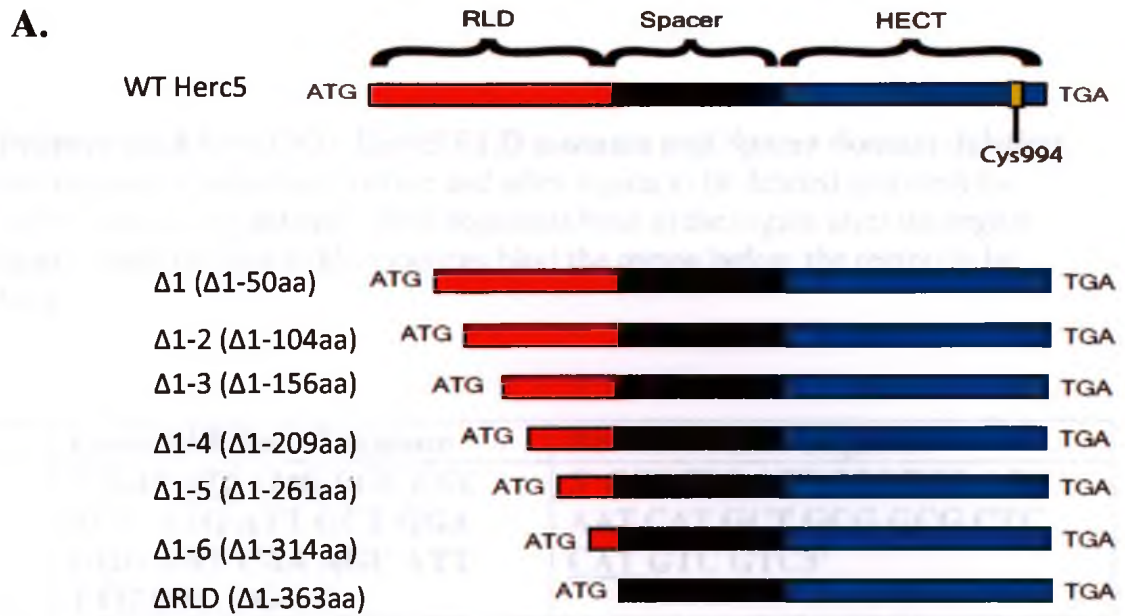


Fig. x RLD mutant design. A) Mutations of the RLD were designed to delete sequentially greater portions of the domain. 7 mutants of the RLD were originally intended, each deleting one blade more of the RLD than the last. B) Primers recognizing the start of the different RLD blades were designed and used for PCR amplification of the different Herc5 RLD gene products. PCR products were run on a 1% agarose gel and visualized using ethidium bromide staining. Δ1, Δ1-3, ΔRLD were successfully cloned into pFLAG; Δ1-2, Δ1-4, Δ1-5, Δ1-6 DNA inserts were unable to be cloned into pFLAG. Primer sequences can be found in Supplementary Table 1.

Table i. Primers used for pCS2+ Herc5 RLD mutants and Spacer domain deletion. Primers are made up of sequences before and after region to be deleted and omit the sequence of the area being deleted. Bold segments bind to the region after the region deleted (head), while the non bold sequences bind the region before the region to be deleted (tail).

Deletion	Forward Primer Sequence	Reverse Primer Sequence
Δ RLD	5' GAC <u>ATG GAG CGC CGC</u> AGC ATG ATT GCT GGA GGG AAT CAA AGC ATT TTG CTC TGG 3'	5' GCT TTG ATT CCC TCC AGC AAT CAT GCT GCG GCG CTC <u>CAT GTC GTC</u> 3'
Δ 1-2RLD	5' GAC <u>ATG GAG CGC CGC</u> AGC CAG GGA GCC GAA CAC ATG CTG 3'	5' GTG TTC GGC TCC CTG GCT GCG GCG CTC <u>CAT GTC</u> GT 3'
Δ 1-5 RLD	5' GAC <u>ATG GAG CGC CGC</u> AGC GAT GGG CTG CTG TTT ACT TTC GGT GC 3'	5' AGT AAA CAG CAG CCC ATC GCT GCG GCG CTC <u>CAT GTC</u> GTC 3'
Δ spacer	5' ATG ATT GCT GGA GGG AGG CCC ACG TTT GAT CTA ACA GTC AGA AGG 3'	5' GAC TGT TAG ATC CCC TCC AGC AAT CAT TAT TAA CTC CTT TTC TGA GG 3'

Table ii. PCR conditions for pCS2+ Herc mutants. A) Conditions for amplification of pCS2+ Herc5 RLD mutants and Spacer deletion mutants B) Thermocycling conditions required for amplification of RLD and Spacer mutants

A.

5ul	10x Reaction buffer
120ng	dsDNA template (pCS2+ Herc5)
1ul	QuikChange® Lightning enzyme
125ng	Forward primer
125ng	Reverse primer
1ul	dNTP mix
1.5ul	QuikSolution reagent
2.5ul (5%)	DMSO
Xul	ddH2O
50ul	Total volume

B.

	Temperature	Time	# of cycles
Initial Denature	95°C	2 minutes	1x
Denature	95°C	20 seconds	18x
Annealing	60°C	10 seconds	18x
Extension	68°C	4 minutes	18x
Final Extension	68°C	5 minutes	1x

2.2 Cell culture, plasmids, and transfection

U2OS, HeLa, 293T and HOS cells were cultured at 37°C and 5% CO₂ in Dulbecco's modified Eagle's medium (DMEM) supplemented with 10% fetal bovine serum (FBS) and 100 IU penicillin/ 100ug/ml streptomycin. Cells for all experiments were seeded in either 6-well dishes containing 2ml of DMEM or in 12-well dishes (BD Biosciences) containing 1ml of DMEM. Herc5 constructs were described previously.

2.21 Transfections

Lipofectamine transfection

Lipofectamine 2000 (Invitrogen) was used for single or dual plasmid transfection of plasmids. A total of 2ug of DNA and 4ul of lipofectamine were transfected into 12-well dishes of HeLa cells at 90% confluency and a total of 4ug of DNA and 10ul of lipofectamine were transfected into each 6-well 10cm² well (BD Biosciences). Protocol included in the kit was followed without modifications. Lipofectamine was used for all confocal microscopy experiments and HIV release assay.

FuGene transfection

FuGene[®] HD (Roche) was used for single plasmid transfection of HeLa cells at 70% confluency. 2ug of DNA and 4ul of FuGene were used for each 6-well, 10cm² well. Protocol included in the kit was followed without modifications. FuGene was used for RTPCR transfection experiments for mRNA expression of Herc5 construct and propidium iodide staining for cell cycle analysis

SuperFect Transfection

SuperFect (Qiagen) was used for single plasmid transfection of HeLa cells at 90% confluency. 2ug of DNA and 10ul of SuperFect transfection reagent were used for each 6-well, 10cm² well. Protocol included with the kit was followed without modifications. SuperFect was used for growth comparison experiment between the different Herc5 construct transfected cells.

2.3 mRNA expression of protein constructs

6-well plates of U2OS were transfected with FuGene® at 70% confluency. Cells were harvested after 24 hours and RNA extraction was performed using PureLink™ RNA Mini Kit (Invitrogen). RNA was then reverse transcribed using M-MLV Reverse Transcriptase (Invitrogen). The protocol supplied with reverse transcriptase was not altered. cDNA was then used to amplify various Herc5 mutants using PCR. 10ul of products were then run on a 1% agarose gel next to a 1Kb DNA ladder (New England Biolabs) (Table iii).

2.4 HIV-1 release Assay (performed by Matthew Woods)

6-well plates of U2OS cells were co-transfected with replication competent HIV-1 (R9 plasmid) and one Herc5 construct using lipofectamine at 70% confluency. 1ml of cell supernatant was collected 48 hours later and stacked on top of 300ul of 20% sucrose. Supernatant was spun at 14000g for 2 hours to collect extracellular virus. Cell pellets were also collected after 48 hours. Once the supernatant was collected, both cell pellet and supernatants were lysed (separately) using RIPA lysis buffer and run on a 10% SDS page gel. Detection of capsid protein and gag polyprotein were done using anti-p24 antibody. Mouse IRDye 680 secondary antibody (LiCOR) was used to illuminate

primary antibody bound to p24 protein and rabbit IRDye 800 antibody (LiCOR) for actin control.

2.5 Growth analysis of Herc5 construct transfected cells

6-well plates of HeLa cells were transfected at 90% confluency using SuperFect transfection reagent (Qiagen) with one of the Herc5 constructs according to the specifications outlined in the included protocol. Three hours after transfection, cells were harvested and 250000 cells were seeded into each well of ten 12-well dishes (two dishes were needed to count each day for growth comparison between constructs for a total of 4 days). For each Herc5 construct, 3 wells were seeded (done in triplicate) for each day the experiment was to be carried out (a total of 12 wells were seeded for each construct). Each day, 3 wells were counted using a hemocytometer for each construct and growth was monitored over 4 days. Growth rates of cells transfected with the different Herc5 constructs were compared to the negative control transfected (pGL3) cells and statistically analyzed using two-way ANOVA.

Table iii. PCR conditions for RTPCR of Herc5 CS2+ mutants. A) Conditions used for PCR reaction performed for RTPCR of Herc5 construct mRNA. B) Thermocycling conditions needed for amplification of Herc5 construct cDNA

A.

5ul	10x Pfu buffer
6ul	MgSO ₄
1ul	10mM dNTPs
1ul	Forward primer (fwd spacer primer)
1ul	Reverse primer (herc5 reverse coding region primer RLD rev)
2.5ul	DMSO
1ul	Pfu enzyme
7ul	cDNA template
25.5ul	Water
50ul	Total

B.

	Temperature	Time	# of cycles
Initial Denature	95°C	3 minutes	1x
Denature	95°C	30 seconds	32x
Annealing	50.5°C	30 seconds	32x
Extension	72°C	4 minutes	32x
Final Extension	72°C	10 minutes	1x

2.6 Confocal Microscopy

Hela cells were seeded in 6-well dishes and transfected using lipofectamine 2000 at 90% confluency. After 24 hours, cells were harvested with PBS EDTA and 3.5×10^5 cells were transferred into 12-well dishes with 18mm coverslips and fresh media. 24 hours after, cells were washed with 1xPBS /1%FBS twice and fixed with a fixing buffer for 10 minutes (19ml 1xPBS, 1ml Formaldehyde, 0.4g Sucrose). Cells were washed twice again with 1xPBS/1%FBS and then permeabilized with a permeabilization buffer for 10minutes (19ml 1xPBS, 1ml 10% NP40, 2g Sucrose). Cells were washed twice with 1xPBS/1%FBS then stained with primary antibody for rev or FLAG (Herc5) (1:1000) for 1 hour. Cells were washed using the 1xPBS/1%FBS 6 times over 15 minutes and stained with a secondary antibody for 1 hour (1:1000). Cells were washed again 6 times over 15 minutes and then mounted on to slides using VECTASHIELD[®] hard set[™] mounting medium with DAPI. Slides were then examined using a Zeiss LSM 510 META confocal microscope mounted on an inverted Axiovert 200 motorized microscope. For statistical analysis, 100 cells were counted for each different condition and were categorized according to their nuclear morphology (either lobed or not lobed) or the Rev localization (nucleolar, nuclear, nuclear boarder, cytoplasmic).

2.7 Propidium Iodide Staining for Cell Cycle analysis

U2OS and 293T cells were transfected using FuGene[®] at 70% confluency. 24hours after transfection, cell cycle control cells were treated with hydroxyurea (1mM) dissolved in water. 24 hours after drug treatment, cells were harvested with PBS/EDTA and washed twice with PBS. Cells were resuspended in 0.5ml of PBS (single cell suspension) and added to 4.5mls of ice cold 70% ethanol and kept on ice for 2 hours to

allow for fixation. Cells were collected by centrifugation at 300xg for 5 minutes and ethanol was decanted. Cells were then washed and resuspended in PBS then collected by centrifugation at 200xg for 5 minutes. PBS was decanted and cells were suspended in 0.5ml of propidium iodide staining solution (10ml 0.1% Triton X-100, 0.5mg DNase free RNaseA, 200ul of 1mg/ml Propidium Iodide) and incubated at 37°C for 15 minutes. Cells were then counted and analyzed using flow cytometry and interpreted using ModFit LT™.

2.8 Statistics

Statistical analysis was performed for experiment 2.5 - Growth analysis of Herc5 transfected cells. Data was analyzed using a two-way ANOVA in the GraphPad Prism 5 program. p values less than 0.05 were considered significant.

Chapter 3: Results

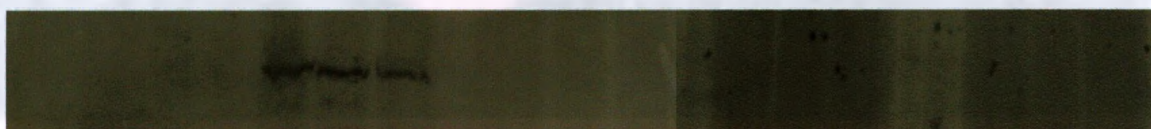
3.1 Generation of Herc5 mutants and RNA expression

Since the E3 ligase function (HECT domain) of Herc5 was shown to be unnecessary for Herc5 to restrict HIV-1 release, the characterization of both the spacer and RLD was necessary to understand the mechanism by which Herc5 was acting as a viral restriction factor. To understand the physiological relevance of the Herc5 spacer and RLD domains, the generation of domain deletions of both the RLD and Spacer regions was essential. Experiments performed with these mutant constructs of Herc5 would allow us to observe the relevance of each domain to Herc5's function. To determine the importance of the RLD for Herc5 restriction of virus, truncations of the RLD were generated using PCR amplification. Forward primers recognizing each blade of the RLD created increasingly

larger truncations of the domain when paired with a reverse primer recognizing the end of the coding region of Herc5 (Fig. x, Supplementary Table 1). A total of 7 deletions were made in this domain and were amplified using PCR (Supplementary Table 2). These deletions were subcloned into the pFLAG vector. Only $\Delta 1$, $\Delta 1-3$, and $\Delta 1-7$ RLD (Δ RLD) were successfully cloned into pFLAG based on sequencing analysis. Western blot of U2OS cells transfected with the pFLAG RLD mutants was performed to test protein expression of the mutant constructs. Wild type CS2⁺ Herc5 was used as a positive control and gave a product of 117kDa. A protein product of roughly 105kDa, 95kDa, and 80kDa was to be expected for successful detection/expression of 1, $\Delta 1-3$, and $\Delta 1-7$ RLD (Δ RLD) respectively. However, none of these mutant constructs were detectable (Fig. 1). MG132 (Sigma) and amantadine-hydrochloride (Sigma) were used to inhibit the proteasome and lysosome respectively to determine if the protein products were being degraded by either of these enzymes. However, no enhancement in expression of the RLD constructs was observed. The $\Delta 1-2$, $\Delta 1-4$, $\Delta 1-5$, $\Delta 1-6$ RLD pFLAG clones were also unable to be obtained. Since $\Delta 1$, $\Delta 1-3$, and Δ RLD pFLAG mutants were unable to express protein and $\Delta 1-2$, $\Delta 1-4$, $\Delta 1-5$, $\Delta 1-6$ RLD mutants were not easily cloned into the pFLAG backbone, RLD mutants were re-cloned in a CS2⁺ plasmid backbone. Primers were redesigned to generate the RLD mutants using modified site directed mutagenesis from the CS2⁺ WT Herc5 construct. Using modified site directed mutagenesis $\Delta 1-2$, $\Delta 1-5$, and $\Delta 1-7$ RLD (Δ RLD) were successfully generated in the CS2⁺ plasmid backbone. Modified site directed mutagenesis was also used to generate the Δ spacer mutation. All constructs were sequenced at Roberts Sequencing Facility and verified using GENtle bioinformatics software. U2OS cells, which do not express Herc5 and therefore eliminated any potential

Ubiquitin	+	+	+	-	-	-	-	-	-	-	-	-	-	-	-
Herc5	-	-	-	+	+	+	-	-	-	-	-	-	-	-	-
ΔRLD	-	-	-	-	-	-	+	+	+	-	-	-	-	-	-
Δ1 RLD	-	-	-	-	-	-	-	-	-	+	+	+	-	-	-
Δ 1-3 RLD	-	-	-	-	-	-	-	-	-	-	-	-	+	+	+
DMSO	+	-	-	+	-	-	+	-	-	+	-	-	+	-	-
Mg132	-	+	-	-	+	-	-	+	-	-	+	-	-	+	-
Amantadine	-	-	+	-	-	+	-	-	+	-	-	+	-	-	+

Herc5



117kDa

Actin



42kDa

Fig. 1 Western blot for protein expression of pFLAG Herc5 RLD mutants in comparison to pCS2⁺ WT Herc5. Polyclonal Herc5 antibody (Abnova) was used to blot for Herc5 constructs. 10uM MG132 (Sigma) was used to inhibit the proteasome and 0.5mM amantadine-HCl (Sigma) was used to inhibit the lysosome. DMSO was used as a control for both MG132 and amantadine effects. Ubiquitin was used as a negative control. Transfections were done using FuGene transfection reagent and harvested 24 hours later. Data shown is representative of two independent trials (n=2).

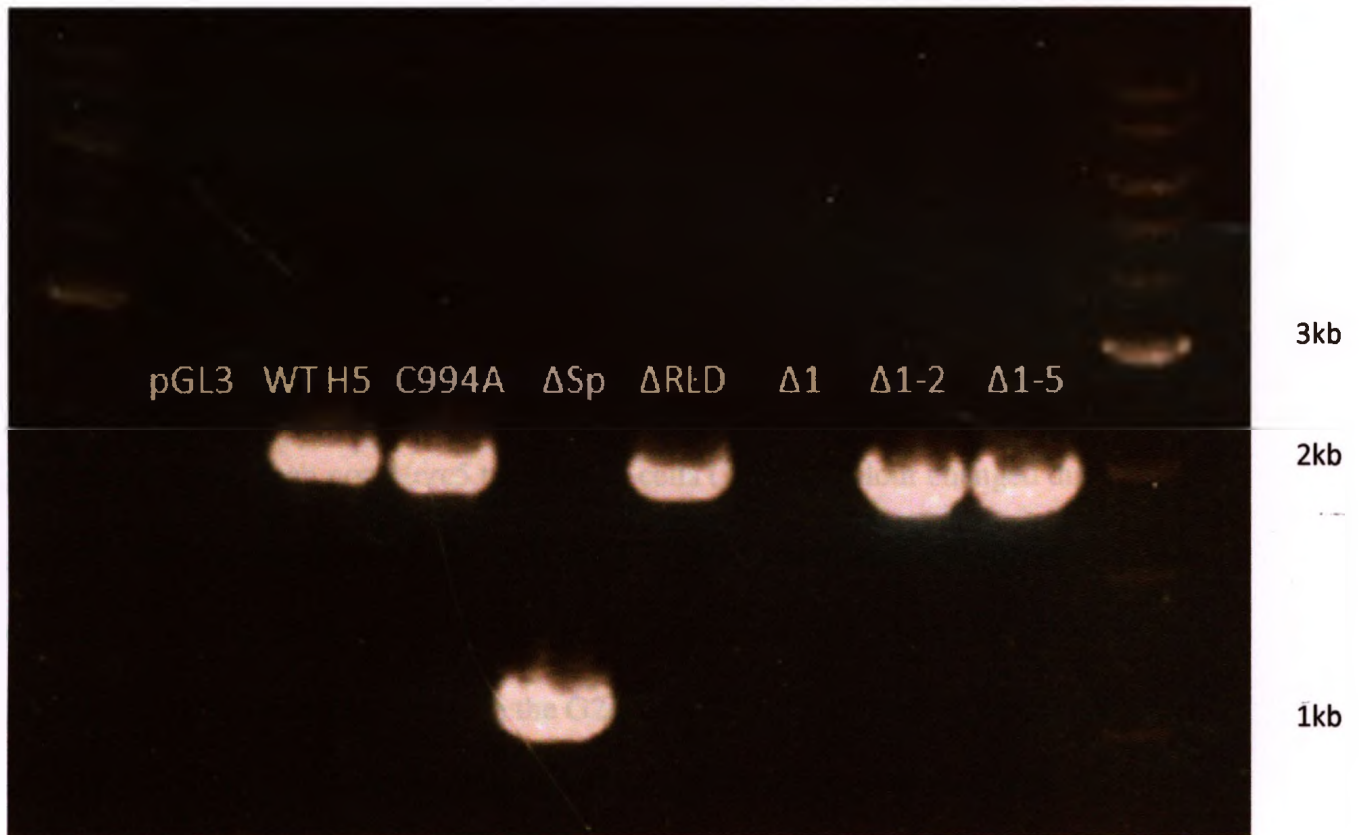


Fig. 2 RTPCR of CS2+ Herc5 constructs from U2OS transfected cells. U2OS cells were transfected with the Herc5 constructs as they are a natural knockdown of Herc5. Total mRNA was extracted 24 hours later and reverse transcribed into cDNA which was then PCR amplified using a forward primer beginning at the spacer region and reverse primer beginning at the end of the HECT domain. For the Δ spacer mutant of Herc5, primers were used so that only the HECT domain was amplified. Δ 1 construct displayed in this 1%DNA agarose gel is in the pFLAG backbone and is part of the first set of Herc5 mutants cloned into the pFLAG backbone. The Herc5 constructs which display mRNA production were those cloned in the CS2+ plasmid backbone.

for background Herc5 mRNA detection, were transfected with mutant constructs and RT PCR was performed to test expression of mRNA (Fig. 2). mRNA production was detectable for all CS2+ Herc5 mutant constructs.

3.2 Effect of Herc5 on cell viability and growth

Observations made in preliminary studies suggested that Herc5-transfected cells grew more slowly than non-Herc5 transfected cells (DMEM colour changed due to greater acidity in media from high confluency of pGL3 transfected and non-transfected cells). In addition, defects in nucleocytoplasmic shuttling of mRNA show retarded growth via restriction of cell cycle in the G2/M stage [131,133,134]. If Herc5 was affecting nucleocytoplasmic shuttling of HIV-1 mRNA, retarded growth would be expected in Herc5 transfected cells. To determine whether Herc5 was affecting replication of cells through this mechanism, growth curves were generated for WT Herc5 and mutant construct transfected HeLa cells over a period of 4 days. Interestingly, Herc5 transfected cells showed a much slower rate of replication in comparison to cells transfected with a promoterless plasmid (pGL3) (Fig. 3). Eliminating E3 ligase activity (C994A) and spacer region of Herc5 did not affect the ability of Herc5 to slow the cell cycle. However, cells transfected with the Δ RLD Herc5 construct displayed a growth pattern comparable to that of the negative control. In addition, when any of the blades of the Herc5 RLD were deleted (Δ 1-2RLD and Δ 1-5RLD) the rate of growth was also comparable to Δ RLD transfected and pGL3 transfected cells (Fig. 3, Supplementary Table 3). This suggests that the RLD of Herc5 is important for the regulation of cell cycle progression and that even a small deletion of its structure will eliminate Herc5's ability to restrict cell cycle. Additionally, this supports the hypothesis that the RLD may

be affecting nucleocytoplasmic shuttling of mRNA by displaying a comparable phenotype. Cell viability tests were also performed on the Herc5 construct transfected cells in which both live and dead cells were counted for each construct. There was no significant difference in the viability of cells when compared across the mutant constructs (data not shown).

3.3 Propidium Iodide staining for cell cycle analysis

Defects in nucleocytoplasmic shuttling of mRNA results in retarded cell cycle, predominantly in the G2/M stage of cell cycle [131]. Section 3.2 demonstrated retarded cell cycle in Herc5 transfected cells; however the stage cell cycle restriction is not clear (if at all). To determine whether Herc5 generates an arrest of cell cycle and whether it is similar to the arrest seen in nucleocytoplasmic mRNA shuttling defective cells (at the G2/M stage of cell cycle), propidium iodide staining for DNA content of cells transfected with WT Herc5, C994A, spacer or RLD mutant constructs was performed and analyzed using flow cytometry. During interphase of the cell cycle, nuclear DNA content of cells duplicates to prepare for mitosis. By the end of G2, the end of interphase, cells contain twice as much DNA as in G1, the beginning of interphase. S phase which occurs between the two stages is the onset of DNA duplication and therefore contains more DNA than G1 but not as much DNA found in G2. The intensity of the PI stain correlates with the amount of DNA in cells and therefore is used to determine the stage of cell cycle.

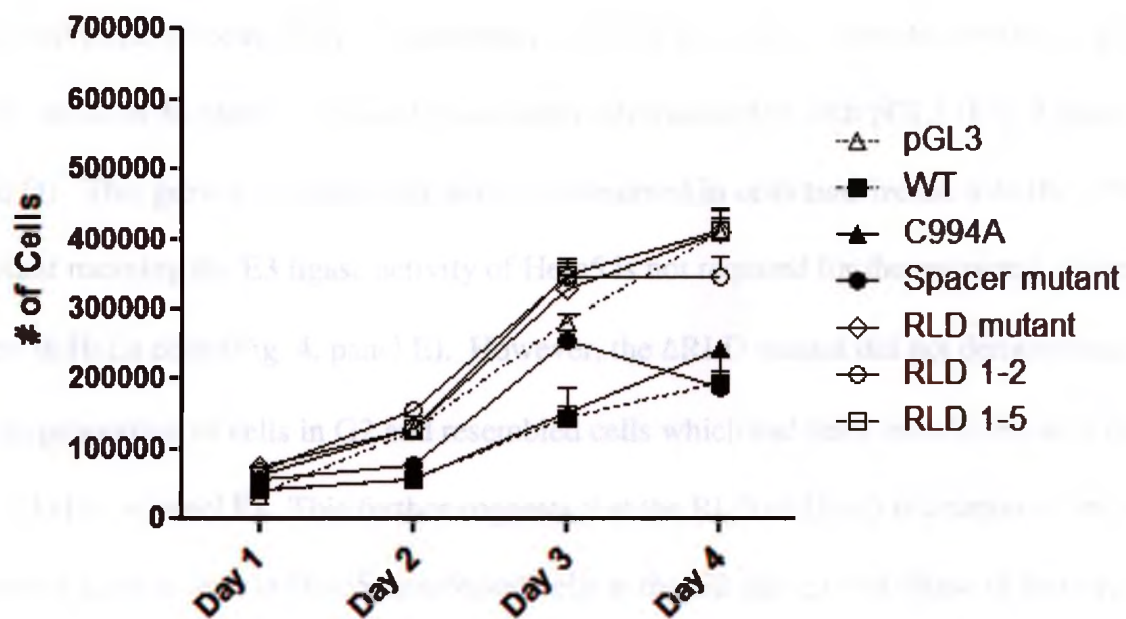
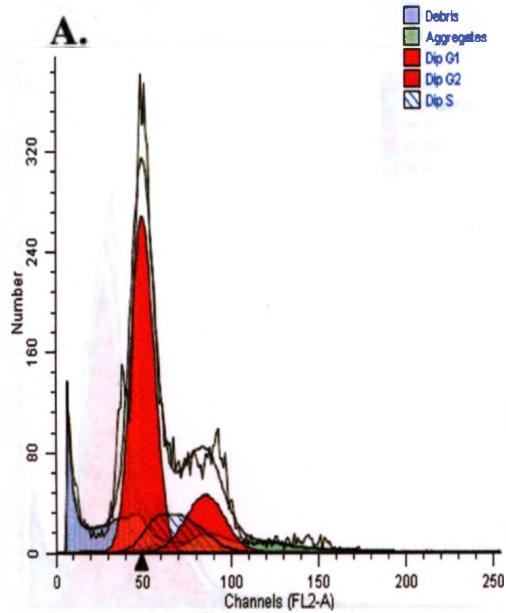
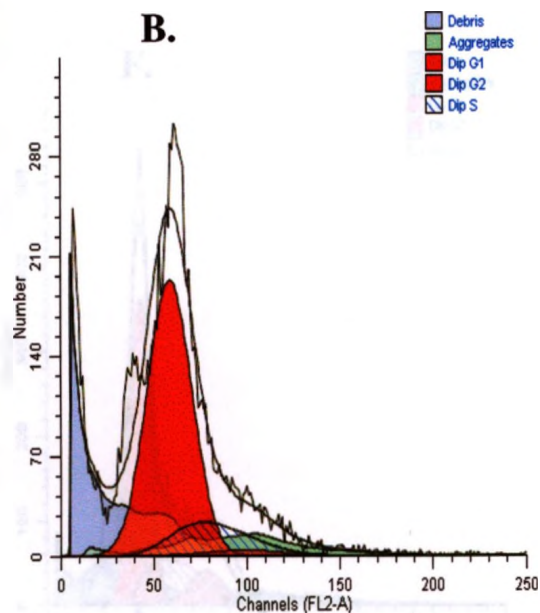


Fig . 3 Growth comparison of Herc5 constructs in HeLa cells. Transfection of HeLa cells was performed using SuperFect transfection reagent. Experiment was performed in triplicate. The mean of three trials was plotted for each day for each construct. Growth rates of all construct transfected cells were compared to pGL3 negative control. Significant differences in growth were observed for WT, C994A, and Δ Spacer ($p < 0.05$) ($n=3$)

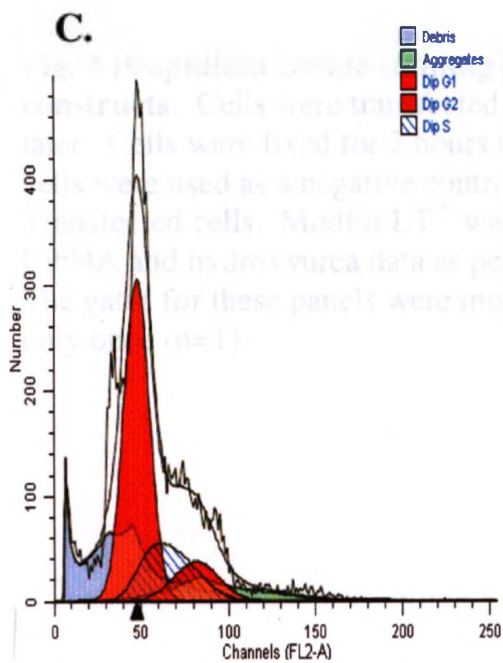
Hydroxyurea, a drug which arrests cell cycle at G1, was used as a positive control for the detection of changes in cell cycle (Fig. 4, panel B). Cells were transfected using FuGene and harvested 48 hours later. Interestingly, 11.25% more Herc5 transfected HeLa cells were in G2 or M phase of the cell cycle than cells transfected with pGL3 (Fig. 4 panel, C and D). This growth characteristic was also observed in cells transfected with the C994A mutant meaning the E3 ligase activity of Herc5 is not required for the restricted growth seen in HeLa cells (Fig. 4, panel E). However, the Δ RLD mutant did not demonstrate a large proportion of cells in G2 and resembled cells which had been transfected with the pGL3 (Fig. 4 panel F). This further suggests that the RLD of Herc5 is necessary for the arrested growth seen in Herc5 transfected cells at the G2 phase or M phase of cell cycle.



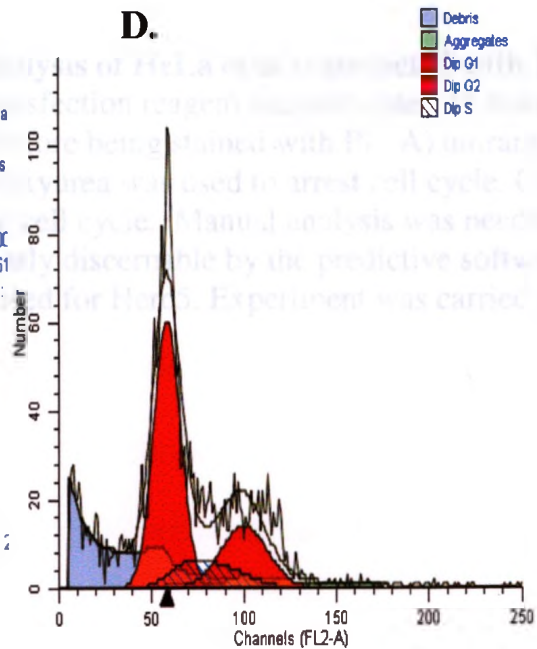
Untreated, G2= 18.73%



Hydroxyurea, G2= 18.73%



pGL3, G2= 13.41%



WT Herc5, G2=24.65%

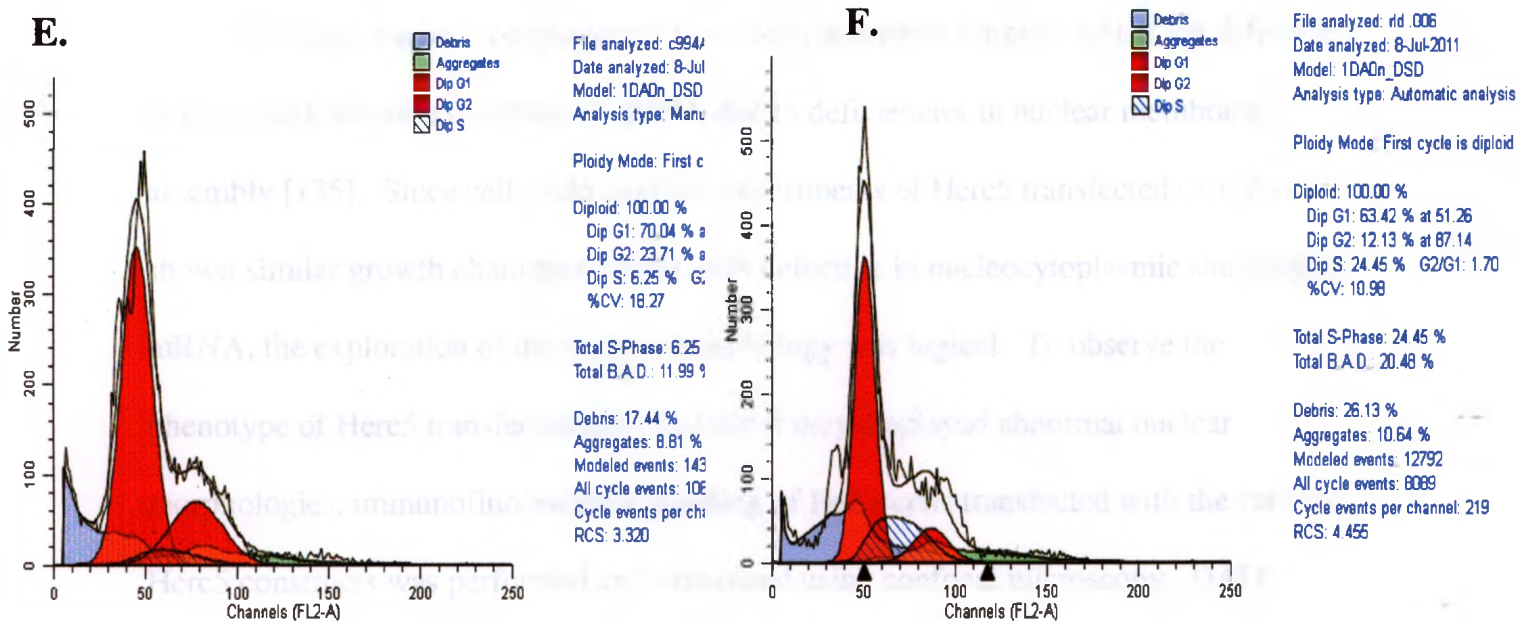
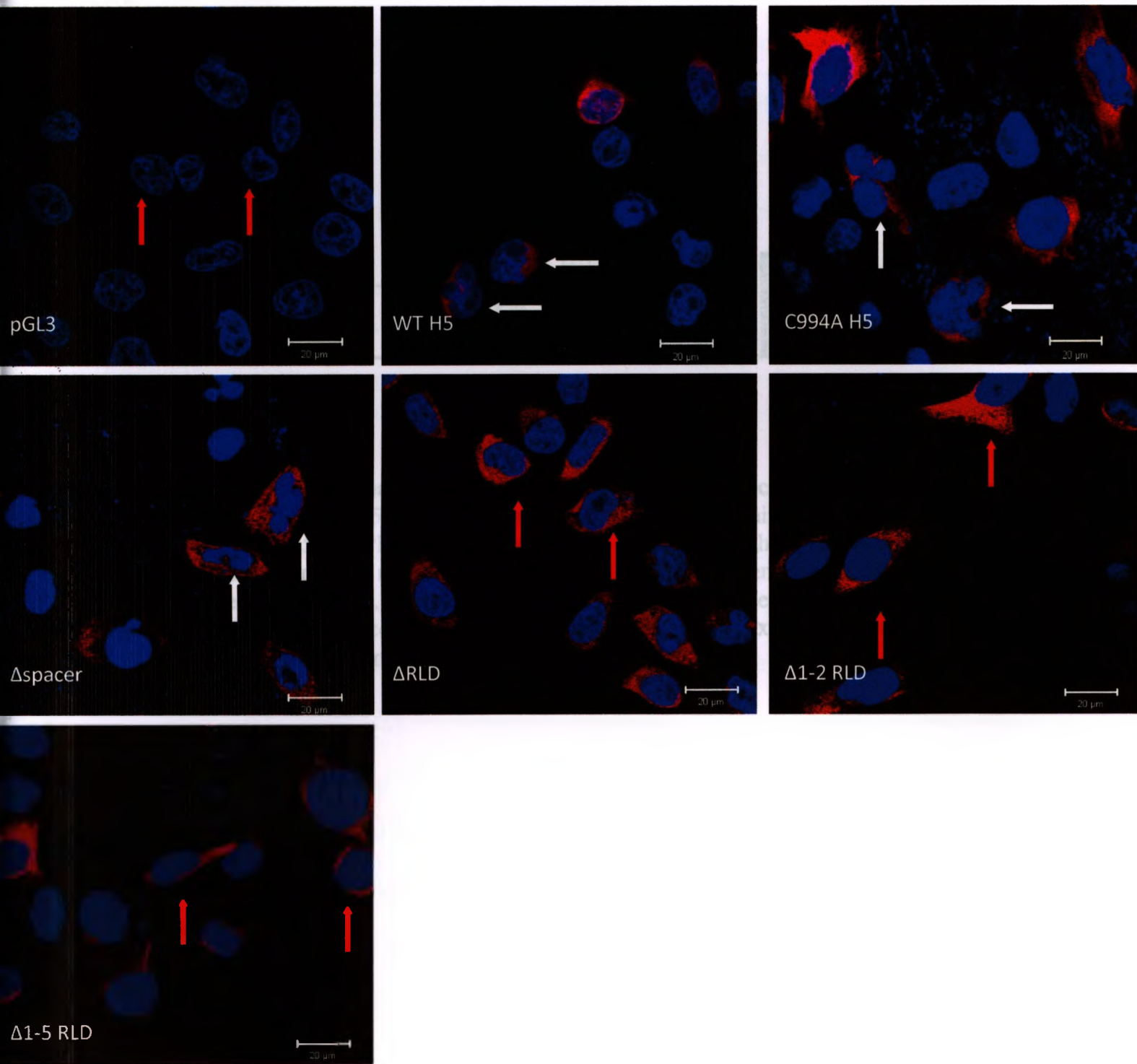


Fig. 4 Propidium Iodide staining for cell cycle analysis of HeLa cells transfected with Herc5 constructs. Cells were transfected with FuGene transfection reagent and harvested 48 hours later. Cells were fixed for 2 hours in 70% ethanol before being stained with PI. A) untransfected cells were used as a negative control B) 1mM Hydroxyurea was used to arrest cell cycle. C-F) Transfected cells. ModFit LT™ was used to analyse cell cycle. Manual analysis was needed for C994A and hydroxyurea data as peaks were not clearly discernable by the predictive software. The gates for these panels were modeled off gates used for Herc5. Experiment was carried out only once (n=1).

3.4 Nuclear morphology

Unusual nuclear morphologies have been described for cells which are defective in nucleocytoplasmic shuttling of mRNA due to deficiencies in nuclear membrane assembly [135]. Since cell cycle analysis experiments of Herc5 transfected cells have shown similar growth characteristics to cells defective in nucleocytoplasmic shuttling of mRNA, the exploration of the nuclear morphology was logical. To observe the phenotype of Herc5 transfected cells and see if they displayed abnormal nuclear morphologies, immunofluorescence labelling of HeLa cells transfected with the various Herc5 constructs was performed and visualized using confocal microscopy. DAPI staining was used for nuclear staining. Interestingly, Herc5 transfected cells had 48% more C-shaped nuclei or nuclei which were lobed and appeared to be dividing into new cells than pGL3 transfected. This same morphology was seen for cells transfected with the C994A mutant of Herc5 (41.5% more than pGL3) as well as the Δ spacer mutant (48% more than pGL3). This phenotype was eliminated when the Δ RLD Herc5 mutant was transfected. When any of the blades of the RLD were deleted (Δ 1-2 or Δ 1-5) the cells still displayed the phenotype representing pGL3 transfected cells which suggests that the full intact RLD structure is necessary for any morphological changes (Fig. 5).

A.



B.

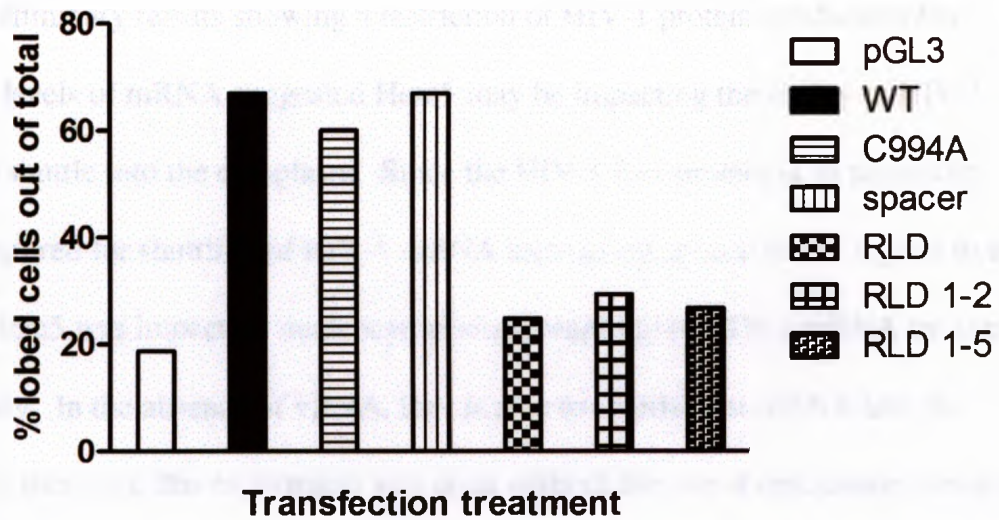


Fig. 5 Lobed nuclear morphology of Herc5 transfected cells. A) confocal microscopy performed on Herc5 construct transfected cells (lipofectamine transfection) Red=Flag tagged Herc5, DAPI/Blue= nucleus. White arrows highlight lobed nuclear morphology, red arrows indicate normal nuclear morphologies. B) percent of cells displaying lobed nuclear phenotypes. At least 100 cells were counted from each Herc5 construct. No statistical analysis could be performed on this data as the experiment was only carried out successfully one time (n=1).

3.5 Rev Localization

Preliminary results showing a restriction of HIV-1 protein production but increased levels of mRNA suggested Herc5 may be impacting the ability of HIV-1 mRNA to shuttle into the cytoplasm. Since the HIV-1 Rev protein is an accessory protein required for shuttling of HIV-1 mRNA into the cytoplasm it was logical to test whether Herc5 was impacting nucleocytoplasmic shuttling of HIV-1 mRNA by altering Rev activity. In the absence of vRNA, Rev is able to shuttle host mRNA into the cytoplasm, therefore this experiment was done without the use of replication competent HIV-1 and only with Rev to specifically examine the effects of Herc5 on its localization. If Herc5 has any effect on Rev's ability to shuttle mRNA from the nucleus, it would still be detectable in the absence of other HIV-1 RNA. Alterations in Rev's ability to shuttle HIV-1 mRNA into the cytoplasm would be accompanied by an observable change in localization of the rev protein - particularly an inability of Rev to shuttle to the cytoplasm and export cellular mRNA in the presence of Herc5. To assess the effect of Herc5 on Rev localization, HeLa cells were co-transfected with one of the various Herc5 constructs and the HIV RNA shuttling protein Rev at an 8:1 ratio. Cells were stained using an anti-Rev antibody and immunofluorescent anti- mouse secondary antibody. DAPI was used to stain the nucleus. Cells transfected with any of the Herc5 constructs or with promoterless vector (pGL3) did not display altered Rev localization. All Rev transfected cells showed Rev contained in the nucleolus of the nucleus where a large concentration of ribosomal RNA is known to be located and transcribed. Rev was not readily detectable in any other cellular compartment or in the cytoplasm (Fig. 6).

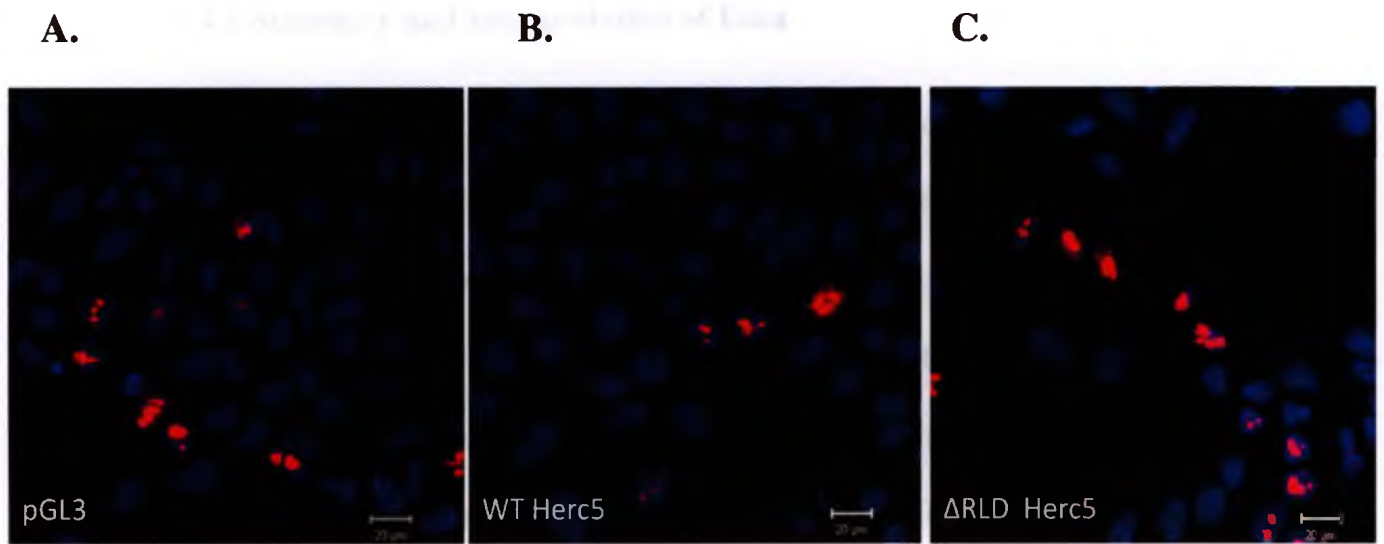


Fig. 6 Rev Localization in HeLa cells transfected with Herc5 mutant constructs. Rev was co-transfected with one of the Herc5 constructs. With each treatment, Rev was found only to localize in the nucleolus of cells. No other localization of Rev or other phenotypes were seen. Red= rev, DAPI/Blue= nucleus. Transfections were performed using lipofectamine (n=3)

Chapter 4: Discussion

4.1 Summary and Interpretation of Data

In summary, our lab has identified a novel HIV restriction factor, Herc5 which may be able to restrict HIV release via two mechanisms: 1) the inhibition of virus release by its E3 ligase and ISGylation of gag, and 2) the inhibition of protein synthesis likely due to an inhibition of RNA trafficking to the cytoplasm for translation resulting in decelerated growth. We have shown that this second mechanism of HIV restriction is not due to Herc5's E3 ligase function since mutating the key C994 residue to alanine, which is necessary for Herc5's ligase activity, did not interfere with Herc5's ability to restrict virus translation. Therefore, creation of Herc5 domain mutants was necessary for comprehending the mechanism by which Herc5 is able to restrict HIV at a pre-translational step. An HIV release assay performed by Matthew Woods (Woods, M., et al., 2011; unpublished) using the RLD and spacer mutants demonstrated the RLD of Herc5 to be important for this second mechanism of restriction due to the inability of Δ RLD Herc5 to restrict virus production. Additionally, the same experiment demonstrated that the spacer domain of Herc5 was not necessary for Herc5 in restricting HIV-1 release. Based on this result as well as preliminary studies that showed increased levels of mRNA (that is not being translated into protein) in the presence of Herc5, we hypothesized that the RLD of Herc5 may be preventing the shuttling of mRNA in the cytoplasm. To test our hypothesis, growth curves of HeLa cells transfected with various domain mutants of Herc5 (including Δ RLD, Δ 1-2 RLD, Δ 1-5RLD) were performed. Growth curve experiments showed that while WT Herc5 showed restricted or retarded cell cycling, the Δ RLD Herc5 and bladed deletions (Δ 1-2, Δ 1-5 RLD) constructs were

able to grow at a rate comparable to cells transfected with a promoterless (pGL3) vector. Propidium iodide staining for nuclear content to determine cell cycle stage demonstrated Herc5 constructs were predominately found in G2 or M phase, whereas the Δ RLD and bladed mutants did not demonstrate any altered cell growth pattern and were predominately found in G1 phase like in pGL3 transfected cells. Based on these results, we have shown that Herc5 is a mediator of cell cycle progression through the activity of its RLD. Additionally, the effects of Herc5 on nuclear morphology are eliminated with any of the RLD mutants which show an increasing reliance of Herc5 on the RLD for its activity.

To elucidate the mechanism and significance of the RLD it must be compared to its most similar homologue, RCC1. Structurally, the RLD is almost identical to the RCC1 protein (Fig. v). As mentioned earlier, the RCC1 is a key regulator of mRNA export to the cytoplasm by acting as a GEF for the Ran GTPase, exchanging Ran-GDP for Ran-GTP. This causes a build up of Ran-GTP in the cytoplasm which generates a GTP energy gradient across the nuclear membrane by which mRNA shuttles across. Interestingly, experiments looking at Herc5 interacting proteins have identified Ran as a binding partner [132- supplementary data]. Due to the high degree of structural homology between the RCC1 and RLD of Herc5 and that Ran is thought to interact with Herc5 and RCC1, it may be possible that the RLD is interacting with Ran similarly to its homologue RCC1 and functioning as a GEF for Ran-GDP converting it into Ran-GTP. Although this has not been directly tested, it has been suggested that Herc5 may act as a GEF for small GTPases like Ran [215]. If this were to occur in the cytoplasm (where Herc5 is found), Herc5 GEF activity may be able to counteract the GTP energy gradient

that normally exists across the nuclear membrane that is required for mRNA shuttling and inhibit or reduce the export of mRNA into the cytoplasm. In addition, cells which are unable to hydrolyze Ran-GTP in the cytoplasm and therefore do not have a defined GTP energy gradient across the nuclear membrane show an arrest at the G2/M stage of cell cycle similar to what we have seen in the presence of Herc5 [133,134]. If the RLD of Herc5 is acting as a GEF for Ran-GDP, it is possible that its conversion into Ran-GTP in the cytoplasm outweighs the rate of hydrolyzing Ran-GTP leading to defective mRNA shuttling and cell cycle possibly an arrest at G2/ M phase. In the presence of Δ RLD Herc5 mutant, the G2/M cell cycle profile seen in WT Herc5 is abolished and resembles the pGL3 negative control. If the RLD of Herc5 is maintaining GEF activity for Ran, we would expect that the deletion of this domain would also display the same phenotype as we have observed in our Δ RLD cell cycle experiments, where Δ RLD Herc5 does not affect cell cycle. That is, deletion of the potential GEF acting domain, Δ RLD, would eliminate cytoplasmic Ran-GDP conversion to Ran-GTP by Herc5. Thus there would no longer be an equalization of Ran-GTP across the nuclear membrane caused by Herc5 GEF activity and instead the cell would resume a normal build up of nuclear Ran-GTP which therefore would allow shuttling of mRNA to the cytoplasm. To further implicate the RLD in Herc5 cell cycle, the E3 ligase activity of Herc5 of Herc5 was necessary for the G2/M phenotype since deletion of these features did not affect the cells' G2/M profile in PI staining experiments.

It was unfortunate that there were technical issues in the processing of the Δ spacer and bladed mutants of the RLD for PI staining and cell cycle analysis. This data would have been valuable in determining whether or not the spacer domain showed the same

G2/M phenotype and allow for greater confidence that the RLD is responsible for the G2/M phenotype. The bladed mutants would have also helped to determine whether the full RLD structure is necessary to observe the cell cycle mediating effects of Herc5. Based on the cell viability and growth analysis experiment, my assumption would be that since the spacer domain maintained slowed growth and that cells transfected with the bladed mutants had normal growth rates, the spacer domain would not be necessary to observe the G2/M phenotype whereas either of the bladed mutations would have shown regular cell cycle progression. Processing issues such as these and fewer than 10,000 cells analysed for certain samples during the PI staining experiment make it increasingly important for the experiment to be repeated at least twice more. The use of 10cm dishes would be more appropriate so that at least 20,000 cells could be collected from each sample and therefore claims of cell cycle arrest would be more statistically relevant. In addition, hydroxyurea treated cells were inhibited almost entirely in G1 and S phase therefore eliminating a second G2 peak. As a result, the ModFit software was not accurately able to model cell cycle peaks automatically for hydroxyurea treated cells. As well, C994A transfected cells displayed a large amount of background staining which also affected ModFit automatic prediction of peaks. Instead, these samples were assessed manually using the same gates used for the analysis of Herc5 cell cycle. Repetition would allow for statistical analysis to be carried out and greater confidence that the results observed are not artificial and reproducible.

RT PCR of Herc5 constructs was performed instead of protein detection using western blot due to an inconsistency for detection of Herc5 protein. Inconsistency in protein detection was not due to transfection since mRNA of Herc5 constructs was

successfully reverse transcribed from U2OS (natural Herc5 knockdowns with no basal production of Herc5). However, Herc5 construct proteins were detectable using confocal microscopy of transfected HeLa cells using the same antibody used for western blot (anti-FLAG). Although HeLa cells are not natural Herc5 knockdowns, the use of FLAG antibody instead of Herc5 antibody allows for detection of only transfected Herc5 constructs. HeLa cells are also much more susceptible to taking up plasmid and therefore are higher expressers of transfected protein. It is possible that the ability to detect Herc5 in confocal microscopy is due to the use of a different cell type rather than a change of detection method. It is also possible, however, that the change in detection ability is due to a change in secondary antibody that was used for confocal microscopy and not for western blot. It might be of greater value to perform nickel column pulldown of Herc5 mutant construct transfected cell lysates. However, re-generation of the Herc5 mutants would need to be done so that they would express a HIS tag needed for the nickel column assay. Performing this assay would allow for greater ability to assess stability of the protein and should be done in parallel with drugs inhibiting proteasomal (MG132) and lysosomal (amantadine) degradation to ensure they are not being prematurely degraded.

Although it is clear that Herc5 transfected cells have altered cell cycle, growth, and are predominately in G2/M stage of cell cycle, it cannot be determined whether the altered growth of Herc5 transfected cells is due to an irreversible arrest of cell cycle at G2/M or a prolongation of G2/M phase based on the experiments performed. Studies that have previously investigated the effects of defective mRNA shuttling to the cytoplasm suggest that cell cycle is restricted rather than prolonged [131,133]. Deursen et al, showed that defects in the CAN protein, which is necessary for nuclear pore formation

and shuttling of mRNA out of the nucleus, causes an arrest of cell cycle predominately in G2 stage. Additionally, Ren et al showed a restriction of cell cycle at G2 when there was accumulation of mRNA in the nucleus and impaired GTP hydrolysis in the cytoplasm. If Herc5 is affecting shuttling of mRNA into the cytoplasm, it is possible that the G2 cell cycle phenotype is due to cell cycle arresting rather than prolongation. However, it has also been noted that increases in the cytoplasmic Ran-GTP binding protein RanBP1, which acts as a co-factor for the Ran-GTP hydrolyzing protein RanGAP1, lead to prolonged mitosis in mammalian cells [136]. Increases in Ran-GTP in the cytoplasm due to Herc5 may cause an upregulation of RanBP1 and affect cell cycle in this manner which might suggest Herc5 is resulting in slower growth of cells rather than restriction in cell cycle. In experiment 3.2, growth analysis was performed on Herc5 and mutant construct transfected cells. Although WT Herc5, C994A, and Δ spacer transfected cells all displayed slower rates of growth, these cells all continued to grow until they reached 100% confluency. This would suggest that growth of these cells was only slowed rather than restricted, however, since transfection rate is not 100% it cannot be ruled out that cells transfected with Herc5 were restricted in growth while untransfected cells in the well continued to grow until the well reached confluency. An important observation that was observed in the Deursen et al study was a normal nuclear envelope assembly of G2 arrested cells. Since we observed abnormal nuclear morphologies in the presence of Herc5 it is possible that cell cycle restriction at G2/M is less likely.

The nuclear morphology experiment shows that the abnormal cell cycling of Herc5 transfected cells is accompanied with a c-shaped or multi-lobed nuclear phenotype. This phenotype can also be supported by a defunct Ran-GTP gradient across the nuclear

membrane. It has been shown in *Xenopus* egg extracts that increased cytoplasmic Ran-GTP disrupts proper assembly of the nuclear envelope leading to abnormally small nuclear morphologies albeit not the same morphologies as we have seen in HeLa cells [224]; however this may be due to cell line variability. Particularly, Ran-GDP in the cytoplasm is necessary for proper nuclear envelope fusion in the process of nuclear assembly [136]. If the Herc5 RLD is contributing to an increased cytoplasmic Ran-GTP concentration by acting as a GEF for Ran, it may lead to the abnormal nuclear morphologies we have observed in HeLa cells transfected with WT Herc5. Herc5 lacking E3 ligase function (C994A) and Δ Spacer Herc5 also display abnormal nuclear morphologies as shown in Figure 5 further implicating the importance of the RLD in this Herc5 phenotype and suggesting that mRNA shuttling defect, cell cycle irregularity, and nuclear morphology abnormality are all due to RLD activity. Interestingly, the use of any of the bladed RLD mutants showed morphology phenotypes that were comparable to pGL3 transfected cells, which strongly suggests the importance of the entire domain in Herc5's cell cycle activity and impact on nuclear morphology. However, this experiment must be repeated at least two more times since it was only performed once successfully and thus no statistical significance can be claimed.

In an HIV-1 release assay using pGL3, WT Herc5, C994A, Δ Spacer, and Δ RLD mutants, the Δ Spacer and C994A Herc5 constructs show equal if not more potent effects in comparison to the WT Herc5 (data not shown) (Woods, M., et al 2011; unpublished). Additionally, although nuclear morphology experiments show a similar propensity for lobed nuclei to occur in WT transfected cells as C994A or Δ Spacer constructs, both C994A and Δ Spacer mutants show a more pronounced abnormal lobed phenotype. These

observations may be explained by the hypothesis that Herc5 might autoregulate itself through ISGylation of its spacer domain to subsequently shutdown the protein function. Therefore, eliminating the E3 ligase activity of Herc5 by C994A point mutation or deletion of the spacer domain could be increasing Herc5 stability, prolonging its activity and subsequently enhancing its effects by preventing/slowing turnover. Western blots performed on Herc5 construct stability show that of all Herc5 modified site directed mutagenesis generated constructs, the Δ spacer mutant is most stable (data not shown). It would be important to do a stability trial for the C994A mutant as well to see if the protein is as stable as the Δ spacer construct. The other well known ISG15 conjugating E3 ligase, EFP, also contains a domain in which multiple alpha helices reside similar to the spacer region of Herc5. AutoISGylation of this domain by EFP leads to negative regulation of its expression and protein turnover [139]. Future experiments should include immunoprecipitation of all Herc5 constructs from transfected cell lysates to compare the levels of intracellular protein. Although immunoprecipitation is only semi-quantitative, large differences in protein expression would be considered significant. If this hypothesis is correct it may help to explain some unusual results seen in the PI staining experiment. Particularly, large amounts of background staining seen for C994A transfected cells which affected ModFit ability to automatically predict peaks for G1, S, and G2. It is possible that the wide peaks for the C994A mutant were due to an incomplete digestion of RNA in cells. Although all cells were treated with RNaseA for an equal amount of time (20 minutes), cells transfected with Herc5 and C994A may have increased levels of RNA in the nucleus if our hypothesis that the RLD domain is restricting trafficking of RNA into the cytoplasm is correct. In addition, C994A may

have even greater amount of RNA build up than Herc5 if the construct is in fact more stable than wild type Herc5. It would be interesting if this wide peak phenomenon was also seen in cells transfected with Δ Spacer Herc5, again since this construct may be more stable and therefore have exaggerated and prolonged effects on cell cycle.

Immunofluorescence of Rev in HeLa cells co-transfected with Herc5 constructs demonstrated that no differences in Rev localization could be detected between any samples. Perhaps due to high the concentration of mRNA that is located in the nucleolus, Rev predominately localizes here and only few Rev molecules are necessary to shuttle RNA to cytoplasm. If such is the case, immunofluorescence may not be sensitive enough to detect cytoplasmic Rev or changes in levels of Rev in the cytoplasm. It should be expected that in pGL3 transfected cells, Rev would be detectable in both the nucleus and cytoplasm. However, if in the negative control Rev is undetectable in the cytoplasm by confocal microscopy, defects in Rev ability to shuttle mRNA into the cytoplasm in the presence of Herc5, as we would expect, would also be undetectable. It is important to find another assay to establish whether or not Herc5 is affecting Rev shuttling in order to determine the mechanism by which Herc5 affects HIV-1 protein production. If Herc5 is able to act as a GEF for Ran in the cytoplasm and offset the GTP gradient across the nuclear membrane, then it would be expected that Rev, which uses the same GTP energy gradient to shuttle HIV-1 mRNA into the cytoplasm, would also be affected and perhaps unable to shuttle out of the nucleus. (See Future directions 4.21 for proposed Rev localization assay).

4.2 Future directions

4.21 Quantification of cytoplasmic Rev in the presence of Herc5 vs pGL3 and Δ RLD transfected cells

Future directions should include an assay that assesses the amount of cytoplasmic rev in the presence of Herc5 vs. Δ RLD Herc5 and pGL3. This would allow us to examine the affect of the RLD of Herc5 on Rev shuttling into and out of the nucleus and further suggest that Herc5 may be affecting the GTP gradient that is required for Rev to shuttle mRNA out of the nucleus. For quantitative analysis of cytoplasmic and nuclear Rev, separation of the two cellular compartments would have to be performed in order to determine their Rev concentrations individually. The ProteoJET™ cytoplasmic and nuclear protein extraction kit could be used for the separation of the cytoplasmic and nuclear fractions of cells transfected with the different Herc5 constructs. Lysates from both the cytoplasmic fraction and nuclear fractions could be run separately on an SDS page gel and blotted for rev contents. Cytoplasmic fractions can be quantitatively compared across samples to determine if there is a difference in rev levels when co-transfected with Herc5 vs. pGL3 (promoterless vector – negative control).

4.22 qRTPCR of HIV mRNA in cytoplasm and nuclear fractions to evaluate shuttling ability in the presence of Herc5 and mutant constructs

qRTPCR could be done for HIV protein mRNA in the cytoplasm and nucleus to determine any differences in mRNA shuttling/distribution that may exist between Herc5 Δ RLD and wild type Herc5 transfected cells. This data would complement the Rev localization data mentioned above. Increased levels of HIV mRNA that are found with

wild type Herc5 may be abolished in the presence of Δ RLD Herc5, which would suggest that this domain is required to restrict the shuttling of HIV mRNA. For example, ultracentrifugation (as an alternative to the ProteoJET™ cytoplasmic and nuclear protein extraction kit) of these cells would be performed to separate nuclear and cytoplasmic fractions. mRNA could be isolated from these fractions and digested to remove DNA. mRNA would then be reverse transcribed into cDNA and could be amplified by PCR with specific primers for HIV protein sequences such as gag forward and reverse primers. This would allow us to quantitatively measure the differences between cytoplasmic and nuclear mRNA in the presence of the Herc5 mutant constructs vs. the wild type and negative control. Again, if the Δ RLD mutant of Herc5 shows similar distribution of mRNA in the cytoplasm and nucleus as the negative control, it would further implicate the RLD in regulating cytoplasmic export of mRNA perhaps through GEF activity.

4.23 Quantification of cytoplasmic Ran-GTP in the presence of Herc5 vs. pGL3 negative control and mutant constructs

To determine if Herc5 has an effect on cytoplasmic Ran-GTP levels, a Ran activation assay kit can be used (Cell Biolabs). This kit uses RanBP1 (a Ran-GTP hydrolyzing enzyme that specifically recognizes GTP bound Ran) agarose beads to selectively pull down activated Ran from cell lysates. Herc5 and mutant construct transfected cells would be harvested and separated of cytoplasmic and nuclear contents through the previously described methodologies. The Ran activation assay kit could be used on the cytoplasmic fraction to quantitatively determine the concentration of Ran-GTP found in the cytoplasm. Cytoplasmic Ran-GTP would be compared in cells

transfected with pGL3, WT and mutant (specifically Δ RLD Herc5) by immunoblotting for Ran.

4.24 Generation of RLD active site mutants to evaluate the impact on Herc5 GEF activity (if any), mRNA shuttling capacity, nuclear morphology, cell cycle progression, growth curve, and rev localization.

Currently we have designed three mutants of Herc5 which contain point mutations within the RLD. We wanted to test the importance of these residues since the homologous sites in RCC1 serve as active sites for RCC1 GEF activity towards Ran [220]. Reduced competency in Herc5 to restrict HIV or mRNA shuttling into the cytoplasm with one or all of these mutations would allow us to further characterize the importance of this domain for HIV restriction. These RLD point mutants should be compared to the Δ RLD mutant and the wild type Herc5 construct in the aforementioned experiments to determine if they completely abolish GEF activity (if any), mRNA shuttling of Herc5, and restrict cell cycle. If so, not only would we have strongly implicated the RLD as a GEF for Ran but also determined key active site residues of Herc5 that are necessary for HIV-1 restriction.

4.25 Generation of an RLD only construct lacking spacer and HECT domains of Herc5

Primers have already been made to amplify the RLD region of Herc5 in the absence of the other domains. It would be interesting to see if this region alone would be able to counteract the Ran-GTP gradient across the nucleus by still acting as a GEF for Ran (if possible) and thus restrict HIV protein production. This would allow us to further

understand the significance of this domain and possibly suggest evolutionary origins of Herc5. Should the domain be able to maintain its GEF activity (if any) and be able to restrict mRNA shuttling, it might suggest that the domain was once a singular protein and either further evolved to contain a spacer and RLD domain perhaps by associating with an ancient ISG15 E3 ligase to acquire stronger antiviral activity.

4.26 Generation of point mutants at lysine residues in the spacer domain to determine if autoISGylation in this domain leads to Herc5 turnover.

To determine the significance of the increased stability seen with the Δ spacer Herc5 construct, point mutations of the lysine residues (where ISGylation occurs [218]) of the spacer domain should be made. Since the other ISG15 E3 ligase, EFP, contains a coiled coil domain that is structurally similar to the spacer domain of Herc5 and is autoISGylated to influence protein degradation, it would be interesting to see if the spacer domain of Herc5 has the same activity. Firstly, stability trials of wild type Herc5 transfected cells in the presence of a deubiquitinating enzyme such as Ubp2 should be performed to determine if protein turnover is due to ubiquitination. Provided that deubiquitination of Herc5 does not increase protein stability, stability trials of wild type Herc5 should be performed in the presence of the de-ISGylating enzyme, Ubp43 and compared to the C994A Herc5 mutant (lacking ISG15 conjugative activity) and wild type Herc5 alone. An increase in stability of the Herc5 construct in the presence of Ubp43 compared to wild type Herc5 and similar to C994A Herc5 stability would suggest that autoISGylation of Herc5 is causing turnover. Next, the spacer domain lysine residue point mutants should be transfected into cells and analyzed for stability and compared to wild type Herc5 stability. This would allow us to determine which residues are necessary

for Herc5 turnover most likely due to ISGylation. To further assess if this is a site for ISG15 binding, wild type Herc5, Δ spacer Herc5, and the lysine residue mutated spacer domain of Herc5 should be transfected into cells in the presence of ISG15 and then immunoprecipitated in the presence of Herc5 (or flag) antibody. The bound product can then be run on a non-denaturing SDS page gel and blotted for ISG15 to determine the capacity of each construct to be modified with ISG15. An inability of ISG15 to bind to Δ spacer and ability to bind to wild type Herc5 would definitively prove the region is ISGylated. With the individual lysine residue point mutants in the spacer domain of Herc5, we can also determine the exact lysines which are targets for autoISGylation. Completion of these experiments would elucidate some of the functional properties of the spacer domain of Herc5.

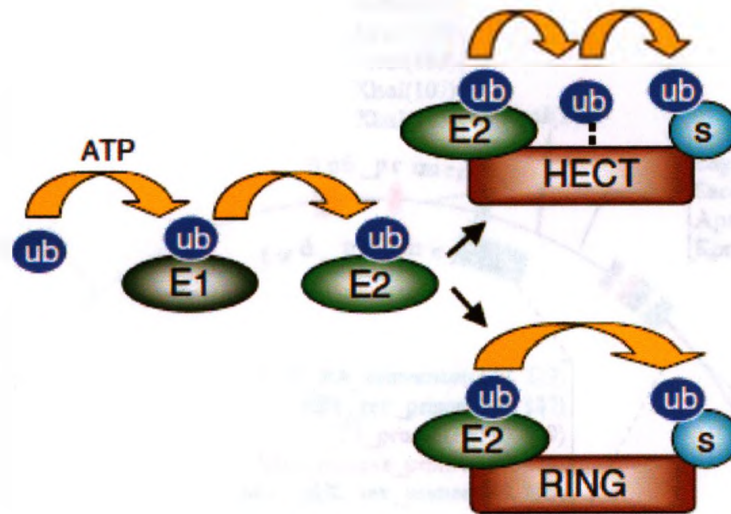
4.27 Evolutionary comparison of Herc5 across various primate species.

In the future, it would also be very interesting to determine the evolutionary conservation of Herc5 amongst primates. Since Herc5 is found in only primates, Herc5 from different primate cell lines can be reverse transcribed using human Herc5 primers- initially. Although these human primers may not be able to amplify Herc5 proteins that exist in other primate species due to sequence variability, some primate species that are sequentially identical or highly similar may yield a Herc5 protein sequence. If not, Herc5 sequences of Rhesus macaques, northern white faced gibbons, Sumatran orangutans, marmosets, and chimpanzees from any of which Herc5 primers can be made. These primers would begin in the non-coding regions of Herc5 so that the coding region of the primate Herc5 sequence would be intact and not contain nucleotide differences that may be present if using human coding region Herc5 primers. These evolutionary comparisons

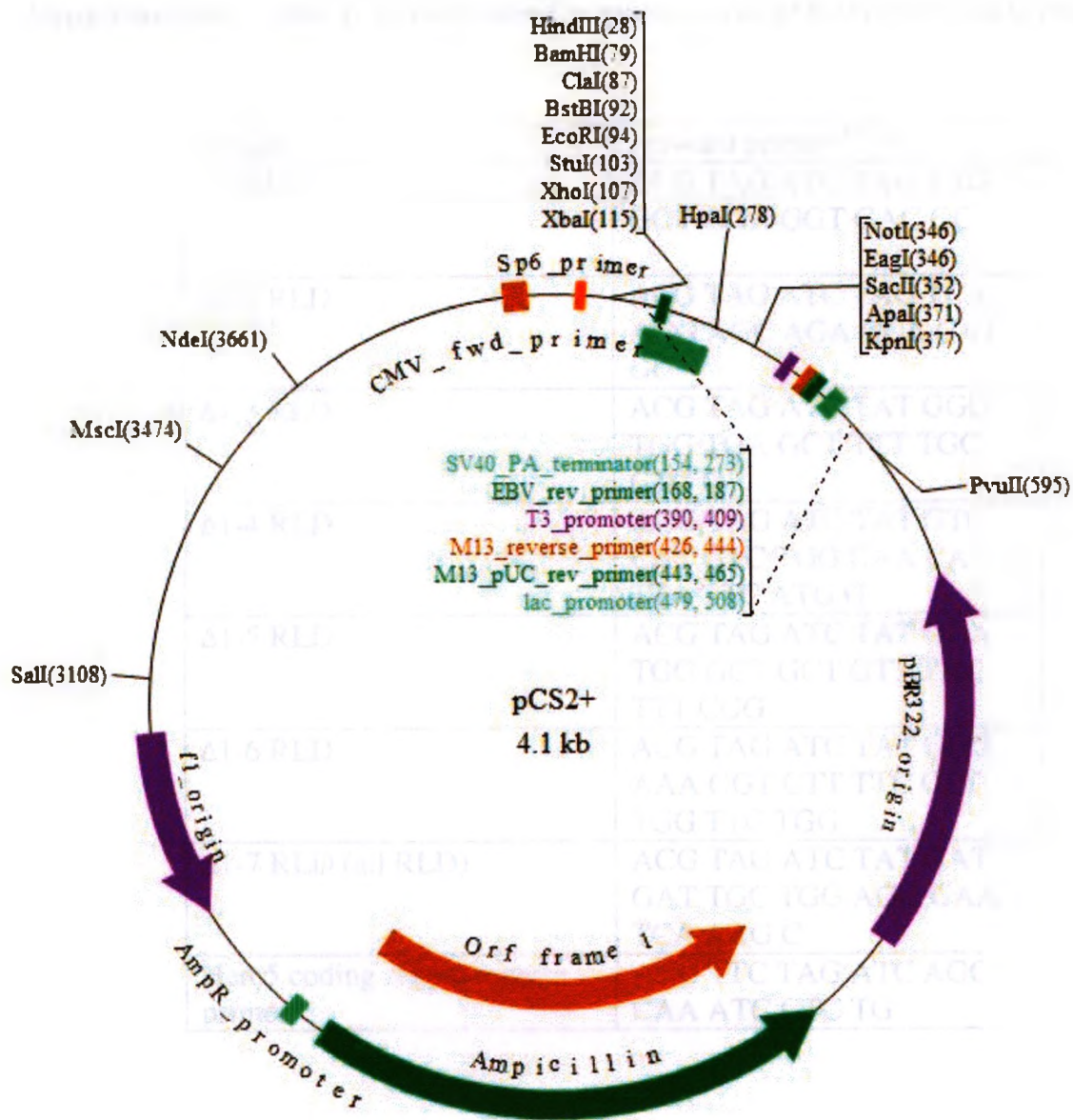
of proteins across species have been performed for other HIV restriction factors such as TRIM22 and TRIM5 α . These studies show that the prevalence of TRIM22 and TRIM5 α within mammalian species is highly selective favouring one protein or the other.

Specifically, the selection of TRIM22 over TRIM5 α in new world monkeys and humans has occurred over the last 23 million years possibly reflecting a change in pathogenic environment [217]. Herc5 isolated from various primate cell lines could be tested on their ability to restrict HIV (or SIV) to assess their antiviral activity and possibly allow us to observe when in evolutionary history Herc5 acquired antiviral activity-particularly by comparing Herc5 antiviral activity in old world and new world monkey cell lines.

Supplementary Figures



Supplementary Figure 1. HECT E3 ligase ubiquitin conjugation vs. RING E3 ligase ubiquitin conjugation [223].



Supplementary Figure 2. pCS2+ plasmid map. Original WT Herc5 construct was cloned in this backbone.

Supplementary Table 1- Primers used for generation of pFLAG Herc5 RLD mutants.

Mutant	Forward primer 5' → 3'
Δ1 RLD	ACG TAG ATC TAG TAG GGT GGA GGT GAC GC
Δ1-2 RLD	ACG TAG ATC TAG TCA AGG AGC AGA GCA CAT GC
Δ1-3 RLD	ACG TAG ATC TAT GGG TGG TGA GCT TTT TGC CTG G
Δ1-4 RLD	ACG TAG ATC TAT GTC CAT GTC TGG CAA CAT TTA TTC ATG G
Δ1-5 RLD	ACG TAG ATC TAT GGA TGG GCT GCT GTT TAC TIT CGG
Δ1-6 RLD	ACG TAG ATC TAT GGG AAA GGT CTT TTC CTT TGG TTC TGG
Δ1-7 RLD (all RLD)	ACG TAG ATC TAT GAT GAT TGC TGG AGG GAA TCA AAG C
Herc5 coding region reverse primer	ACG TTC TAG ATC AGC CAA ATC CTC TG

Supplementary Table 2. PCR conditions for amplification of pFLAG Herc5 RLD constructs

A.

5ul	10x pfu reaction buffer w/o MgSO ₄
6ul	MgSO ₄
1ul	dNTP
1ul	Forward primer
1ul	Reverse primer
2.5ul	DMSO (5%)
120ng	Template CS2 ⁺ Herc5
1ul	pfu
To 50ul	water
50ul	Total volume

B.

	Temperature	Time	# of cycles
Initial Denature	95°C	3 minutes	1x
Denature	95°C	30 seconds	32x
Annealing	50.5°C	30 seconds	32x
Extension	72°C	4 minutes	32x
Final Extension	72°C	10 minutes	1x

Supplementary Table 3. Statistical analysis of cell cycle growth curve generated using two-way ANOVA in GraphPad Prism 5.

Two-way RM ANOVA		Matching by cols		
Source of Variation	% of total variation	P value		
Interaction	4.71	0.0004		
Day	82.83	< 0.0001		
Treatment	7.97	< 0.0001		
Subjects (matching)	0.8137	0.5766		
Source of Variation	P value summary	Significant?		
Interaction	***	Yes		
Day	****	Yes		
Treatment	****	Yes		
Subjects (matching)	ns	No		
Source of Variation	Df	Sum-of-squares	Mean square	F
Interaction	24	1.475e+011	6.145e+009	2.994
Day	4	2.594e+012	6.486e+011	316.0
Treatment	6	2.497e+011	4.162e+010	22.86
Subjects (matching)	14	2.548e+010	1.820e+009	0.8869
Residual	56	1.149e+011	2.052e+009	
Number of missing values	0			
Bonferroni multiple comparisons	Number of comparisons: 30			
pGL3 vs WT				
Treatment	pGL3	WT	Difference	95% CI of diff.
Day 1	36000	43000	7000	-112607 to 126607
Day 2	127000	59000	-68000	-187607 to 51607
Day 3	283333	146667	-136667	-256273 to -17060
Day 4	410000	196667	-213333	-332940 to -93727
Treatment	Difference	t	P value	Summary
Day 1	7000	0.1914	P > 0.05	ns
Day 2	-68000	1.859	P > 0.05	ns
Day 3	-136667	3.737	P < 0.05	*
Day 4	-213333	5.834	P < 0.0001	****
pGL3 vs C994A				
Treatment	pGL3	C994A	Difference	95% CI of diff.
Day 1	36000	43000	7000	-112607 to 126607
Day 2	127000	59000	-68000	-187607 to 51607
Day 3	283333	153333	-130000	-249607 to -10393
Day 4	410000	243333	-166667	-286273 to -47060

Treatment	Difference	t	P value	Summary
Day 1	7000	0.1914	P > 0.05	ns
Day 2	-68000	1.859	P > 0.05	ns
Day 3	-130000	3.555	P < 0.05	*
Day 4	-166667	4.558	P < 0.001	***

pGL3 vs Spacer mutant

Treatment	pGL3	Spacer mutant	Difference	95% CI of diff.
Day 1	36000	59000	23000	-96607 to 142607
Day 2	127000	79000	-48000	-167607 to 71607
Day 3	283333	256667	-26667	-146273 to 92940
Day 4	410000	190000	-220000	-339607 to -100393

Treatment	Difference	t	P value	Summary
Day 1	23000	0.6289	P > 0.05	ns
Day 2	-48000	1.313	P > 0.05	ns
Day 3	-26667	0.7292	P > 0.05	ns
Day 4	-220000	6.016	P < 0.0001	****

pGL3 vs RLD mutant

Treatment	pGL3	RLD mutant	Difference	95% CI of diff.
Day 1	36000	76000	40000	-79607 to 159607
Day 2	127000	130000	3000	-116607 to 122607
Day 3	283333	330000	46667	-72940 to 166273
Day 4	410000	410000	0.0	-119607 to 119607

Treatment	Difference	t	P value	Summary
Day 1	40000	1.094	P > 0.05	ns
Day 2	3000	0.08204	P > 0.05	ns
Day 3	46667	1.276	P > 0.05	ns
Day 4	0.0	0.0	P > 0.05	ns

pGL3 vs RLD 1-2

Treatment	pGL3	RLD 1-2	Difference	95% CI of diff.
Day 1	36000	71000	35000	-84607 to 154607
Day 2	127000	158000	31000	-88607 to 150607
Day 3	283333	346667	63333	-56273 to 182940
Day 4	410000	346667	-63333	-182940 to 56273

Treatment	Difference	t	P value	Summary
Day 1	35000	0.9571	P > 0.05	ns
Day 2	31000	0.8477	P > 0.05	ns
Day 3	63333	1.732	P > 0.05	ns
Day 4	-63333	1.732	P > 0.05	ns

pGL3 vs RLD 1-5

Treatment	pGL3	RLD 1-5	Difference	95% CI of diff.
Day 1	36000	63000	27000	-92607 to 146607
Day 2	127000	132000	5000	-114607 to 124607
Day 3	283333	350000	66667	-52940 to 186273

Treatment	Difference	t	P value	Summary
Day 1	27000	0.7383	P > 0.05	ns
Day 2	5000	0.1367	P > 0.05	ns
Day 3	66667	1.823	P > 0.05	ns
Day 4	3333	0.09115	P > 0.05	ns

References

1. Pickart, C. M. & Eddins, M. J. Ubiquitin: structures, functions, mechanisms. *Biochim. Biophys. Acta* **1695**, 55-72 (2004).
2. Pickart, C. M. Mechanisms underlying ubiquitination. *Annu. Rev. Biochem.* **70**, 503-533 (2001).
3. Di Fiore, P. P., Polo, S. & Hofmann, K. When ubiquitin meets ubiquitin receptors: a signalling connection. *Nat. Rev. Mol. Cell Biol.* **4**, 491-497 (2003).
4. Hofmann, K. & Falquet, L. A ubiquitin-interacting motif conserved in components of the proteasomal and lysosomal protein degradation systems. *Trends Biochem. Sci.* **26**, 347-350 (2001).
5. Donaldson, K. M., Yin, H., Gekakis, N., Supek, F. & Joazeiro, C. A. Ubiquitin signals protein trafficking via interaction with a novel ubiquitin binding domain in the membrane fusion regulator, Vps9p. *Curr. Biol.* **13**, 258-262 (2003).
6. Shih, S. C. *et al.* A ubiquitin-binding motif required for intramolecular monoubiquitylation, the CUE domain. *EMBO J.* **22**, 1273-1281 (2003).
7. Scheffner, M., Huibregtse, J. M., Vierstra, R. D. & Howley, P. M. The HPV-16 E6 and E6-AP complex functions as a ubiquitin-protein ligase in the ubiquitination of p53. *Cell* **75**, 495-505 (1993).
8. Hatakeyama, S., Jensen, J. P. & Weissman, A. M. Subcellular localization and ubiquitin-conjugating enzyme (E2) interactions of mammalian HECT family ubiquitin protein ligases. *J. Biol. Chem.* **272**, 15085-15092 (1997).
9. Huibregtse, J. M., Scheffner, M., Beaudenon, S. & Howley, P. M. A family of proteins structurally and functionally related to the E6-AP ubiquitin-protein ligase. *Proc. Natl. Acad. Sci. U. S. A.* **92**, 5249 (1995).
10. Scheffner, M. & Staub, O. HECT E3s and human disease. *BMC Biochem.* **8 Suppl 1**, S6 (2007).
11. Scheffner, M., Nuber, U. & Huibregtse, J. M. Protein ubiquitination involving an E1-E2-E3 enzyme ubiquitin thioester cascade. *Nature* **373**, 81-83 (1995).
12. Schwarz, S. E., Rosa, J. L. & Scheffner, M. Characterization of human hect domain family members and their interaction with UbcH5 and UbcH7. *J. Biol. Chem.* **273**, 12148-12154 (1998).
13. Garcia-Gonzalo, F. R. & Rosa, J. L. The HERC proteins: functional and evolutionary insights. *Cell Mol. Life Sci.* **62**, 1826-1838 (2005).

14. Shearwin-Whyatt, L., Dalton, H. E., Foot, N. & Kumar, S. Regulation of functional diversity within the Nedd4 family by accessory and adaptor proteins. *Bioessays* **28**, 617-628 (2006).
15. Ingham, R. J., Gish, G. & Pawson, T. The Nedd4 family of E3 ubiquitin ligases: functional diversity within a common modular architecture. *Oncogene* **23**, 1972-1984 (2004).
16. Huang, L. *et al.* Structure of an E6AP-UbcH7 complex: insights into ubiquitination by the E2-E3 enzyme cascade. *Science* **286**, 1321-1326 (1999).
17. Verdecia, M. A. *et al.* Conformational flexibility underlies ubiquitin ligation mediated by the WWP1 HECT domain E3 ligase. *Mol. Cell* **11**, 249-259 (2003).
18. Wang, M. & Pickart, C. M. Different HECT domain ubiquitin ligases employ distinct mechanisms of polyubiquitin chain synthesis. *EMBO J.* **24**, 4324-4333 (2005).
19. Kim, H. T. *et al.* Certain pairs of ubiquitin-conjugating enzymes (E2s) and ubiquitin-protein ligases (E3s) synthesize nondegradable forked ubiquitin chains containing all possible isopeptide linkages. *J. Biol. Chem.* **282**, 17375-17386 (2007).
20. Scialpi, F. *et al.* Itch self-polyubiquitylation occurs through lysine-63 linkages. *Biochem. Pharmacol.* **76**, 1515-1521 (2008).
21. Lim, K. L. & Lim, G. G. K63-linked ubiquitination and neurodegeneration. *Neurobiol. Dis.* **43**, 9-16 (2011).
22. Kim, H. C. & Huijbrechtse, J. M. Polyubiquitination by HECT E3s and the determinants of chain type specificity. *Mol. Cell. Biol.* **29**, 3307-3318 (2009).
23. Hengstermann, A. *et al.* Growth suppression induced by downregulation of E6-AP expression in human papillomavirus-positive cancer cell lines depends on p53. *J. Virol.* **79**, 9296-9300 (2005).
24. Lu, C., Pribanic, S., Debonneville, A., Jiang, C. & Rotin, D. The PY motif of ENaC, mutated in Liddle syndrome, regulates channel internalization, sorting and mobilization from subapical pool. *Traffic* **8**, 1246-1264 (2007).
25. Zhou, R., Patel, S. V. & Snyder, P. M. Nedd4-2 catalyzes ubiquitination and degradation of cell surface ENaC. *J. Biol. Chem.* **282**, 20207-20212 (2007).
26. Hannoun, Z., Greenhough, S., Jaffray, E., Hay, R. T. & Hay, D. C. Post-translational modification by SUMO. *Toxicology* **278**, 288-293 (2010).
27. Vertegaal, A. C. *et al.* Distinct and overlapping sets of SUMO-1 and SUMO-2 target proteins revealed by quantitative proteomics. *Mol. Cell. Proteomics* **5**, 2298-2310 (2006).

28. Rodriguez, M. S., Dargemont, C. & Hay, R. T. SUMO-1 conjugation in vivo requires both a consensus modification motif and nuclear targeting. *J. Biol. Chem.* **276**, 12654-12659 (2001).
29. Hay, R. T. Role of ubiquitin-like proteins in transcriptional regulation. *Ernst Schering Res. Found. Workshop* (**57**), 173-192 (2006).
30. Sharrocks, A. D. PIAS proteins and transcriptional regulation--more than just SUMO E3 ligases? *Genes Dev.* **20**, 754-758 (2006).
31. Desterro, J. M. *et al.* SUMO-1 modification alters ADAR1 editing activity. *Mol. Biol. Cell* **16**, 5115-5126 (2005).
32. Zhao, J. Sumoylation regulates diverse biological processes. *Cell Mol. Life Sci.* **64**, 3017-3033 (2007).
33. Hartner, J. C., Walkley, C. R., Lu, J. & Orkin, S. H. ADAR1 is essential for the maintenance of hematopoiesis and suppression of interferon signaling. *Nat. Immunol.* **10**, 109-115 (2009).
34. Wang, Y. & Samuel, C. E. Adenosine deaminase ADAR1 increases gene expression at the translational level by decreasing protein kinase PKR-dependent eIF-2alpha phosphorylation. *J. Mol. Biol.* **393**, 777-787 (2009).
35. Lin, X., Liang, M., Liang, Y. Y., Brunicardi, F. C. & Feng, X. H. SUMO-1/Ubc9 promotes nuclear accumulation and metabolic stability of tumor suppressor Smad4. *J. Biol. Chem.* **278**, 31043-31048 (2003).
36. Roysland, K. *et al.* Analyzing direct and indirect effects of treatment using dynamic path analysis applied to data from the Swiss HIV Cohort Study. *Stat. Med.* (2011).
37. Steffan, J. S. *et al.* SUMO modification of Huntingtin and Huntington's disease pathology. *Science* **304**, 100-104 (2004).
38. Cai, Q. & Robertson, E. S. Ubiquitin/SUMO modification regulates VHL protein stability and nucleocytoplasmic localization. *PLoS One* **5**, e12636 (2010).
39. Atkins, D. J. *et al.* Concomitant deregulation of HIF1alpha and cell cycle proteins in VHL-mutated renal cell carcinomas. *Virchows Arch.* **447**, 634-642 (2005).
40. Shiio, Y. & Eisenman, R. N. Histone sumoylation is associated with transcriptional repression. *Proc. Natl. Acad. Sci. U. S. A.* **100**, 13225-13230 (2003).
41. Kochs, G., Garcia-Sastre, A. & Martinez-Sobrido, L. Multiple anti-interferon actions of the influenza A virus NS1 protein. *J. Virol.* **81**, 7011-7021 (2007).

42. Mibayashi, M. *et al.* Inhibition of retinoic acid-inducible gene I-mediated induction of beta interferon by the NS1 protein of influenza A virus. *J. Virol.* **81**, 514-524 (2007).
43. Satterly, N. *et al.* Influenza virus targets the mRNA export machinery and the nuclear pore complex. *Proc. Natl. Acad. Sci. U. S. A.* **104**, 1853-1858 (2007).
44. Xu, K. *et al.* Modification of nonstructural protein 1 of influenza A virus by SUMO1. *J. Virol.* **85**, 1086-1098 (2011).
45. Mi, Z., Fu, J., Xiong, Y. & Tang, H. SUMOylation of RIG-I positively regulates the type I interferon signaling. *Protein Cell.* **1**, 275-283 (2010).
46. Gong, L. & Yeh, E. T. Identification of the activating and conjugating enzymes of the NEDD8 conjugation pathway. *J. Biol. Chem.* **274**, 12036-12042 (1999).
47. Xirodimas, D. P. Novel substrates and functions for the ubiquitin-like molecule NEDD8. *Biochem. Soc. Trans.* **36**, 802-806 (2008).
48. Nakayama, K. I. & Nakayama, K. Regulation of the cell cycle by SCF-type ubiquitin ligases. *Semin. Cell Dev. Biol.* **16**, 323-333 (2005).
49. Kawakami, T. *et al.* NEDD8 recruits E2-ubiquitin to SCF E3 ligase. *EMBO J.* **20**, 4003-4012 (2001).
50. Edgar, B. A. & Orr-Weaver, T. L. Endoreplication cell cycles: more for less. *Cell* **105**, 297-306 (2001).
51. Tateishi, K., Omata, M., Tanaka, K. & Chiba, T. The NEDD8 system is essential for cell cycle progression and morphogenetic pathway in mice. *J. Cell Biol.* **155**, 571-579 (2001).
52. Baroth, M., Orlich, M., Thiel, H. J. & Becher, P. Insertion of cellular NEDD8 coding sequences in a pestivirus. *Virology* **278**, 456-466 (2000).
53. Gu, B. *et al.* The RNA helicase and nucleotide triphosphatase activities of the bovine viral diarrhea virus NS3 protein are essential for viral replication. *J. Virol.* **74**, 1794-1800 (2000).
54. Narasimhan, J. *et al.* Crystal structure of the interferon-induced ubiquitin-like protein ISG15. *J. Biol. Chem.* **280**, 27356-27365 (2005).
55. Chang, Y. G. *et al.* Different roles for two ubiquitin-like domains of ISG15 in protein modification. *J. Biol. Chem.* **283**, 13370-13377 (2008).

56. Malakhov, M. P. *et al.* High-throughput immunoblotting. Ubiquitin-like protein ISG15 modifies key regulators of signal transduction. *J. Biol. Chem.* **278**, 16608-16613 (2003).
57. Malakhova, O. A. *et al.* Protein ISGylation modulates the JAK-STAT signaling pathway. *Genes Dev.* **17**, 455-460 (2003).
58. Jeon, Y. J., Yoo, H. M. & Chung, C. H. ISG15 and immune diseases. *Biochim. Biophys. Acta* **1802**, 485-496 (2010).
59. Feng, Q. *et al.* UBE1L causes lung cancer growth suppression by targeting cyclin D1. *Mol. Cancer Ther.* **7**, 3780-3788 (2008).
60. Desai, S. D. *et al.* Elevated expression of ISG15 in tumor cells interferes with the ubiquitin/26S proteasome pathway. *Cancer Res.* **66**, 921-928 (2006).
61. D'Cunha, J. *et al.* In vitro and in vivo secretion of human ISG15, an IFN-induced immunomodulatory cytokine. *J. Immunol.* **157**, 4100-4108 (1996).
62. Durfee, L. A., Lyon, N., Seo, K. & Huibregtse, J. M. The ISG15 conjugation system broadly targets newly synthesized proteins: implications for the antiviral function of ISG15. *Mol. Cell* **38**, 722-732 (2010).
63. Zhao, C., Hsiang, T. Y., Kuo, R. L. & Krug, R. M. ISG15 conjugation system targets the viral NS1 protein in influenza A virus-infected cells. *Proc. Natl. Acad. Sci. U. S. A.* **107**, 2253-2258 (2010).
64. Kim, M. J. & Yoo, J. Y. Inhibition of hepatitis C virus replication by IFN-mediated ISGylation of HCV-NS5A. *J. Immunol.* **185**, 4311-4318 (2010).
65. Bleul, C. C., Wu, L., Hoxie, J. A., Springer, T. A. & Mackay, C. R. The HIV coreceptors CXCR4 and CCR5 are differentially expressed and regulated on human T lymphocytes. *Proc. Natl. Acad. Sci. U. S. A.* **94**, 1925-1930 (1997).
66. Strebel, K. Virus-host interactions: role of HIV proteins Vif, Tat, and Rev. *AIDS* **17 Suppl 4**, S25-34 (2003).
67. Chan, D. C., Fass, D., Berger, J. M. & Kim, P. S. Core structure of gp41 from the HIV envelope glycoprotein. *Cell* **89**, 263-273 (1997).
68. Erickson-Viitanen, S. *et al.* Cleavage of HIV-1 gag polyprotein synthesized in vitro: sequential cleavage by the viral protease. *AIDS Res. Hum. Retroviruses* **5**, 577-591 (1989).
69. Lillehoj, E. P. *et al.* Purification and structural characterization of the putative gag-pol protease of human immunodeficiency virus. *J. Virol.* **62**, 3053-3058 (1988).

70. Freed, E. O., Myers, D. J. & Risser, R. Characterization of the fusion domain of the human immunodeficiency virus type 1 envelope glycoprotein gp41. *Proc. Natl. Acad. Sci. U. S. A.* **87**, 4650-4654 (1990).
71. Auewarakul, P., Wacharapornin, P., Srichatrapimuk, S., Chutipongtanate, S. & Puthavathana, P. Uncoating of HIV-1 requires cellular activation. *Virology* **337**, 93-101 (2005).
72. Briones, M. S., Dobard, C. W. & Chow, S. A. Role of human immunodeficiency virus type 1 integrase in uncoating of the viral core. *J. Virol.* **84**, 5181-5190 (2010).
73. Bachis, A., Cruz, M. I. & Mocchetti, I. M-tropic HIV envelope protein gp120 exhibits a different neuropathological profile than T-tropic gp120 in rat striatum. *Eur. J. Neurosci.* **32**, 570-578 (2010).
74. Cartier, C. *et al.* Active cAMP-dependent protein kinase incorporated within highly purified HIV-1 particles is required for viral infectivity and interacts with viral capsid protein. *J. Biol. Chem.* **278**, 35211-35219 (2003).
75. Wacharapornin, P., Lauhakirti, D. & Auewarakul, P. The effect of capsid mutations on HIV-1 uncoating. *Virology* **358**, 48-54 (2007).
76. Lanchy, J. M. *et al.* Dynamics of the HIV-1 reverse transcription complex during initiation of DNA synthesis. *J. Biol. Chem.* **275**, 12306-12312 (2000).
77. Whitcomb, J. M. & Hughes, S. H. Retroviral reverse transcription and integration: progress and problems. *Annu. Rev. Cell Biol.* **8**, 275-306 (1992).
78. Abbondanzieri, E. A. *et al.* Dynamic binding orientations direct activity of HIV reverse transcriptase. *Nature* **453**, 184-189 (2008).
79. Sarafianos, S. G. *et al.* Crystal structure of HIV-1 reverse transcriptase in complex with a polypurine tract RNA:DNA. *EMBO J.* **20**, 1449-1461 (2001).
80. Popov, S. *et al.* Viral protein R regulates nuclear import of the HIV-1 pre-integration complex. *EMBO J.* **17**, 909-917 (1998).
81. Goldgur, Y. *et al.* Three new structures of the core domain of HIV-1 integrase: an active site that binds magnesium. *Proc. Natl. Acad. Sci. U. S. A.* **95**, 9150-9154 (1998).
82. Maignan, S., Guilloteau, J. P., Zhou-Liu, Q., Clement-Mella, C. & Mikol, V. Crystal structures of the catalytic domain of HIV-1 integrase free and complexed with its metal cofactor: high level of similarity of the active site with other viral integrases. *J. Mol. Biol.* **282**, 359-368 (1998).

83. Cai, M. *et al.* Solution structure of the N-terminal zinc binding domain of HIV-1 integrase. *Nat. Struct. Biol.* **4**, 567-577 (1997).
84. Lodi, P. J. *et al.* Solution structure of the DNA binding domain of HIV-1 integrase. *Biochemistry* **34**, 9826-9833 (1995).
85. Wang, J. Y., Ling, H., Yang, W. & Craigie, R. Structure of a two-domain fragment of HIV-1 integrase: implications for domain organization in the intact protein. *EMBO J.* **20**, 7333-7343 (2001).
86. Chen, J. C. *et al.* Crystal structure of the HIV-1 integrase catalytic core and C-terminal domains: a model for viral DNA binding. *Proc. Natl. Acad. Sci. U. S. A.* **97**, 8233-8238 (2000).
87. Guiot, E. *et al.* Relationship between the oligomeric status of HIV-1 integrase on DNA and enzymatic activity. *J. Biol. Chem.* **281**, 22707-22719 (2006).
88. Faure, A. *et al.* HIV-1 integrase crosslinked oligomers are active in vitro. *Nucleic Acids Res.* **33**, 977-986 (2005).
89. Delelis, O. *et al.* Insight into the integrase-DNA recognition mechanism. A specific DNA-binding mode revealed by an enzymatically labeled integrase. *J. Biol. Chem.* **283**, 27838-27849 (2008).
90. Li, M. & Craigie, R. Processing of viral DNA ends channels the HIV-1 integration reaction to concerted integration. *J. Biol. Chem.* **280**, 29334-29339 (2005).
91. Gao, K., Butler, S. L. & Bushman, F. Human immunodeficiency virus type 1 integrase: arrangement of protein domains in active cDNA complexes. *EMBO J.* **20**, 3565-3576 (2001).
92. Ren, G., Gao, K., Bushman, F. D. & Yeager, M. Single-particle image reconstruction of a tetramer of HIV integrase bound to DNA. *J. Mol. Biol.* **366**, 286-294 (2007).
93. Rana, T. M. & Jeang, K. T. Biochemical and functional interactions between HIV-1 Tat protein and TAR RNA. *Arch. Biochem. Biophys.* **365**, 175-185 (1999).
94. Dingwall, C. *et al.* HIV-1 tat protein stimulates transcription by binding to a U-rich bulge in the stem of the TAR RNA structure. *EMBO J.* **9**, 4145-4153 (1990).
95. Fujinaga, K. *et al.* A minimal chimera of human cyclin T1 and tat binds TAR and activates human immunodeficiency virus transcription in murine cells. *J. Virol.* **76**, 12934-12939 (2002).

96. Gold, M. O., Yang, X., Herrmann, C. H. & Rice, A. P. PITALRE, the catalytic subunit of TAK, is required for human immunodeficiency virus Tat transactivation in vivo. *J. Virol.* **72**, 4448-4453 (1998).
97. Herrmann, C. H. & Rice, A. P. Lentivirus Tat proteins specifically associate with a cellular protein kinase, TAK, that hyperphosphorylates the carboxyl-terminal domain of the large subunit of RNA polymerase II: candidate for a Tat cofactor. *J. Virol.* **69**, 1612-1620 (1995).
98. Dahmus, M. E. Reversible phosphorylation of the C-terminal domain of RNA polymerase II. *J. Biol. Chem.* **271**, 19009-19012 (1996).
99. Zhu, Y. *et al.* Transcription elongation factor P-TEFb is required for HIV-1 tat transactivation in vitro. *Genes Dev.* **11**, 2622-2632 (1997).
100. Dorr, A. *et al.* Transcriptional synergy between Tat and PCAF is dependent on the binding of acetylated Tat to the PCAF bromodomain. *EMBO J.* **21**, 2715-2723 (2002).
101. Kiernan, R. E. *et al.* HIV-1 tat transcriptional activity is regulated by acetylation. *EMBO J.* **18**, 6106-6118 (1999).
102. Deng, L. *et al.* Acetylation of HIV-1 Tat by CBP/P300 increases transcription of integrated HIV-1 genome and enhances binding to core histones. *Virology* **277**, 278-295 (2000).
103. Greger, I. H., Demarchi, F., Giacca, M. & Proudfoot, N. J. Transcriptional interference perturbs the binding of Sp1 to the HIV-1 promoter. *Nucleic Acids Res.* **26**, 1294-1301 (1998).
104. Vlach, J. *et al.* Induction of Sp1 phosphorylation and NF-kappa B-independent HIV promoter domain activity in T lymphocytes stimulated by okadaic acid. *Virology* **208**, 753-761 (1995).
105. Mahanta, S. K., Scholl, T., Yang, F. C. & Strominger, J. L. Transactivation by CIITA, the type II bare lymphocyte syndrome-associated factor, requires participation of multiple regions of the TATA box binding protein. *Proc. Natl. Acad. Sci. U. S. A.* **94**, 6324-6329 (1997).
106. Raha, T., Cheng, S. W. & Green, M. R. HIV-1 Tat stimulates transcription complex assembly through recruitment of TBP in the absence of TAFs. *PLoS Biol.* **3**, e44 (2005).
107. Verrijzer, C. P., Chen, J. L., Yokomori, K. & Tjian, R. Binding of TAFs to core elements directs promoter selectivity by RNA polymerase II. *Cell* **81**, 1115-1125 (1995).

108. Feinberg, M. B., Baltimore, D. & Frankel, A. D. The role of Tat in the human immunodeficiency virus life cycle indicates a primary effect on transcriptional elongation. *Proc. Natl. Acad. Sci. U. S. A.* **88**, 4045-4049 (1991).
109. Sheldon, M., Ratnasabapathy, R. & Hernandez, N. Characterization of the inducer of short transcripts, a human immunodeficiency virus type 1 transcriptional element that activates the synthesis of short RNAs. *Mol. Cell. Biol.* **13**, 1251-1263 (1993).
110. Zhou, W., Parent, L. J., Wills, J. W. & Resh, M. D. Identification of a membrane-binding domain within the amino-terminal region of human immunodeficiency virus type 1 Gag protein which interacts with acidic phospholipids. *J. Virol.* **68**, 2556-2569 (1994).
111. Pettit, S. C., Gulnik, S., Everitt, L. & Kaplan, A. H. The dimer interfaces of protease and extra-protease domains influence the activation of protease and the specificity of GagPol cleavage. *J. Virol.* **77**, 366-374 (2003).
112. Pettit, S. C., Everitt, L. E., Choudhury, S., Dunn, B. M. & Kaplan, A. H. Initial cleavage of the human immunodeficiency virus type 1 GagPol precursor by its activated protease occurs by an intramolecular mechanism. *J. Virol.* **78**, 8477-8485 (2004).
113. Oliva, R. *et al.* Structural investigation of the HIV-1 envelope glycoprotein gp160 cleavage site, 2: relevance of an N-terminal helix. *ChemBiochem* **4**, 727-733 (2003).
114. Freed, E. O. HIV-1 gag proteins: diverse functions in the virus life cycle. *Virology* **251**, 1-15 (1998).
115. Murakami, T. & Freed, E. O. Genetic evidence for an interaction between human immunodeficiency virus type 1 matrix and alpha-helix 2 of the gp41 cytoplasmic tail. *J. Virol.* **74**, 3548-3554 (2000).
116. Miyauchi, K. *et al.* The membrane-spanning domain of gp41 plays a critical role in intracellular trafficking of the HIV envelope protein. *Retrovirology* **7**, 95 (2010).
117. Franzusoff, A., Volpe, A. M., Josse, D., Pichuanes, S. & Wolf, J. R. Biochemical and genetic definition of the cellular protease required for HIV-1 gp160 processing. *J. Biol. Chem.* **270**, 3154-3159 (1995).
118. Raja, N. U., Vincent, M. J. & Jabbar, M. A. Analysis of endoproteolytic cleavage and intracellular transport of human immunodeficiency virus type 1 envelope glycoproteins using mutant CD4 molecules bearing the transmembrane endoplasmic reticulum retention signal. *J. Gen. Virol.* **74** (Pt 10), 2085-2097 (1993).
119. Bouloy, M. *et al.* Genetic evidence for an interferon-antagonistic function of rift valley fever virus nonstructural protein NSs. *J. Virol.* **75**, 1371-1377 (2001).

120. Marie, I., Durbin, J. E. & Levy, D. E. Differential viral induction of distinct interferon-alpha genes by positive feedback through interferon regulatory factor-7. *EMBO J.* **17**, 6660-6669 (1998).
121. Bowie, A. G. & Hago, I. R. The role of Toll-like receptors in the host response to viruses. *Mol. Immunol.* **42**, 859-867 (2005).
122. Uematsu, S. *et al.* Interleukin-1 receptor-associated kinase-1 plays an essential role for Toll-like receptor (TLR)7- and TLR9-mediated interferon- α induction. *J. Exp. Med.* **201**, 915-923 (2005).
123. Yoneyama, M. *et al.* The RNA helicase RIG-I has an essential function in double-stranded RNA-induced innate antiviral responses. *Nat. Immunol.* **5**, 730-737 (2004).
124. Kawai, T. *et al.* IPS-1, an adaptor triggering RIG-I- and Mda5-mediated type I interferon induction. *Nat. Immunol.* **6**, 981-988 (2005).
125. Kerkmann, M. *et al.* Activation with CpG-A and CpG-B oligonucleotides reveals two distinct regulatory pathways of type I IFN synthesis in human plasmacytoid dendritic cells. *J. Immunol.* **170**, 4465-4474 (2003).
126. Novick, D., Cohen, B. & Rubinstein, M. The human interferon alpha/beta receptor: characterization and molecular cloning. *Cell* **77**, 391-400 (1994).
127. Kim, S. H., Cohen, B., Novick, D. & Rubinstein, M. Mammalian type I interferon receptors consists of two subunits: IFN α R1 and IFN α R2. *Gene* **196**, 279-286 (1997).
128. Kisseleva, T., Bhattacharya, S., Braunstein, J. & Schindler, C. W. Signaling through the JAK/STAT pathway, recent advances and future challenges. *Gene* **285**, 1-24 (2002).
129. Horvath, C. M. The Jak-STAT pathway stimulated by interferon alpha or interferon beta. *Sci. STKE* **2004**, tr10 (2004).
130. Goh, W. C., Manel, N. & Emerman, M. The human immunodeficiency virus Vpr protein binds Cdc25C: implications for G2 arrest. *Virology* **318**, 337-349 (2004).
131. van Deursen, J., Boer, J., Kasper, L. & Grosveld, G. G2 arrest and impaired nucleocytoplasmic transport in mouse embryos lacking the proto-oncogene CAN/Nup214. *EMBO J.* **15**, 5574-5583 (1996).
132. Wong, J. J., Pung, Y. F., Sze, N. S. & Chin, K. C. HERC5 is an IFN-induced HECT-type E3 protein ligase that mediates type I IFN-induced ISGylation of protein targets. *Proc. Natl. Acad. Sci. U. S. A.* **103**, 10735-10740 (2006).
133. Ren, M., Coutavas, E., D'Eustachio, P. & Rush, M. G. Effects of mutant Ran/TC4 proteins on cell cycle progression. *Mol. Cell. Biol.* **14**, 4216-4224 (1994).

134. Bischoff, F. R., Krebber, H., Smirnova, E., Dong, W. & Ponstingl, H. Co-activation of RanGTPase and inhibition of GTP dissociation by Ran-GTP binding protein RanBP1. *EMBO J.* **14**, 705-715 (1995).
135. Hetzer, M., Bilbao-Cortes, D., Walther, T. C., Gruss, O. J. & Mattaj, I. W. GTP hydrolysis by Ran is required for nuclear envelope assembly. *Mol. Cell* **5**, 1013-1024 (2000).
136. Kalab, P., Pu, R. T. & Dasso, M. The ran GTPase regulates mitotic spindle assembly. *Curr. Biol.* **9**, 481-484 (1999).
137. Azuma, Y. *et al.* Conserved histidine residues of RCC1 are essential for nucleotide exchange on Ran. *J. Biochem.* **120**, 82-91 (1996).
138. Izaurralde, E., Kutay, U., von Kobbe, C., Mattaj, I. W. & Gorlich, D. The asymmetric distribution of the constituents of the Ran system is essential for transport into and out of the nucleus. *EMBO J.* **16**, 6535-6547 (1997).
139. Zou, W., Wang, J. & Zhang, D. E. Negative regulation of ISG15 E3 ligase EFP through its autoISGylation. *Biochem. Biophys. Res. Commun.* **354**, 321-327 (2007).
140. Watts, J. M. *et al.* Architecture and secondary structure of an entire HIV-1 RNA genome. *Nature* **460**, 711-716 (2009).
141. Meyer, B. E. & Malim, M. H. The HIV-1 Rev trans-activator shuttles between the nucleus and the cytoplasm. *Genes Dev.* **8**, 1538-1547 (1994).
142. Malim, M. H., Hauber, J., Le, S. Y., Maizel, J. V. & Cullen, B. R. The HIV-1 rev trans-activator acts through a structured target sequence to activate nuclear export of unspliced viral mRNA. *Nature* **338**, 254-257 (1989).
143. Truant, R. & Cullen, B. R. The arginine-rich domains present in human immunodeficiency virus type 1 Tat and Rev function as direct importin beta-dependent nuclear localization signals. *Mol. Cell. Biol.* **19**, 1210-1217 (1999).
144. Henderson, B. R. & Percipalle, P. Interactions between HIV Rev and nuclear import and export factors: the Rev nuclear localisation signal mediates specific binding to human importin-beta. *J. Mol. Biol.* **274**, 693-707 (1997).
145. Fankhauser, C., Izaurralde, E., Adachi, Y., Wingfield, P. & Laemmli, U. K. Specific complex of human immunodeficiency virus type 1 rev and nucleolar B23 proteins: dissociation by the Rev response element. *Mol. Cell. Biol.* **11**, 2567-2575 (1991).
146. Wen, W., Meinkoth, J. L., Tsien, R. Y. & Taylor, S. S. Identification of a signal for rapid export of proteins from the nucleus. *Cell* **82**, 463-473 (1995).

147. Neville, M., Stutz, F., Lee, L., Davis, L. I. & Rosbash, M. The importin-beta family member Crm1p bridges the interaction between Rev and the nuclear pore complex during nuclear export. *Curr. Biol.* **7**, 767-775 (1997).
148. Fornerod, M., Ohno, M., Yoshida, M. & Mattaj, I. W. CRM1 is an export receptor for leucine-rich nuclear export signals. *Cell* **90**, 1051-1060 (1997).
149. Stade, K., Ford, C. S., Guthrie, C. & Weis, K. Exportin 1 (Crm1p) is an essential nuclear export factor. *Cell* **90**, 1041-1050 (1997).
150. Bischoff, F. R. & Gorlich, D. RanBP1 is crucial for the release of RanGTP from importin beta-related nuclear transport factors. *FEBS Lett.* **419**, 249-254 (1997).
151. Chamond, N., Locker, N. & Sargueil, B. The different pathways of HIV genomic RNA translation. *Biochem. Soc. Trans.* **38**, 1548-1552 (2010).
152. Nicholson, M. G., Rue, S. M., Clements, J. E. & Barber, S. A. An internal ribosome entry site promotes translation of a novel SIV Pr55(Gag) isoform. *Virology* **349**, 325-334 (2006).
153. Miele, G. & Lever, A. M. Expression of mutant and wild-type gag proteins for gene therapy in HIV-1 infection. *Gene Ther.* **3**, 357-361 (1996).
154. Ricci, E. P., Soto Rifo, R., Herbreteau, C. H., Decimo, D. & Ohlmann, T. Lentiviral RNAs can use different mechanisms for translation initiation. *Biochem. Soc. Trans.* **36**, 690-693 (2008).
155. Sonenberg, N. & Hinnebusch, A. G. Regulation of translation initiation in eukaryotes: mechanisms and biological targets. *Cell* **136**, 731-745 (2009).
156. Balvay, L., Lopez Lastra, M., Sargueil, B., Darlix, J. L. & Ohlmann, T. Translational control of retroviruses. *Nat. Rev. Microbiol.* **5**, 128-140 (2007).
157. Kieft, J. S. Viral IRES RNA structures and ribosome interactions. *Trends Biochem. Sci.* **33**, 274-283 (2008).
158. Pflugsten, J. S. & Kieft, J. S. RNA structure-based ribosome recruitment: lessons from the Dicistroviridae intergenic region IRESes. *RNA* **14**, 1255-1263 (2008).
159. Scarlata, S. & Carter, C. Role of HIV-1 Gag domains in viral assembly. *Biochim. Biophys. Acta* **1614**, 62-72 (2003).
160. Dalton, A. K., Ako-Adjei, D., Murray, P. S., Murray, D. & Vogt, V. M. Electrostatic interactions drive membrane association of the human immunodeficiency virus type 1 Gag MA domain. *J. Virol.* **81**, 6434-6445 (2007).

161. Derdowski, A., Ding, L. & Spearman, P. A novel fluorescence resonance energy transfer assay demonstrates that the human immunodeficiency virus type 1 Pr55Gag I domain mediates Gag-Gag interactions. *J. Virol.* **78**, 1230-1242 (2004).
162. Demirov, D. G., Ono, A., Orenstein, J. M. & Freed, E. O. Overexpression of the N-terminal domain of TSG101 inhibits HIV-1 budding by blocking late domain function. *Proc. Natl. Acad. Sci. U. S. A.* **99**, 955-960 (2002).
163. Carpick, B. W. *et al.* Characterization of the solution complex between the interferon-induced, double-stranded RNA-activated protein kinase and HIV-I transactivating region RNA. *J. Biol. Chem.* **272**, 9510-9516 (1997).
164. Dey, M. *et al.* Mechanistic link between PKR dimerization, autophosphorylation, and eIF2alpha substrate recognition. *Cell* **122**, 901-913 (2005).
165. Rojas, M., Arias, C. F. & Lopez, S. Protein kinase R is responsible for the phosphorylation of eIF2alpha in rotavirus infection. *J. Virol.* **84**, 10457-10466 (2010).
166. Maitra, R. K. & Silverman, R. H. Regulation of human immunodeficiency virus replication by 2',5'-oligoadenylate-dependent RNase L. *J. Virol.* **72**, 1146-1152 (1998).
167. Marie, I., Svab, J., Robert, N., Galabru, J. & Hovanessian, A. G. Differential expression and distinct structure of 69- and 100-kDa forms of 2-5A synthetase in human cells treated with interferon. *J. Biol. Chem.* **265**, 18601-18607 (1990).
168. Maitra, R. K. *et al.* HIV-1 TAR RNA has an intrinsic ability to activate interferon-inducible enzymes. *Virology* **204**, 823-827 (1994).
169. Yap, M. W., Nisole, S. & Stoye, J. P. A single amino acid change in the SPRY domain of human Trim5alpha leads to HIV-1 restriction. *Curr. Biol.* **15**, 73-78 (2005).
170. Kajaste-Rudnitski, A. *et al.* TRIM22 inhibits HIV-1 transcription independently of its E3 ubiquitin ligase activity, Tat, and NF-kappaB-responsive long terminal repeat elements. *J. Virol.* **85**, 5183-5196 (2011).
171. Barr, S. D., Smiley, J. R. & Bushman, F. D. The interferon response inhibits HIV particle production by induction of TRIM22. *PLoS Pathog.* **4**, e1000007 (2008).
172. Ritchie, K. J. & Zhang, D. E. ISG15: the immunological kin of ubiquitin. *Semin. Cell Dev. Biol.* **15**, 237-246 (2004).
173. Okumura, A., Lu, G., Pitha-Rowe, I. & Pitha, P. M. Innate antiviral response targets HIV-1 release by the induction of ubiquitin-like protein ISG15. *Proc. Natl. Acad. Sci. U. S. A.* **103**, 1440-1445 (2006).

174. Pincetic, A., Kuang, Z., Seo, E. J. & Leis, J. The interferon-induced gene ISG15 blocks retrovirus release from cells late in the budding process. *J. Virol.* **84**, 4725-4736 (2010).
175. Kerscher, O., Felberbaum, R. & Hochstrasser, M. Modification of proteins by ubiquitin and ubiquitin-like proteins. *Annu. Rev. Cell Dev. Biol.* **22**, 159-180 (2006).
176. Harty, R. N., Pitha, P. M. & Okumura, A. Antiviral activity of innate immune protein ISG15. *J. Innate Immun.* **1**, 397-404 (2009).
177. Shi, H. X. *et al.* Positive regulation of interferon regulatory factor 3 activation by Herc5 via ISG15 modification. *Mol. Cell. Biol.* **30**, 2424-2436 (2010).
178. Ono, A., Ablan, S. D., Lockett, S. J., Nagashima, K. & Freed, E. O. Phosphatidylinositol (4,5) bisphosphate regulates HIV-1 Gag targeting to the plasma membrane. *Proc. Natl. Acad. Sci. U. S. A.* **101**, 14889-14894 (2004).
179. Halwani, R., Khorchid, A., Cen, S. & Kleiman, L. Rapid localization of Gag/GagPol complexes to detergent-resistant membrane during the assembly of human immunodeficiency virus type 1. *J. Virol.* **77**, 3973-3984 (2003).
180. Jenkins, Y. *et al.* Biochemical analyses of the interactions between human immunodeficiency virus type 1 Vpr and p6(Gag). *J. Virol.* **75**, 10537-10542 (2001).
181. Selig, L. *et al.* Interaction with the p6 domain of the gag precursor mediates incorporation into virions of Vpr and Vpx proteins from primate lentiviruses. *J. Virol.* **73**, 592-600 (1999).
182. Greatorex, J., Gallego, J., Varani, G. & Lever, A. Structure and stability of wild-type and mutant RNA internal loops from the SL-1 domain of the HIV-1 packaging signal. *J. Mol. Biol.* **322**, 543-557 (2002).
183. Amarasinghe, G. K. *et al.* NMR structure of the HIV-1 nucleocapsid protein bound to stem-loop SL2 of the psi-RNA packaging signal. Implications for genome recognition. *J. Mol. Biol.* **301**, 491-511 (2000).
184. Paoletti, A. C., Shubsda, M. F., Hudson, B. S. & Borer, P. N. Affinities of the nucleocapsid protein for variants of SL3 RNA in HIV-1. *Biochemistry* **41**, 15423-15428 (2002).
185. Yuan, Y., Kerwood, D. J., Paoletti, A. C., Shubsda, M. F. & Borer, P. N. Stem of SL1 RNA in HIV-1: structure and nucleocapsid protein binding for a 1 x 3 internal loop. *Biochemistry* **42**, 5259-5269 (2003).
186. Kerwood, D. J., Cavaluzzi, M. J. & Borer, P. N. Structure of SL4 RNA from the HIV-1 packaging signal. *Biochemistry* **40**, 14518-14529 (2001).

187. Wan, M. & Loh, B. N. Expression and purification of active form of HIV-1 protease from *E. coli*. *Biochem. Mol. Biol. Int.* **35**, 899-912 (1995).
188. Pettit, S. C., Lindquist, J. N., Kaplan, A. H. & Swanstrom, R. Processing sites in the human immunodeficiency virus type 1 (HIV-1) Gag-Pro-Pol precursor are cleaved by the viral protease at different rates. *Retrovirology* **2**, 66 (2005).
189. Darke, P. L. *et al.* HIV-1 protease specificity of peptide cleavage is sufficient for processing of gag and pol polyproteins. *Biochem. Biophys. Res. Commun.* **156**, 297-303 (1988).
190. Stuchell, M. D. *et al.* The human endosomal sorting complex required for transport (ESCRT-I) and its role in HIV-1 budding. *J. Biol. Chem.* **279**, 36059-36071 (2004).
191. von Schwedler, U. K. *et al.* The protein network of HIV budding. *Cell* **114**, 701-713 (2003).
192. Dussupt, V. *et al.* The nucleocapsid region of HIV-1 Gag cooperates with the PTAP and LYPXnL late domains to recruit the cellular machinery necessary for viral budding. *PLoS Pathog.* **5**, e1000339 (2009).
193. Scott, A. *et al.* Structural and mechanistic studies of VPS4 proteins. *EMBO J.* **24**, 3658-3669 (2005).
194. Shim, S., Merrill, S. A. & Hanson, P. I. Novel interactions of ESCRT-III with LIP5 and VPS4 and their implications for ESCRT-III disassembly. *Mol. Biol. Cell* **19**, 2661-2672 (2008).
195. Nakasato, N. *et al.* A ubiquitin E3 ligase Efp is up-regulated by interferons and conjugated with ISG15. *Biochem. Biophys. Res. Commun.* **351**, 540-546 (2006).
196. Takeuchi, T., Inoue, S. & Yokosawa, H. Identification and Herc5-mediated ISGylation of novel target proteins. *Biochem. Biophys. Res. Commun.* **348**, 473-477 (2006).
197. Ji, Y. *et al.* The ancestral gene for transcribed, low-copy repeats in the Prader-Willi/Angelman region encodes a large protein implicated in protein trafficking, which is deficient in mice with neuromuscular and spermiogenic abnormalities. *Hum. Mol. Genet.* **8**, 533-542 (1999).
198. Hochrainer, K. *et al.* The human HERC family of ubiquitin ligases: novel members, genomic organization, expression profiling, and evolutionary aspects. *Genomics* **85**, 153-164 (2005).
199. Renault, L. *et al.* The 1.7 Å crystal structure of the regulator of chromosome condensation (RCC1) reveals a seven-bladed propeller. *Nature* **392**, 97-101 (1998).

200. Renault, L., Kuhlmann, J., Henkel, A. & Wittinghofer, A. Structural basis for guanine nucleotide exchange on Ran by the regulator of chromosome condensation (RCC1). *Cell* **105**, 245-255 (2001).
201. Ohtsubo, M., Okazaki, H. & Nishimoto, T. The RCC1 protein, a regulator for the onset of chromosome condensation locates in the nucleus and binds to DNA. *J. Cell Biol.* **109**, 1389-1397 (1989).
202. Bischoff, F. R. & Ponstingl, H. Mitotic regulator protein RCC1 is complexed with a nuclear ras-related polypeptide. *Proc. Natl. Acad. Sci. U. S. A.* **88**, 10830-10834 (1991).
203. Bischoff, F. R. & Ponstingl, H. Catalysis of guanine nucleotide exchange on Ran by the mitotic regulator RCC1. *Nature* **354**, 80-82 (1991).
204. Quimby, B. B. & Dasso, M. The small GTPase Ran: interpreting the signs. *Curr. Opin. Cell Biol.* **15**, 338-344 (2003).
205. Rosa, J. L., Casaroli-Marano, R. P., Buckler, A. J., Vilaro, S. & Barbacid, M. p619, a giant protein related to the chromosome condensation regulator RCC1, stimulates guanine nucleotide exchange on ARF1 and Rab proteins. *EMBO J.* **15**, 4262-4273 (1996).
206. Garcia-Gonzalo, F. R. & Rosa, J. L. The HERC proteins: functional and evolutionary insights. *Cell Mol. Life Sci.* **62**, 1826-1838 (2005).
207. Takeuchi, T., Inoue, S. & Yokosawa, H. Identification and Herc5-mediated ISGylation of novel target proteins. *Biochem. Biophys. Res. Commun.* **348**, 473-477 (2006).
208. Dastur, A., Beaudenon, S., Kelley, M., Krug, R. M. & Huibregtse, J. M. Herc5, an interferon-induced HECT E3 enzyme, is required for conjugation of ISG15 in human cells. *J. Biol. Chem.* **281**, 4334-4338 (2006).
209. Versteeg, G. A. *et al.* Species-specific antagonism of host ISGylation by the influenza B virus NS1 protein. *J. Virol.* **84**, 5423-5430 (2010).
210. Tang, Y. *et al.* Herc5 attenuates influenza A virus by catalyzing ISGylation of viral NS1 protein. *J. Immunol.* **184**, 5777-5790 (2010).
211. Shi, H. X. *et al.* Positive regulation of interferon regulatory factor 3 activation by Herc5 via ISG15 modification. *Mol. Cell. Biol.* **30**, 2424-2436 (2010).
212. Burkhard, P., Stetefeld, J. & Strelkov, S. V. Coiled coils: a highly versatile protein folding motif. *Trends Cell Biol.* **11**, 82-88 (2001).

213. Chan, D. C., Chutkowski, C. T. & Kim, P. S. Evidence that a prominent cavity in the coiled coil of HIV type 1 gp41 is an attractive drug target. *Proc. Natl. Acad. Sci. U. S. A.* **95**, 15613-15617 (1998).
214. Zou, W., Wang, J. & Zhang, D. E. Negative regulation of ISG15 E3 ligase EFP through its autoISGylation. *Biochem. Biophys. Res. Commun.* **354**, 321-327 (2007).
215. Mitsui, K. *et al.* A novel human gene encoding HECT domain and RCC1-like repeats interacts with cyclins and is potentially regulated by the tumor suppressor proteins. *Biochem. Biophys. Res. Commun.* **266**, 115-122 (1999).
216. Zhao, C., Hsiang, T. Y., Kuo, R. L. & Krug, R. M. ISG15 conjugation system targets the viral NS1 protein in influenza A virus-infected cells. *Proc. Natl. Acad. Sci. U. S. A.* **107**, 2253-2258 (2010).
217. Sawyer, S. L., Emerman, M. & Malik, H. S. Discordant evolution of the adjacent antiretroviral genes TRIM22 and TRIM5 in mammals. *PLoS Pathog.* **3**, e197 (2007).
218. Zhang, D. & Zhang, D. E. Interferon-stimulated gene 15 and the protein ISGylation system. *J. Interferon Cytokine Res.* **31**, 119-130 (2011).
219. Jimenez-Sousa, M. A. *et al.* Gene expression profiling in the first twelve weeks of treatment in chronic hepatitis C patients. *Enferm. Infecc. Microbiol. Clin.* (2011).
220. Azuma, Y., Renault, L., Garcia-Ranea, J. A., Valencia, A., Nishimoto, T., Wittinghofer, A. Model of the Ran-RCC1 interaction using biochemical and docking experiments. *JMB.* **289**, 1119-1130 (2009).
221. Narasimhan, J., Wang, M., Fu, Z., Klein, J. M., Haas, A. L., Kim, J. P. Crystal structure of the Interferon-induced ubiquitin-like protein ISG15. *JBC.* **280**, 27356-27365 (2005).
222. Garcia-Gonzalo, F. R., Rosa, J. L. The Herc proteins: functional and evolutionary insights. *Cell. Mol. Life Sci.* **62**, 1826-1838 (2005).
223. Nethe, M., Hordijk, P. L. The role of ubiquitinylation and degradation in RhoTPase signaling. *Journal of Cell Science.* **123**, 4011-4018 (2010).
224. Hughes, M., Zhang, C., Avis, J. M., Hutchinson, C. J., Clarke, P. R. The role of the Ran GTPase in nuclear assembly and DNA replication: characterization of the effects of Ran mutants. *Journal of cell Science.* **111**, 3017-3026 (1998).